

**AN EXPERIMENTAL STUDY ON SURFACTANT-ALTERNATING-GAS
PROCESS**

by

© Mahsa Moayedi

A thesis submitted to the

School of Graduate Studies

In partial fulfillment of the requirements for the degree of

Master of Engineering

Faculty of Engineering and Applied Science

Memorial University of Newfoundland

October 2015

St. John's

Newfoundland and Labrador

ABSTRACT

Foam, produced during surfactant enhanced water-alternating-gas (SAG) injection, reduces the mobility ratio by increasing the displacement fluid (gas) viscosity; furthermore, it can block high permeability zones leading to increased recovery efficiency. This study presents a comparative laboratory study of two nonionic surfactants (Ivey-Sol 108 and TX-100) in a series of SAG coreflooding tests. The effects of surfactant type, concentration, brine salinity, injection scheme and the addition of a sacrificial adsorption agent to the secondary waterflooding on oil recovery were evaluated. Several foam stability measurement tests using dynamic and static methods were conducted to examine the foam stability of the different solutions that were used in coreflooding tests. Two main mechanisms behind the use of surfactants to enhance oil recovery are (1) reduction in interfacial tension and (2) alteration of wettability. Both the interfacial tension and contact angle of the surfactant solution and rock used in coreflooding were also characterized at experimental conditions to examine their effect on oil recovery.

It was found that optimized SAG experiment improved the total oil recovery by 13% compared to the water-alternating-gas (WAG) experiment and TX-100 is superior to Ivey-sol 108 for reducing the interfacial tension (IFT), producing foam, altering wettability toward intermediate and improving recovery. More stable and stronger foam can be generated by using low salinity brine and concentrations of surfactant above critical micelle concentration (CMC); furthermore, recovery of oil increased using low salinity solutions and higher concentrations of surfactants. The addition of sodium lignosulfonate (SLS) to the secondary waterflooding can prevent surfactant adsorption onto the rock surface, therefore maintaining a higher concentration of surfactant, leading to increased oil recovery.

ACKNOWLEDGEMENTS

First and foremost, I would like to thank God, whose many blessings have made me who I am today.

My profound and sincere gratitude goes to my able supervisor, Dr. Lesley James for her perpetual support, guidance and encouragement throughout this research work.

I also thank the Hibernia Management and Development Company (HMDC), Chevron Canada, the Natural Sciences and Engineering Research Council of Canada (NSERC), the Canada Foundation for Innovation (CFI), and the Research and Development Corporation (RDC) for their financial support without which this work could not have been performed.

I would also like to express my sincere thanks to Dr. Shehadeh Masalmeh for the valuable comments on the results and discussions and all the faculty members and my friends for their constant encouragement and support.

Finally, my heartfelt thanks to my parents, sister, and brother for their everlasting love and support to finish this project.

TABLE OF CONTENTS

ABSTRACT	i
ACKNOWLEDGEMENTS	ii
LIST OF TABLES	vi
LIST OF FIGURES	vii
LIST OF ABBREVIATIONS	xi
1. INTRODUCTION	1
1.1 Background	1
1.2 EOR Screening Criteria.....	2
1.3 Principles of Enhanced Oil Recovery (EOR).....	3
1.3.1 Improving Mobility Ratio	3
1.3.2 Increasing Capillary Number	4
1.4 Research Objective and Scope	4
1.5 Thesis Organization.....	5
2. LITERATURE REVIEW	7
2.1 Interfacial Tension.....	8
2.2 Wettability	9
2.3 Surfactant Flooding	11
2.3.1 Surfactant Structure	11
2.3.2 Capillary Desaturation Curve	12
2.4 Surfactant-Alternating-Gas (SAG) Flooding	14
2.5 Foam Principles.....	15
2.6 Foam Generation Mechanisms.....	17
2.6.1 Snap-off.....	17
2.6.2 Lamella-division	18
2.6.3 Leave-behind.....	18
2.7 Mobility Reduction Factor (MRF)	19
2.8 Foam Destruction	20
2.8.1 Foam Disjoining Pressure	20
2.8.2 Limiting Capillary Pressure	21

2.9	Factors to be Considered in Designing Foam Flooding Applications	24
2.9.1	Foam Flooding Screening Criteria.....	24
2.9.2	Foam Injection Mode	26
2.9.3	Foaming Ability and Foam Stability.....	27
2.9.4	Adsorption.....	29
2.9.5	Salinity	31
2.9.6	IFT Reduction	33
2.9.7	Wettability of Rock and Wettability Alteration by Surfactants.....	34
2.9.8	Thermal Stability	34
2.10	Foam Field Applications	35
3.	EXPERIMENTAL APPARATUS AND PROCEDURE	38
3.1	Experimental Fluids	38
3.2	Experimental Methods	40
3.2.1	Dynamic Test (Air Injection).....	40
3.2.2	Static Test (Bottle Shake)	43
3.2.3	Lessons Learned in Foam Test	45
3.2.4	Interfacial Tension and Contact Angle Measurement	45
3.2.5	Lessons Learned in IFT and Wettability Measurement.....	48
3.2.6	Core Cleaning	48
3.2.7	Low Pressure Coreflooding	51
3.2.8	Lessons Learned in Coreflooding Tests.....	57
4.	RESULTS AND DISCUSSION.....	58
4.1	Dynamic Test Results and Discussion	58
4.2	Static Test Results and Discussion.....	62
4.3	IFT and Contact Angle Results and Discussion.....	66
4.3.1	Effect of Surfactant Type and Concentration on IFT and Wettability.....	66
4.3.2	Effect of Salinity on Interfacial Tension and Wettability	68
4.4	Coreflooding Test Results and Discussion.....	69
4.4.1	Errors in Coreflooding Experiments.....	70
4.4.2	Comparison of WAG and SAG injection	72
4.4.3	Effect of Surfactant Type and Concentration on Oil Recovery	73

4.4.4	Effect of Salinity on Oil Recovery.....	75
4.4.5	Effect of Injection Scheme on Oil Recovery	77
4.4.6	Effect of Sacrificial Adsorption Agent on Oil Recovery	79
4.4.7	Optimal Oil Recovery	81
4.5	Considerations for Field Implementation.....	83
4.6	Economic Analysis.....	85
5.	CONCLUSION AND RECOMMENDATIONS.....	88
5.1	Summary of Findings and Conclusions	88
5.2	Recommendations and Future Work.....	90
	REFERENCES.....	92
	APPENDIX.....	100
	APPENDIX A: Error Analysis.....	100
	APPENDIX B: Porosity and Absolute Permeability Measurement.....	103
	B-1: Porosity Measurement and Pore Volume Calculation.....	103
	B-2: Absolute Permeability Measurement:	104
	APPENDIX C: Raw Data	105
	C-1: Foam Stability Test Raw Data.....	105
	C-2: IFT and Contact Angle Raw Data	107
	C-3: Coreflooding Raw Data.....	115
	APPENDIX D: Sample Calculation.....	152
	D-1: Dead Volume Calculation (volume of outlet section):.....	152
	D-2: Coreflooding Material Balance Calculation.....	155
	D-3: IFT and Contact Angle Sample Calculation	164
	APPENDIX E: Economic Analysis	166
	APPENDIX F: Paper.....	168

LIST OF TABLES

Table 1.1 Summary of screening criteria for EOR methods (after Taber et al., 1997).....	2
Table 3.1 Brine compositions	39
Table 3.2 Surfactants and SLS properties.....	39
Table 3.3 Berea sandstone properties	39
Table 3.4 Foaming assessment methods.....	40
Table 4.1 Solutions used in the bottle test	62
Table 4.2 Interfacial tensions (IFT) and contact angles of different solutions	67
Table 4.3 Errors in Coreflooding Experiments.....	71
Table 4.4 Summary of the experimental runs.....	71
Table 4.5 Reservoir characteristics	85
Table 4.6 Economic analysis of WAG and SAG injection.....	86

LIST OF FIGURES

Figure 1.1 Oil recovery mechanisms (Schimdt, 1990)	1
Figure 2.1 Possible effects of foam on the transport of gas in porous media, (A) Gravity override, (B) Viscous fingering, and (C) Flow diversion to low permeability zones (after Sharma et al., 1986)	8
Figure 2.2 Three possible states of wettability in oil reservoirs	10
Figure 2.3 Schematic of a surfactant molecule and micelle structure (Kopeliovich, 2013)	12
Figure 2.4 Schematic of trapped oil droplet in a capillary tube	12
Figure 2.5 Effect of pore-size distribution on the Capillary Desaturation Curve (CDC), (Skjæveland and Kleppe, 1992)	13
Figure 2.6 Effect of wettability on the residual saturation of wetting and non-wetting phase (Skjæveland and Kleppe, 1992)	14
Figure 2.7 Comparison of gas, WAG and SAG injections (after The EOR Alliance, 2014)	15
Figure 2.8 Illustration of foam system in 2D (Schramm and Wassmuth 1994)	16
Figure 2.9 Schematic of snap-off mechanism (Ransohoff and Radke 1988)	18
Figure 2.10 Lamella division mechanisms (Kovscek and Radke, 1994)	18
Figure 2.11 Leave-behind lamella generation mechanism (Kovscek and Radke, 1994)	19
Figure 2.12 Schematic of a foam film	20
Figure 2.13 The disjoining pressure as a function of film thickness showing the presence of limiting capillary pressure (P_c^*) (after Afsharpour, 2009)	22

Figure 2.14 Schematic example of gas-water capillary pressure in porous media: foam is stable below the limiting capillary pressure (Khatib and Hirasaki, 1988).....	23
Figure 2.15 Foam selection and placement in EOR projects (after Turta and Singhal, 2002)	26
Figure 3.1 Schematic of the air injection foam assessment apparatus.....	41
Figure 3.2 Air injection apparatus in the glass bath cylinder	42
Figure 3.3 Neslab RTE-100 water bath	42
Figure 3.4 Gilmont GF-2160 flow meter.....	43
Figure 3.5 Boston Round Bottle	44
Figure 3.6 Vinci Interfacial Tension (IFT 700) apparatus.....	46
Figure 3.7 IFT apparatus schematic.....	46
Figure 3.8 Soxhlet apparatus schematic.....	50
Figure 3.9 Fresh toluene in still pot	50
Figure 3.10 Distillation process (a) after 25 minutes, (b) after 45 minutes, (c) after three days..	51
Figure 3.11 Schematic of the coreflooding apparatus	52
Figure 3.12 Low Pressure coreflooding setup	53
Figure 3.13 Coreflooding outlet section (8: phase separator, 9: Emdyne MK 2000 gasmeter) ...	53
Figure 3.14 Keller LEO3 pressure transducer	54
Figure 3.15 Equilibar back pressure regulator (model # EB1LF1)	54
Figure 3.16 Custom made three phase separator	54
Figure 4.1 Collapse of Ivey-sol 108 foam, (a) t = 5 minutes, (b) t = 7 minutes, (c) t = 10 minutes, (d) t = 15 minutes.....	59
Figure 4.2 Dynamic foam test using different surfactant solutions in the absence of oil.....	60

Figure 4.3 Initial foam volume and foam collapse time of different surfactant solutions in the presence of oil, using the air injection method	61
Figure 4.4 Foam height at 0 time generated by different solutions (solution from left to right in turn is: T1, T2, T3, T4, I1, I2, I3 and I4)	63
Figure 4.5 Foam height at 1 hour generated by different solutions (solution from left to right in turn is: T1, T2, T3, T4, I1, I2, I3, and I4)	63
Figure 4.6 Foam height at 4 hours generated by different solutions (solution from left to right in turn is: T1, T2, T3, T4, I1, I2, I3, and I4)	63
Figure 4.7 Foam stability of different surfactant solutions in the absence of oil.....	64
Figure 4.8 Condition of foam generated by different solutions after 5 minutes in the presence of 10 vol% oil (Solutions from left to right in turn are: T1, T2, T3, T4, I1, I2, I3, and I4)	65
Figure 4.9 Foam stability of different surfactant solutions in the presence of oil	65
Figure 4.10 Comparison between the foam stability of different surfactant solutions in the presence and absence of oil	66
Figure 4.11 IFT at different surfactant concentrations.	68
Figure 4.12 Contact angle of oil drop on Berea sandstone in bulk of different solutions: (a) 7000 ppm TDS brine, (b) 21,000 ppm TDS brine, (c) TX-100 at CMC with 21000 ppm TDS, (d) TX-100 at 0.3 wt% + CMC with 21000 ppm TDS	69
Figure 4.13 Comparison of WAG and SAG injection.....	72
Figure 4.14 Pressure profile during WAG and SAG injection.	73
Figure 4.15 Effect of surfactant types and concentration on residual oil recovery	74
Figure 4.16 Pressure profile during SAG injection	75

Figure 4.17 Effect of salinity on total oil recovery	76
Figure 4.18 Pressure profile during SAG injection	77
Figure 4.19 Effect of injection scheme (starting with gas or surfactant) after secondary water flooding.....	78
Figure 4.20 Pressure profile during two experiments with different injection schemes	78
Figure 4.21 Color of 0.5 wt% SLS solutions (a) after production, (b) before injection	80
Figure 4.22 Effect of addition of SLS to the secondary waterflooding on total oil recovery.....	80
Figure 4.23 Pressure profile comparison in the absence and presence of sodium lignosulfonate in the secondary waterflooding.....	81
Figure 4.24 Optimization of experiments	82
Figure 4.25 Pressure profile comparison	82
Figure 4.26 Net Present Value (NPV) for SAG and WAG injection	87

LIST OF ABBREVIATIONS

A	Area (cm ²)
ASTM	American Society of Testing and Materials
AFNOR	Association Frances Normalization
AOS	Alpha olefin sulfonate
ASP	Alkaline-Surfactant-Polymer
cm	Centimeter
CaCl ₂	Calcium chloride
CDC	Capillary desaturation curve
CFB	Central fault block
CMC	Critical micelle concentration (wt%)
CLS	Calcium lignosulfonate
CO ₂	Carbon dioxide
cP	Centipoises
G	Free energy (Nm)
dP	Differential pressure (psi)
DIN	Deutsches Institut für Normung
EOR	Enhance oil recovery
FAWAG	Foam assisted water alternating gas
ft/d	Foot per day
f _w	Fractional flow of water
G	Gibbs free energy (Nm)
g/mol	Grams per mole
gmol/L	Gram mole per liter
h*	Critical thickness
ISO	International Standardization Organization
in	Inches
IFT	Interfacial tension (mN/m)
k	Permeability (mD)
KI	Potassium iodide

L	Length (cm)
M	Mobility
MRF	Mobility reduction factor
mm	Milli meter
mD	Milli Darcy
mN/m	Milli newton per meter
MPa	Mega pascal
mPa.s	Milli pascal second
m/s	Meter per second
N_c	Capillary number
NC	Not critical
N_2	Nitrogen
$Na_2B_4O_7 \cdot 10H_2O$	Sodium tetraborate decahydrate
NaCl	Sodium chloride
Na_3PO_4	Trisodium phosphate
$Na_2P_3O_{10}$	Sodium triphosphate
Na_2SO_4	Sodium sulfate
$NaHCO_3$	Sodium bicarbonate
NPV	Net present value
OD	Outside diameter (in)
O1	Produced oil during secondary waterflooding (cm ³)
O2	Total produced oil during tertiary recovery (cm ³)
O3	Total produced oil (cm ³)
OOIP	Original oil in place (cm ³)
P_A	Pressure in phase A
P_c	Capillary pressure
P_c^*	Limiting capillary pressure
P_{in}	Inlet pressure (psi)
P_{out}	Outlet pressure (psi)
ppm	Parts per million
psi	Pound per square inch

PV	Pore Volume (cm ³)
Q	Flow rate (cm ³ /s)
R	Principal radius
ROIP	Residual oil in place (cm ³)
SAG	Surfactant-alternating-gas
SLS	Sodium lignosulfonate
S _w	Water saturation
S _w [*]	Critical water saturation
S _{wc}	Connate water saturation
S _{or}	Residual oil saturation
TDS	Total dissolved solid
u	Darcy velocity
WAG	Water-alternating-gas
WFB	Western fault block
Π	Disjoining pressure
Π _{vw}	Van der waals pressure
Π _{EL}	Electrostatic pressure
ΔP	Differential pressure (psi)
θ	Contact angle
σ	Interfacial tension (mN/m)
σ _{AB}	Interfacial tension between phase A and phase B
κ	Foam film mean curvature
κ _i	Effective permeability
μ _i	Fluid viscosity (cP)
λ _i	Mobility of phase i
ρ	Density (g/cm ³)

1. INTRODUCTION

1.1 Background

The natural energy of a hydrocarbon reservoir is sufficient to produce only a small fraction of the initial hydrocarbons in place. Remaining oil is trapped as a result of the interplay between viscous, gravity and capillary forces in the porous media. Enhanced Oil Recovery (EOR) refers to the process of extracting oil with the methods other than the conventional mechanisms as shown in Figure 1.1. As indicated in this figure the use of surfactants is a chemical EOR method. The scope of this thesis is to examine the alternating injection of surfactant and gas to improve the microscopic and macroscopic volumetric sweep efficiencies.

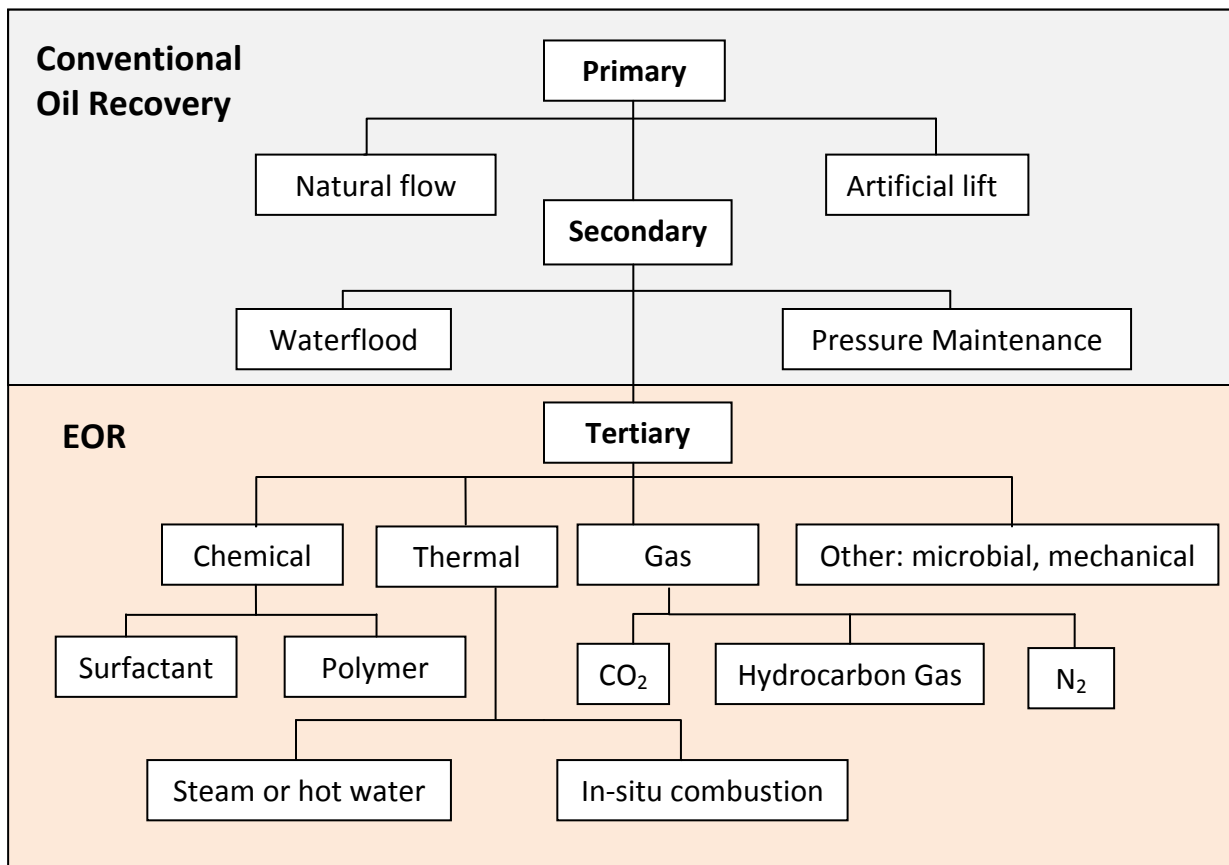


Figure 1.1 Oil recovery mechanisms (Schimdt, 1990)

1.2 EOR Screening Criteria

Taber et al. (1997) proposed enhanced oil recovery screening criteria based on both field results and oil recovery mechanisms. The major considerations for the EOR processes are both the fluid properties and the reservoir characteristics. The screening criteria for SAG injection should contain the criteria for both enhanced waterflooding and gas injection.

Table 1.1 Summary of screening criteria for EOR methods (after Taber et al., 1997)

	Oil Properties		Reservoir Characteristics				
EOR Method	Gravity (°API)	Viscosity (cP)	Oil Saturation (%PV)	Formation Type	Average Perm. (mD)	Depth (ft)	T (°F)
Gas Injection Methods (Miscible)							
N ₂	> 35	< 0.4	> 40	Sandstone/ Carbonate	NC	> 6000	NC
Hydrocarbon	> 23	< 3	> 30	Sandstone/ Carbonate	NC	> 4000	NC
CO ₂	> 22	< 10	> 20	Sandstone/ Carbonate	NC	> 2500	NC
Immiscible gases	> 12	< 600	> 35	NC	NC	> 1800	NC
Enhanced Waterflooding							
Micellar, Polymer, ASP	> 20	< 35	> 35	Sandstone	> 10	> 9000	> 200
Polymer flooding	> 15	< 150, > 10	> 50	Sandstone	> 50	< 11500	> 100
Thermal/Mechanic							
Combustion	> 35	< 5000	> 50	Sandstone	> 50	< 11,5000	100
Steam	> 8	< 200,000	> 40	Sandstone	> 200	< 4500	NC
Surface Mining	7 to 10	Zero Cold flow	> 8 wt% sand	Mineable Tar sand	NC	> 3:1 Overburden to sand ratio	NC

NC: not critical

1.3 Principles of Enhanced Oil Recovery (EOR)

The main goal of any EOR process is to increase oil recovery by reducing the mobility ratio and/or increasing the capillary number.

1.3.1 Improving Mobility Ratio

Effective permeability (κ_i) is a measure of the conductance of a porous medium for one fluid phase when the medium is saturated with more than one fluid. The Mobility of phase i (λ_i) is the effective permeability (κ_i) of that phase divided by its viscosity (μ_i).

$$\lambda_i = \frac{\kappa_i}{\mu_i}. \quad (1)$$

Mobility ratio (M) is defined as the mobility of the displacing fluid over the mobility of displaced fluid. For maximum displacement efficiency, $M \leq 1$ is a favorable mobility ratio.

$$M = \frac{\lambda_{\text{displacing fluid}}}{\lambda_{\text{displaced fluid}}}. \quad (2)$$

If $M > 1$, such as when the viscosity of the displacing fluid is much lower than the displaced fluid, the displacing fluid, will flow past the displaced fluid and viscous fingering will occur.

The mobility ratio M can be reduced by:

- Decreasing the viscosity of the displaced fluid (oil),
- Increasing the viscosity of displacing fluid,
- Increasing the effective permeability to oil,
- Decreasing the effective permeability to the displacing fluid.

1.3.2 Increasing Capillary Number

The saturation of the remaining oil in the reservoir is a function of the capillary number (N_c), which is usually defined as the ratio of viscous to capillary forces

$$N_c = \frac{\text{Viscous Forces}}{\text{Capillary Forces}} = \frac{u\mu}{\sigma\cos\theta} \quad (3)$$

where u is the Darcy velocity (m/s), μ is the viscosity of the displacing fluid (mPa.s), θ is the contact angle between the oil-water interface and the rock surface, and σ is the interfacial tension (mN/m) between the displacing and displaced fluids.

As the capillary number increases, the oil displacement efficiency also increases. It was reported that three orders of magnitude increase in capillary number will result in recovery of 50% of the oil from waterflooded reservoir and an increase of four orders of magnitude is required to displace 100% oil from a core (Donaldson et al. 1989).

The overall efficiency of an EOR process is a function of both microscopic and macroscopic sweep efficiency. The microscopic sweep efficiency depends on the interfacial interactions including interfacial tension and dynamic contact angle while macroscopic efficiency is influenced by density of the fluids and rock heterogeneity.

1.4 Research Objective and Scope

Most of previous research conducted in the area of surfactants has focused on their ability to lower IFT while largely disregarding the wettability effects. Three to four orders of magnitude reduction in interfacial tension would be required to improve the recovery of residual oil. Earlier literature (discussed in chapter 2) addressed the issue of nonionic surfactants failure to achieve

ultralow interfacial tension, and whether they could be used effectively to recover residual oil in surfactant flooding. In reservoirs containing harsh brine anionic surfactants will precipitate but nonionic surfactants remain soluble with a high resistance to precipitation which makes them good candidates for consideration in real reservoirs. In this study, nonionic surfactants and gas are injected in alternating mode and their abilities to generate in-situ foam and alter the wettability of Berea sandstone rock to improve oil recovery are investigated. The objectives of this experimental study are to examine and compare two nonionic surfactants and find the optimal experimental surfactant enhanced water-alternating-gas (SAG) injection conditions for recovery efficiency using different tests including two foam stability tests, interfacial tension and wettability measurements and coreflooding experiments. This research is directed toward the study of the effects of surfactant type (Ivey-Sol 108 and TX-100), surfactant concentration (CMC and 0.3 wt% + CMC), brine salinity (7000 ppm and 21000 ppm TDS), injection scheme (Surfactant-Gas-Surfactant and Gas-Surfactant-Gas) and the addition of sacrificial adsorption agent on SAG process at selected reservoir conditions in a Berea sandstone.

1.5 Thesis Organization

The thesis is organized into five chapters. This chapter includes some background. Chapter 2 reviews the literature. Chapter 3 describes the experimental apparatus and procedure. In order to accomplish the proposed objectives, coreflooding experiments, static and dynamic foam stability tests, interfacial tension and contact angle measurements have been completed. Coreflooding experiments were conducted using a 1 ft Berea sandstone core, Hibernia crude oil as the oleic phase and different surfactant solutions at various concentrations with different salinity brines as the aqueous phase, along with pure N₂ as the injecting gas. The recoveries were calculated in

each experiment to evaluate the effect of selected factors. The results and discussion are presented in chapter 4. Chapter 5 comprises conclusion and recommendations for the future.

2. LITERATURE REVIEW

Enhanced oil recovery (EOR) refers to all the processes (other than waterflooding) in which energy and chemicals are used to establish pressure gradients, reduce interfacial tensions or the mobility of the driving fluid, and alter the permeability of selected zones in order to increase oil production (Boon, 1984).

The current challenges in gas injection as an EOR method are flow of gas in high permeability portions of heterogeneous rock (Figure 2.1C), density contrast between gas and oil which causes gravity override where a less dense fluid flows on the top of a reservoir unit (Figure 2.1A), and viscosity contrast between gas and oil causes viscous fingering where the interface of oil and gas bypasses sections of reservoir as it moves along, creating an uneven, or fingered, profile in the reservoir (Figure 2.1B). A potential solution to overcome these problems is foaming of the gas, which was first proposed by Bond and Holbrook in 1958. Possible effects of foam on overcoming gravity override, viscous fingering and flow in high permeability zones are illustrated in Figure 2.1A to 2.1C respectively.

One method to generate foam is to alternate the injection of gas and surfactant solution (SAG) into the reservoir. The higher microscopic efficiency of the gas (the fraction of oil which is recovered in the swept part of the reservoir) combined with the higher macroscopic vertical sweep efficiency (the fraction of total reservoir which is swept) of the water can significantly improve the total efficiency of the process, as compared to pure gas or water injections. Moreover, the addition of surfactant to the water phase adds potentially two benefits to the water cycle; a reduction in the interfacial tension of the oil-water interface and the wettability alteration of the rock.

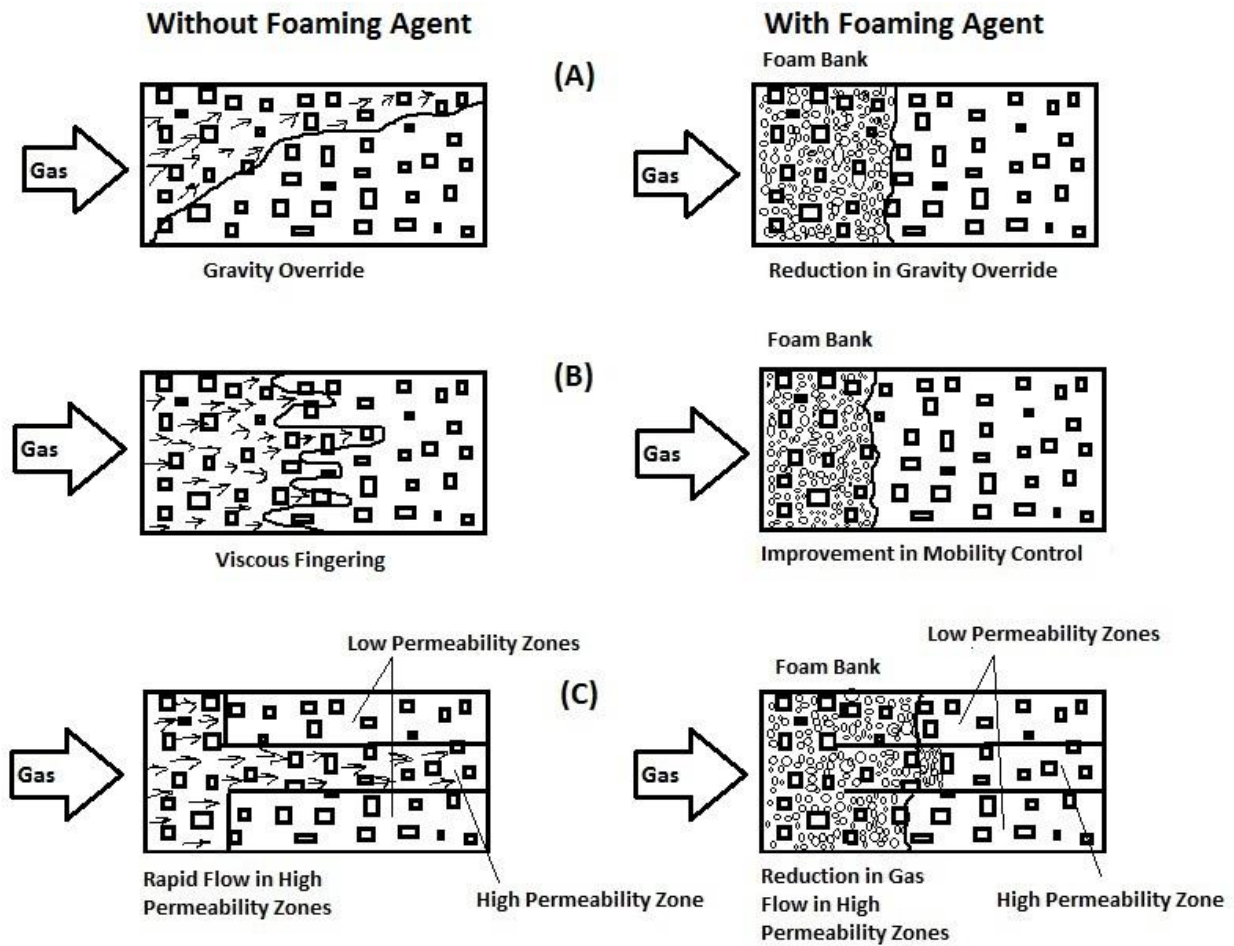


Figure 2.1 Possible effects of foam on the transport of gas in porous media, (A) Gravity override, (B) Viscous fingering, and (C) Flow diversion to low permeability zones (after Sharma et al., 1986)

2.1 Interfacial Tension

Interfacial tension (σ (N/m)) is defined as the change in Gibbs surface free energy (dG (Nm)) per change in area (dA (m^2)):

$$\sigma = \frac{dG}{dA} . \quad (4)$$

The pendant drop method, which is used to determine the interfacial tension, is based on the Young-Laplace equations. The general Young-Laplace equation is given as:

$$P_c = P_A - P_B = \sigma_{AB} \left(\frac{1}{R_1} + \frac{1}{R_2} \right) \quad (5)$$

where the capillary pressure (P_c) is the pressure difference between the pressure in phase A (P_A) and the pressure in phase B (P_B), σ_{AB} is the surface/interfacial tension between phase A and phase B, and the two principal radii, R_1 and R_2 , are orthogonal and tangent to the surface.

2.2 Wettability

The wettability of a surface shows the tendency of a liquid to spread on, or adheres to (wet), a solid substrate or surface. The wettability of a porous medium plays an important role in determining the displacement effectiveness of injected fluids and ultimate oil recovery. Homogeneous wettability is classified into three categories namely water-wet, oil-wet, or intermediate-wet, and the heterogeneous state of wettability is referred to mixed-wet. As is shown in Figure 2.2 contact angle determines the wettability of the rock. A reservoir is water-wet when the contact angle between the rock and an oil drop on the rock surface is less than 90° . An oil-wet rock has an angle greater than 90° and intermediate-wet creates the angle of 90° .

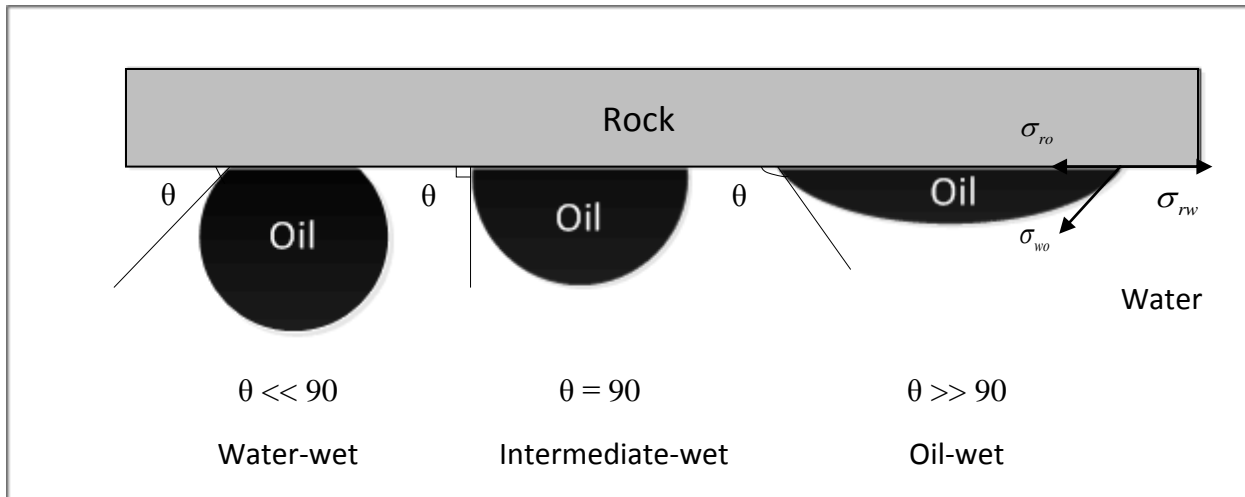


Figure 2.2 Three possible states of wettability in oil reservoirs

In mixed wettability condition some parts of the pore surface are water-wet and others are oil-wet. The generally accepted theory is that the small pores are occupied by water and are water-wet, while larger pores are more likely oil-wet and have a continuous path (Salathiel, 1973).

Thomas Young (1829) proposed treating the contact angle of a liquid with a surface as the mechanical equilibrium of a drop resting on a plane solid surface under restraints of three surface tensions. σ_{wo} (at the interface of water and oil), σ_{ro} (at the interface of rock and oil) and σ_{rw} (at the interface of rock and water) (Figure 2.2).

$$\sigma_{ro} + \sigma_{wo} \cos(180 - \theta) - \sigma_{rw} = 0 \quad (6)$$

Complete wetting is when $\theta = 180$, thus

$$\sigma_{ro} + \sigma_{wo} = \sigma_{rw} \quad \text{OR} \quad \sigma_{wo} \leq \sigma_{rw} \quad \text{OR} \quad \sigma_{\text{adhesive}} \leq \sigma_{\text{substrate}} \quad (7)$$

Effective wetting requires the surface tension of the adhesive to be less than or equal to that of the substrate.

2.3 Surfactant Flooding

The purpose of surfactant flooding is to recover the capillary trapped oil after waterflooding by reducing interfacial tension between the oil and water. The oil bank is generated due to the coalescence of trapped oil droplets.

2.3.1 Surfactant Structure

A surfactant molecule has a hydrophobic hydrocarbon chain and a hydrophilic head group resulting in the adsorption of a surfactant molecule at an interface. This leads to a reduction in surface or interfacial tension and an alteration in the wettability of the surface. Surfactants are generally classified into four different groups according to the presence of formally charged hydrophilic groups in its head including (I) anionic, (II) nonionic, (III) cationic, and (VI) zwitterionic.

A micelle is an aggregate of surfactant molecules dispersed in a liquid colloid. The critical micelle concentration (CMC) denotes the surfactant concentration over which surfactant molecules associate to form micelles and surfactant solution shows an abrupt change in physicochemical properties (Moroi, 1992). Figure 2.3 shows a schematic of a surfactant molecule and a typical micelle structure. As illustrated in Figure 2.3 when a micelle forms in aqueous solution above the CMC, the surfactant monomers aggregate (self-assemble) with the tails inside the micelle shielded from water and the heads at the micelle surface in contact with water.

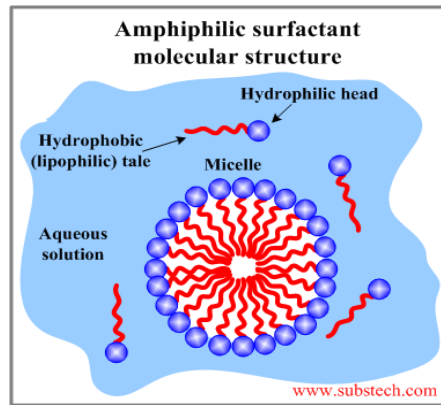


Figure 2.3 Schematic of a surfactant molecule and micelle structure (Kopeliovich, 2013)

Nonionic surfactants in surfactant-alternating-gas (SAG) injection may be better suited for reservoirs with high total dissolved solids, since the ions in ionic surfactants can form precipitate phases causing the surfactant to become insoluble (Verkruyse et al., 1985).

2.3.2 Capillary Desaturation Curve

The shape of trapped oil (non-wetting phase) droplet in a capillary tube is shown in Figure 2.4.

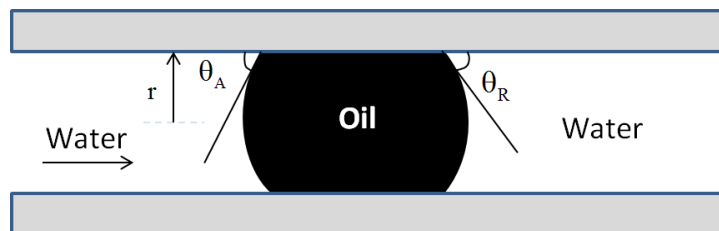


Figure 2.4 Schematic of trapped oil droplet in a capillary tube

A pressure gradient should exist along the trapped oil to displace it from left to right (Chatzis, 2003). i.e.,

$$\Delta P_{\text{mobilization}} \geq \frac{2\sigma}{r} (\cos \theta_R - \cos \theta_A). \quad (8)$$

This illustrates when the interfacial tension between water and oil is reduced by surfactants the minimum pressure gradient to move the oil droplet will decrease.

The relationship between residual oil saturation (immobile oil saturation after conventional (gas or water displacement) and capillary number is illustrated with the Capillary Desaturation Curve (CDC) which varies with wettability and pore-size distribution. As is shown in Figure 2.5, residual oil saturation starts to drop when pore sizes become narrower at high capillary numbers (N_c). At low capillary numbers ($< 10^{-6}$) and high capillary numbers ($> 10^{-3}$) reservoirs with a wide pore-size distribution have the higher residual oil saturation. In Figure 2.6 the wetting phase is shifted to the right of CDC of the non-wetting phase by two orders of magnitude implying that the surfactant flood should have higher efficiency in water-wet reservoirs.

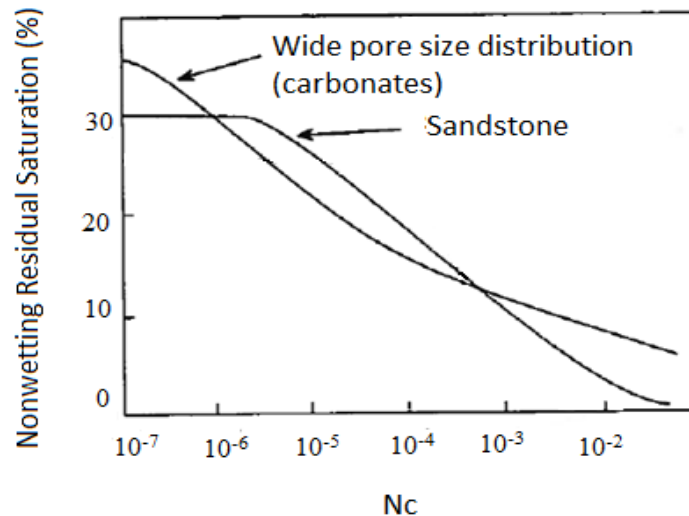


Figure 2.5 Effect of pore-size distribution on the Capillary Desaturation Curve (CDC), (Skjæveland and Kleppe, 1992).

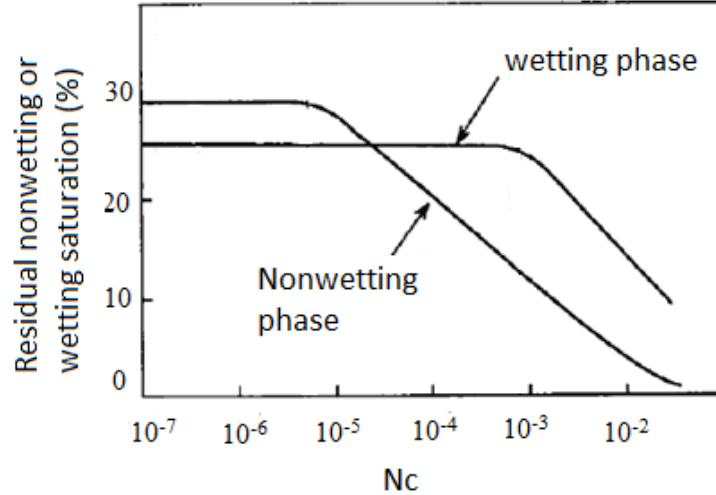


Figure 2.6 Effect of wettability on the residual saturation of wetting and non-wetting phase (Skjæveland and Kleppe, 1992).

2.4 Surfactant-Alternating-Gas (SAG) Flooding

The goal of surfactant-alternating-gas flooding is to benefit from the advantages of both surfactant and gas flooding by alternating the injection of both. As it is illustrated in Figure 2.7A and 2.7B water-alternating-gas injection can improve sweep efficiency compared to continuous gas injection, but the recovery is still affected by gravity segregation and reservoir heterogeneity. The addition of surfactant with foaming ability to the water cycle can reduce the mobility of the gas phase, which will reduce channeling, viscous fingering, and gravity override (Figure 2.7C). Donaldson and Chilingarian (1989) reported that foam increases the trapped gas saturation in porous media. As gas saturation increases, oil saturation decreases; furthermore, a high trapped gas saturation would result in a higher pressure gradient and usually would reduce gas mobility.

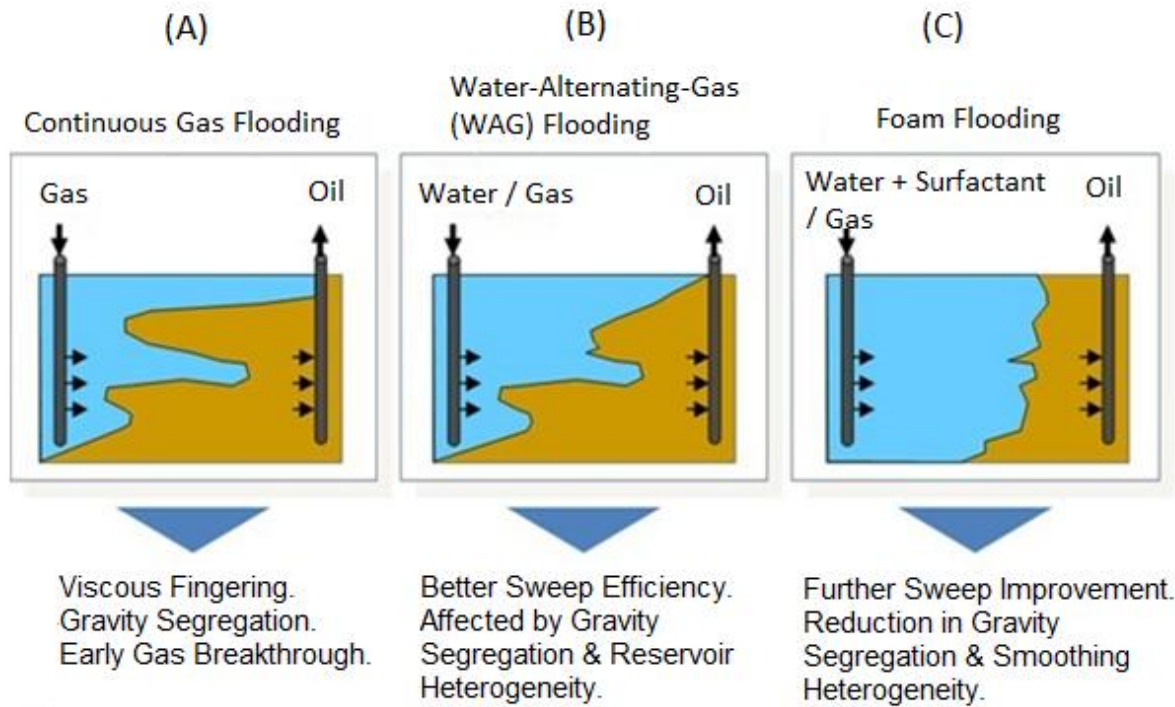


Figure 2.7 Comparison of gas, WAG and SAG injections (after The EOR Alliance, 2014)

2.5 Foam Principles

Foam is generated when gas is dispersed into a continuous liquid phase. The gas is the discontinuous phase organized in gas bubbles. The bubbles contact each other by thin liquid films, called foam films or lamella. The foam films are in direct contact with the liquid phase and the neighboring foam films via plateau borders. A plateau border is the connection point of three lamellas, at an angle of 120° . A 2D schematic of foam structure is shown in Figure 2.8. In three dimensions, four Plateau borders meet at a point at the tetrahedral ($\sim 109^\circ$) angle. Surfactants prevent the bubble from coalescence (Schramm and Wassmuth, 1994).

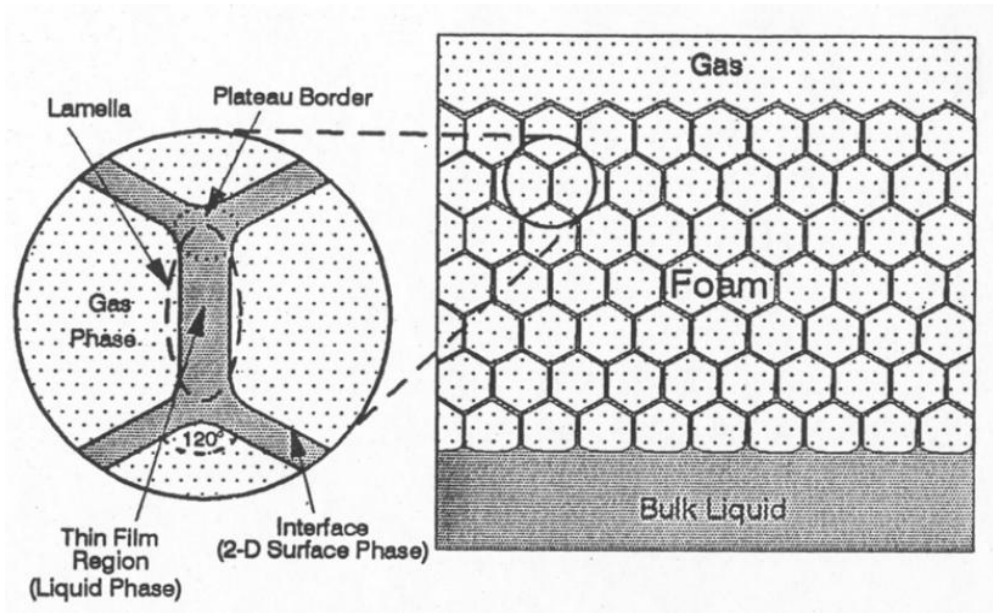


Figure 2.8 Illustration of foam system in 2D (Schramm and Wassmuth 1994)

Foam can vary based on multiple factors (Marsden et al., 1967):

1) *Foam quality* is defined by the volume of gas over the volume of liquid present; Wet foam exists when the foam quality is below 0.5 and spherical gas bubbles move with little restriction from adjacent bubbles. When the foam quality is greater than 0.5, the foam is considered dry and bubbles have less freedom. A foam quality greater than 0.75 indicates that the bubbles are crowded and no spherical shape is observed. Foam quality depends on the surfactant type and the method of foam generation.

2) *Foam texture* describes the bubble size and bubble size distribution, which depends on the surfactant type, foam generation method, and foam quality. Bubble size will decrease with an increase in surfactant concentration or a decrease in foam quality.

3) *Foam rheology* describes foam behavior as a non-Newtonian fluid. Foam true viscosity is difficult to quantify due to the coalescence rate, and in porous media, the regeneration rate. It is

common to express foam in terms of foam mobility, calculated from Darcy's law, and defined as the ratio of effective permeability to apparent viscosity which is defined as the shear stress applied to a fluid divided by the shear rate.

2.6 Foam Generation Mechanisms

Based on visual observation, there are three well-known foam generation mechanisms: snap-off, lamella-division, and leave behind.

2.6.1 Snap-off

When a gas bubble penetrates into a pore and expands, the capillary pressure decreases, which causes a pressure gradient in the liquid phase leading to flow from the surrounding liquid into the pore throat. If the capillary pressure drops below a critical value, the liquid will snap off a gas bubble (Ransohoff and Radke, 1988). The snap-off mechanism is illustrated in Figure 2.9. This process will repeat only if sufficient liquid is present and if the interfacial curvature at the pore throat is larger than the curvature in the surrounding pores (Kovscek and Radke, 1996, 2003). This is the only foam mechanism that is completely mechanical and that may occur in the absence of surfactant. The role of the surfactant is to stabilize the developed bubble and prevent it from coalescing (Kovscek and Radke, 1994).

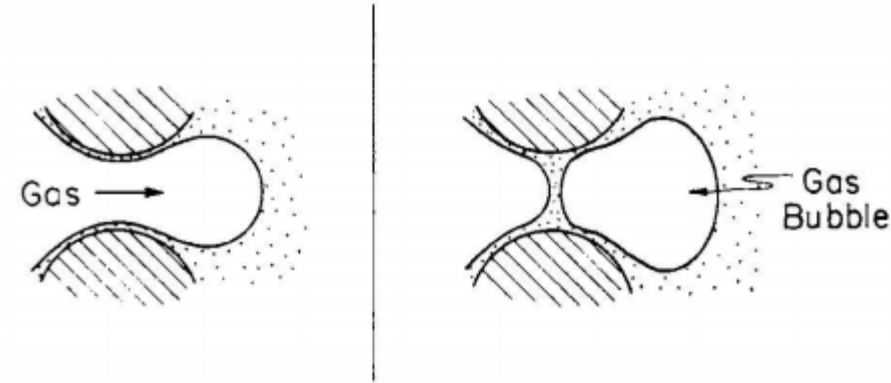


Figure 2.9 Schematic of snap-off mechanism (Ransohoff and Radke 1988)

2.6.2 Lamella-division

Lamella division occurs when one pre-existing bubble or lamella splits into two separate ones at branch points in porous media due to the capillary forces; in other words, some type of lamella generation must have already occurred (Ransohoff and Radke, 1988). The lamella division mechanism is shown in Figure 2.10. The frequency of this mechanism depends on: branch points, bubble sizes, and local capillary pressure fluctuation (Kovscek and Radke, 1994).

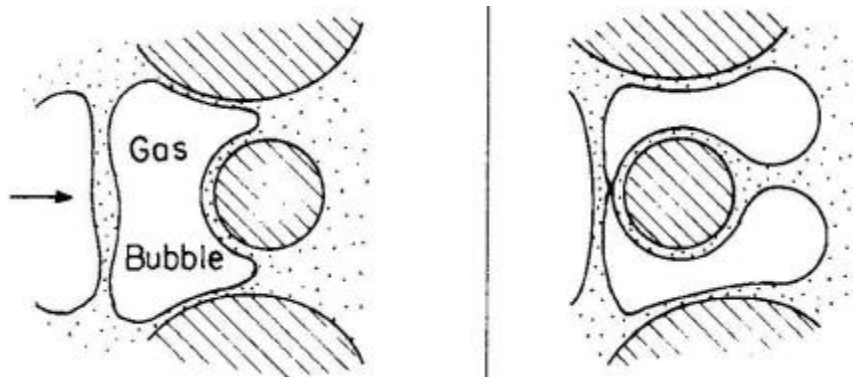


Figure 2.10 Lamella division mechanisms (Kovscek and Radke, 1994).

2.6.3 Leave-behind

The leave-behind mechanism, which is shown schematically in Figure 2.11, occurs when two non-wetting phase fronts approach the same wetting phase filled pore from different directions

leaving behind wet surfaces that may bridge together to form lamella. This method contributes the lamella created by leave-behind mechanisms, which may reduce gas permeability by blocking flow paths to gas.

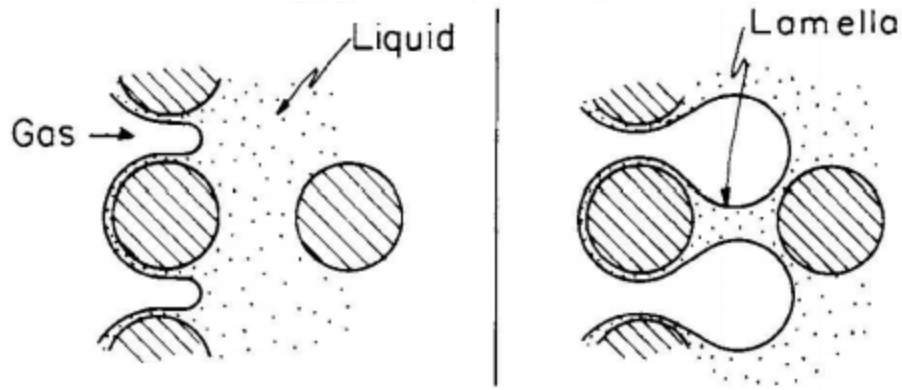


Figure 2.11 Leave-behind lamella generation mechanism (Kovscek and Radke, 1994).

2.7 Mobility Reduction Factor (MRF)

The mobility reduction factor (MRF) is a factor to characterize the strength of generated foam and it is defined as:

$$\text{MRF} = \frac{\Delta P_{\text{foam}}}{\Delta P_{\text{no foam}}} \quad (9)$$

ΔP_{foam} and $\Delta P_{\text{no foam}}$ are the measured differential pressure across the porous media with and without foam respectively. A high differential pressure indicates the presence of strong foam inside the core. A sustained MRF and differential pressure trend can be attributed to the stability of the foam (Shafian et al., 2013).

2.8 Foam Destruction

The efficiency of a foam-assisted EOR process depends on the stability and regeneration rate of foam. The foam needs to be stable in order to affect oil recovery by stabilizing the displacement process, blocking the high permeability zones and diverting the fluid into unswept zones. The stability of the foam films are influenced by many factors such as surfactant type, surfactant concentration, salinity, gravitational drainage, adsorption kinetics, gas diffusion through foam films, capillary pressure, mechanical fluctuations, and surface forces (Kornev et al., 1999).

2.8.1 Foam Disjoining Pressure

The foam films are thin free standing layers of aqueous solution surrounded by gas from both sides. A schematic of a foam film is illustrated in Figure 2.12. Foam disjoining pressure (Π) is the film thickness dependence of the interaction between two film surfaces. According to DLVO theory (Derjaguin and Landau, 1941; Verwey and Oberbeek, 1948), two foam film surfaces will interact with each other and the interaction is the combination of repulsive electrostatic pressures (Π_{EL}) and attractive Van der Waals (Π_{vw}) pressures due to the existence of an electric double layer which appears on surface of liquid film.

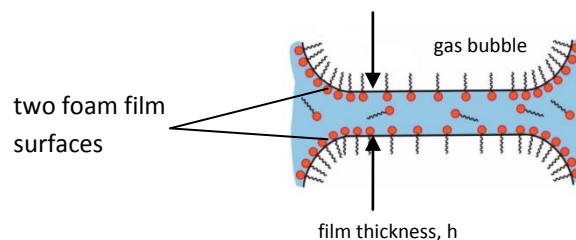


Figure 2.12 Schematic of a foam film

Highly negative disjoining pressure indicates strong negative attractive forces between two film surfaces that make foam film unstable, whereas positive repulsive forces make foam film stable. These two pressures act on the film surface and balance the capillary pressure. At equilibrium (quasi-static situation) the disjoining pressure of foam film equals the capillary pressure, i.e.

$$\Pi = \Pi_{EL} - \Pi_{vw} = P_c = 2\sigma\kappa \quad (10)$$

where σ is the gas/water interfacial tension and κ is its mean curvature (Farajzadeh et al., 2012). Typically, equilibrium is reached for aqueous films of thickness 20 to 100 nm (Mysels et al., 1959 and Bergeron 1999).

If $\Pi_{EL} > \Pi_{vw} + P_c$, the film surfaces are well apart and the foam film is stable but if $\Pi_{EL} < \Pi_{vw} + P_c$, the two foam film surfaces are in contact and the foam film is unstable. The strength of the electrostatic component of the disjoining pressure depends on the concentration of electrolytes in the aqueous phase and the density of the charges on the gas/liquid interfaces. The disjoining pressure varies with salinity, surfactant type and concentration (Farajzadeh et al., 2012).

2.8.2 Limiting Capillary Pressure

Khatib and Hirasaki (1988) reported the existence of a limiting capillary pressure, above which coalescence occurs. The limiting capillary pressure depends on the saturation of the wetting phase and rock properties. Figure 2.13 shows the presence of limiting capillary pressure and the relationship between disjoining pressure and foam thickness.

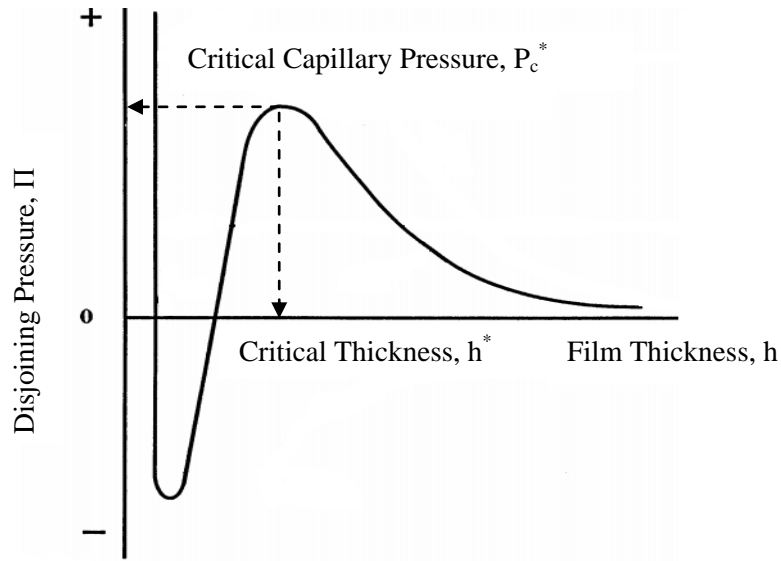


Figure 2.13 The disjoining pressure as a function of film thickness showing the presence of limiting capillary pressure (P_c^*) (after Afsharpoor, 2009)

A typical plot of capillary pressure is illustrated in Figure 2.14. The magnitude of the capillary pressure increases as the saturation of the wetting phase decreases. Since the lamella in porous media is considered to be flat, the imposed capillary pressure on foam films residing in pore throats is balanced with the disjoining pressure. Therefore, if the capillary pressure in porous media exceeds a limiting value, the foam becomes unstable. The limiting capillary pressure (P_c^*) corresponds to the liquid saturation (S_w^*) below which foam films are unstable. The limiting capillary pressure is a function of porous media permeability (hence r), surfactant type, surfactant concentration, electrolyte concentration (affect the contact angle), and foam flow rate (changing the dynamic contact angle at the front and end of the bubble) (Jiménezet and Radke, 1989).

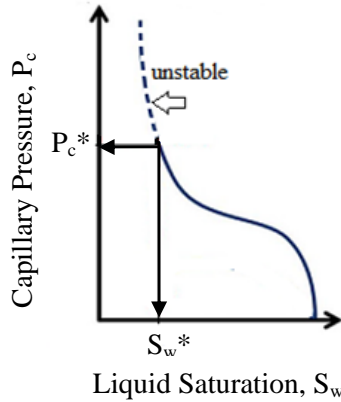


Figure 2.14 Schematic example of gas-liquid capillary pressure in porous media: foam is stable below the limiting capillary pressure (Khatib and Hirasaki, 1988).

Kibodeaux and Rossen (1997) conducted experiments in consolidated porous media, and measured unexpectedly high capillary pressure during foam flow. First, they injected hundreds of pore volumes of brine and then changed the back pressure intermittently between 0 and 100 psig to assure that minimum volume of gas was in the core. For the next step, the back pressure was set at 147 psia and dozens of pore volumes of surfactant solution were injected. Then, gas was injected along with the surfactant solution at the water fractional flow of $0.2 \leq f_w \leq 0.002$. They reported that the water saturation, S_w , decreased and capillary pressure, P_c , increased when the fractional flow of injected water was reduced, down to the point where foam abruptly collapsed. At this point, the limiting capillary pressure, P_c^* , was measured at 12 psi.

Xu and Rossen (2003) presented experimental fractional-flow curves for two surfactant types, Bio-terge AS-40 and Shell NEODOL 91-8, in a Berea sandstone core, in the absence of oil, at high foam quality. They used Berea sandstone and a back pressure of 150 psi in their experiments. To obtain the fractional flow curve, fixed superficial velocities of liquid and gas were injected in incremental steps and the average water saturation was measured by a mass

balance at each step. In their studies, foams were sufficiently stable and persistent for successful SAG process. The fractional flow methods were used to predict displacement behavior on the field scale. A hypothetical field scale 1D displacement was predicted from the data. Foam did not break completely at a single value of S_w . Foam weakened in the fractional flow between $0.037 < f_w < 0.019$, as has been reported in other experimental (Wassmuth et al., 2001) and theoretical (Kam and Rossen, 2002) studies.

In the presence of oil, it has been found that oil penetration, disturbance propagation, and lamellae rupture will cause foam destabilization. Oil may penetrate either by solubilisation or emulsification. Solubilisation occurs only if the surfactant concentration is greater than the critical micelle concentration (CMC) where micelles are present as a structured layer in foam films. This causes the foam films to rupture in a stepwise transition and the rate of film thinning increases with solubilised oil. Moreover, when a gas bubble approaches the interface of two immiscible fluids, a pseudoemulsion or asymmetric film can form. The destabilizing effect of oil depends on the type of oil and surfactant used (Rateman, 1989).

2.9 Factors to be Considered in Designing Foam Flooding Applications

Surfactant capabilities and injection modes are the main parameters that should be considered in designing foam flooding applications. They will be discussed in this section.

2.9.1 Foam Flooding Screening Criteria

Since surfactants are the main components for foam generation, many of the screening criteria are similar to the criteria for surfactant flooding. Two of the important criteria discussed in the literature include low salinity reservoirs, and high permeability, heterogeneous reservoirs

(Sheng, 2011). The presence of oil and very high temperatures (e.g., $> 200^{\circ}\text{C}$) causes challenges to foam stability. Many field applications of foams (discussed in section 2.10) are at low residual oil saturation since oil has a detrimental effect on the foaming ability of surfactants and low residual oil is favorable so that stable foams can be generated (Sheng, 2013).

It has been reported that the most important factors in foam assisted EOR projects are the (a) method of foam injection into the reservoir, which can be as preformed foam, co-injection foam, or surfactant-alternating-gas (SAG) foam, (b) reservoir pressure and (c) permeability. In a steam-foam project, which is a low pressure application (0.7 to 3.5 MPa), foam with the quality in the range of 45 - 80% is used and co-injection is preferred. Injection cycles as short as seven days are common. Under suitable conditions a decrease of 20% in water cut and 6 - 12% increase in recovery of OOIP can be obtained. In high pressure application, such as miscible gas flooding, foam results in high mobility and injectivity reduction (Turta and Singhal, 2002).

Turta and Singhal (2002) classified suitable foam injection mode in Figure 2.15. For a successful foam application, one has to determine the kind of problem to be solved, which of the injection well is causing the problem, and which is the offending well, and whether the foam should be applied at a production well or an injection well. As it is illustrated a suitable method of foam injection is selected according to the desired distance of foam propagation, pressure and permeability of the reservoir. As they suggested for reducing mobility in the reservoirs with the pressure higher than 3 MPa, or in low pressure with permeability less than 200 mD, SAG injection should be used as the method of foam injection.

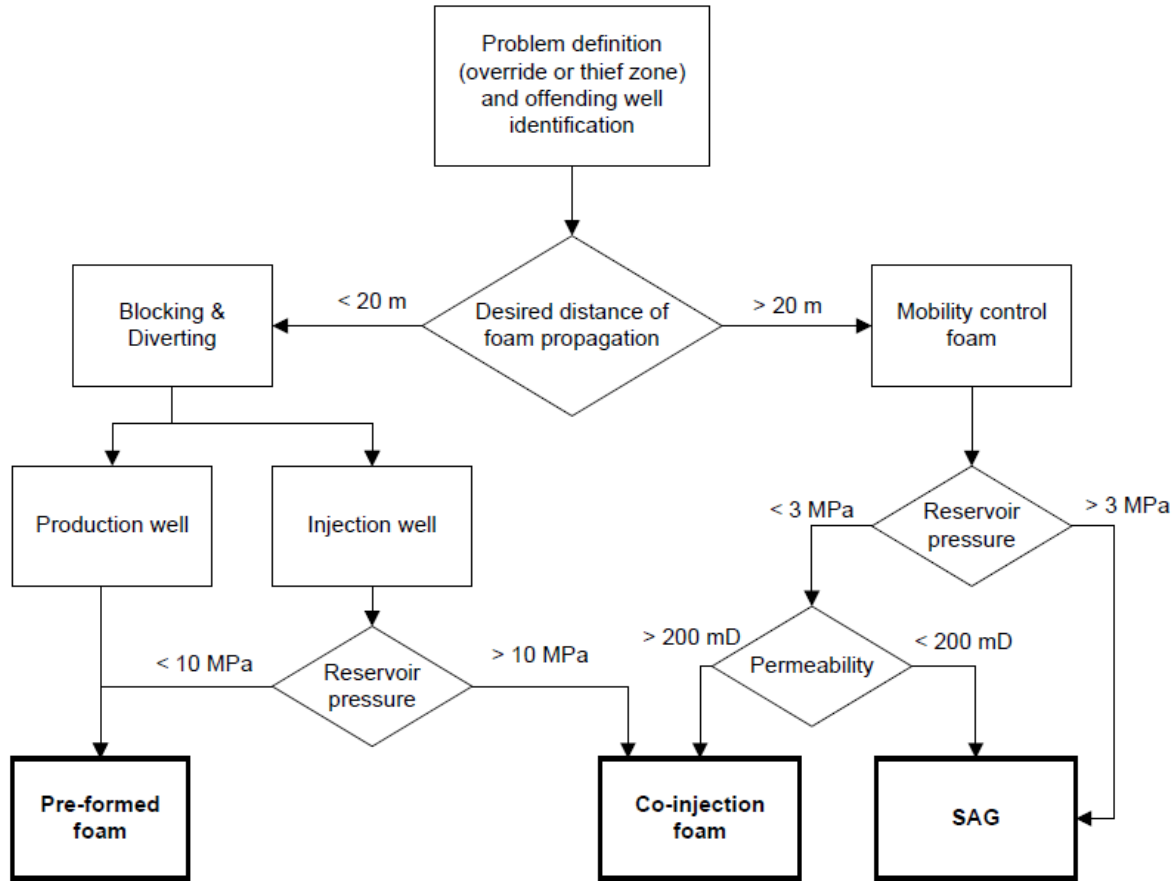


Figure 2.15 Foam selection and placement in EOR projects (after Turta and Singhal, 2002)

2.9.2 Foam Injection Mode

There are three type of foam injection to the reservoirs:

1. *Pre-formed foam* is generated outside the porous medium by using a foam generator at the surface, or during downward flow through the tubing and in the perforations, before entering into the formation.
2. *Co-injection foam* is formed in-situ (near the injector) where surfactant and gas are injected simultaneously into the reservoir.

3. *SAG foam* is generated by alternate injection of surfactant and gas to the reservoir. Foam is produced during drainage of surfactant solution by gas.

SAG injection has several advantages over co-injection in subsurface applications; the pressure build-up during gas injection can be controlled by a specific injection pressure in the SAG process. SAG injection minimizes contact between water and gas in surface facilities, which is important when using acidic gases such as CO₂ (Heller, 1994). It has been reported that alternating injection of a small amount of gas and liquid can improve the foam generation in the near-well region (Rossen and Gauglitz, 1990). SAG has the potential to increase gas injectivity as water is displaced from the near-well region during gas injection, foam weakens, gas mobility rises and injectivity increases (Shi and Rossen, 1998).

2.9.3 Foaming Ability and Foam Stability

Moradi-Araghi et al. (1997) used CO₂-foam in different laboratory experiments to select a suitable surfactant with the best foaming ability and foam stability to use in South Cowden Unit. Four surfactants, Chaser CD-1045, Chaser CD-1050, Foamer NES-25 and Rhodapex CD-128, were evaluated for their foaming properties. According to their experiments, Foamer NES-25 exhibited the best performance achieving 50-60% foam quality while the optimum foam quality for Chaser CD-1045, Chaser CD-1050 and Rhodapex CD-128 that achieved was 70%. They also found that foams produced by co-injection of surfactant and CO₂ produced the best results than those made by SAG process. The performance of the foams produced by the SAG process deteriorated with the slug size.

Shafian et al. (2013) used X-ray to monitor foam generation and propagation in porous media using ROS as the foaming agent. Experiments were carried out on Berea sandstone and reservoir cores and with different surfactant types. A slug of surfactant solution was injected followed by gas prior to co-injection of surfactant and gas (83% foam quality). The results showed efficient mobility control by achieving required MRF in presence of ROS surfactant. The presence of oil, and especially the highly paraffinic crude oil, had a detrimental effect on foaming ability and foam propagation; moreover, they found that moderate MRF are obtained at high flow rate, as in the near wellbore area, and higher MRF are obtained at lower flow rates, which ensure good mobility control and sweep efficiency when the foam propagates within the reservoir.

Wenxiang and Jianhua (2010) used a glass capillary test to evaluate the effects of surfactant type, surfactant texture, alkaline concentration, salinity of brine, temperature and crude oil property on the foaming ability of ORS41, B-100, and a mixture of a nonionic surfactant and B-100. The mixture of nonionic and B100 had the best overall foaming capability. They suggested critical values of surfactant concentration, and alkaline concentration for foam flooding. They found that the foaming ability of the studied surfactants decreased with salinity, temperature and content of light components in crude oil. Of the different surfactant types studied, surfactant included sulfate was superior to the one included sulfonate in foaming ability. For a single type of surfactant, the foaming ability increased with the increase of carbon chain, but decreased when the carbon chain increased to a certain length.

Liave and Olsen (1994) evaluated the application of mixed surfactant foams as an alternative method for mobility control behind a low-concentration chemical flood in laboratory experiments. Their results indicated that even at low concentrations, the use of alternating slug cycles of gas and selected mixed surfactants resulted in significantly higher differential pressures

compared to the individual surfactant components. Foams generated with the specific mixture of surfactants were more stable, even in the presence of oil. The synergistic effect of enhancing foam-generation behavior and stability of these types of systems can improve foam performance in mobility control through porous media.

2.9.4 Adsorption

A surfactant should propagate deeply into the reservoir in order to stabilize foam and reduce the mobility of gas. When a surfactant is adsorbed on the rock surface, the loss of surfactant due to adsorption affects the propagation of surfactant and its effectiveness to stabilize foam films. Many researchers have investigated the mechanisms of surfactant adsorption onto the rock surface and have proposed different approaches to prevent the loss of surfactants, such as the use of a lower cost sacrificial agent.

The application of lignosulfonate, an inexpensive byproduct of the paper industry, as a sacrificial adsorption agent in CO₂-foam, was patented by Kalfoglou et al. in 1997. They reported that since lignosulfonate contains anionic charges it reduced the surfactant adsorption onto their limestone sample by 16 - 35%.

Safarzadeh and Nejad (2011) conducted experiments to evaluate the effect of a sacrificial agent, gas phase and surfactant concentration on the adsorption of sodium dodecyl sulfate (SDS) on silica; moreover, they conducted a series of SAG tests to investigate the effect of surfactant concentration, injection rates, and the presence of calcium lignosulfonate (CLS) as a sacrificial adsorption agent on oil recovery. They found adsorption decreased when using nitrogen rather than methane. They also found that SAG injection increased ultimate recovery up to 10%

compared to WAG injection. The addition of CLS increased the total oil recovery by 2%, while it decreased the adsorption of surfactant by approximately 22% during the SAG test.

Syahputra et al. (2000) conducted coreflooding experiments in a composite core to evaluate the mobility reduction of foam and oil recovery. They showed that lignosulfonate generates strong foam when mixed with other surfactants which resulted in a significant improvement in oil recovery. They reported a reduction in the IFT when an increased lignosulfonate concentration was used in the absence of surfactant. The IFTs of the mixtures of surfactant and lignosulfonate increased with the concentration of lignosulfonate. Lower interfacial tension is favorable to generate more stable foam for lignosulfonate and lignosulfonate/surfactant mixtures. Co-injection of CO₂ and lignosulfonate as a sacrificial agent with various concentrations of surfactant CD1045 resulted in delaying CO₂ breakthrough time in the high permeability region and diverting displacing fluid into the low permeability region which increased oil production. Additives such as a lignosulfonate improved both the oil recovery and economics of the project.

Chiwetelu et al (1980) studied various co-surfactants for use with lignosulfonate-based surfactant solutions to test their ability to improve the oil recovery of pure lignosulfoate solutions. They found that after a cumulative injection of 2.7 PV of brine, a final oil recovery of 83% was obtained. At 1 wt% lignosulfonate concentration no additional oil was produced, but at 3 wt% and 6 wt% solutions, additional recoveries of 2% and 4% respectively were achieved.

Hong et al (1987) studied injection of ammonium lignosulfonate in the Glenn Pool field located in Oklahoma, United States. A 2 wt% lignosulfonate solution was injected for 10 days. They found that 50% of the injected lignosulfonate was adsorbed and more oil was produced in the test pattern. The low cost lignosulfonate injection was beneficial to oil recovery.

Kuhlman et al (2000) studied the adsorption and propagation of surfactants in Berea cores and reported a reduction in surfactant adsorption onto the rock surface when the surfactant concentration was below CMC. They further concluded that adsorption can be decreased by using a mixture of ethoxylated with ethoxylated sulfonates and by reducing the ethoxylate chain length in alcohol ethoxy sulfonates.

Lawson (1978) examined adsorption of cationic and nonionic and anionic surfactants on sandstones and carbonates. He found that nonionic surfactant adsorption on sandstone was high and relatively insensitive to salinity. Adsorption on carbonates was lower than on sandstone. For anionic surfactants, he found that adsorption isotherms were Langmuirian and multivalent cations were found to increase the adsorption. Salts of large anions and common detergent builder such as Borax ($\text{Na}_2\text{B}_4\text{O}_7 \cdot 10\text{H}_2\text{O}$), sodium triphosphate ($\text{Na}_5\text{P}_3\text{O}_{10}$), and trisodium phosphate (Na_3PO_4) reduce the adsorption of anionic surfactants because the rock surface was rendered inaccessible to surfactant molecule through the adsorption of the large sacrificial adsorbent anions.

Liu et al. (2005) measured the adsorption of Chaser CD-1045 surfactant onto kaolinite and they reported that adsorption increased with salinity for both NaCl and CaCl_2 with the divalent salt system inducing a higher adsorption onto the kaolinite.

2.9.5 Salinity

Many reservoirs contain harsh brine which is not amenable to anionic surfactants. The ability of nonionic surfactants to remain soluble with a high resistance to precipitation in harsh brines makes them good candidates for consideration in real reservoirs (Verkruyse and Salter, 1985). Contrary to this generalization, Liu et al. (2005) reported Chaser CD-1045 as an anionic

surfactant that had excellent foaming ability and high resistance to brine salinity at the concentration of 0.025 wt% or higher.

Brine salinity has been to have a significant effect on the interfacial tension (IFT), reservoir wettability and oil recovery. Saline water is classified into three categories by the US Geological Survey (Perlman, 2014); slightly saline water has around 1000 to 3000 ppm of TDS. Moderately saline water is roughly about 3000 to 10,000 ppm TDS, and highly saline water is in the range of 10,000 to 35,000 ppm TDS. Based on the fact that the proper salinity of dissolved solids in the injection water may yield the highest oil recovery, the application of suitable water salinity is important to improve oil recovery.

Generally, an increase in salinity will result in foam destabilization or, depending on the surfactant, have little effect. High salinity water breaks foam by decreasing the electrostatic double layer forces or by diminishing surfactant solubilisation in brine (Alkan et al., 1991).

Many researchers confirmed that low salinity water (total dissolved solids of less than 2000-8000 ppm) has significant impact on wettability and higher oil recovery based on their laboratory studies conducted over a period of many years. It has also been reported that low salinity effects were observed both in a secondary and tertiary flooding mode (Zheng, 2012).

Tang and Morrow (1999) explained that during low salinity water injection, fines may be washed away resulting in the exposure of primary surfaces that are more water-wet, but during high salinity water injection, fines retain their oil-wet nature resulting in lower sweep efficiency.

Lager et al. (2006) reported that cation exchange between the mineral surface and invading brine is the primary mechanism causing higher oil recovery during low salinity water injection.

Cai et al. (1996) conducted experiments to measure interfacial tension of ten normal-alkanes in water/brine and hydrocarbon mixture in water/brine systems by using the pendant drop instrument under high pressure conditions. They reported that higher salinity had higher interfacial tension and the increase depended on the salinity, but was insensitive to the specific salt and pressure.

Abdel-Wali (1996) added oleic acid to crude oil to investigate the effect of polar compounds, which behavior was like an anionic surfactant, and lowered interfacial tension. The optimum concentration of oleic acid to achieve the lowest interfacial tension was 0.8 wt%. Water salinity in the range of 0 to 200,000 ppm TDS NaCl was used, but the lowest interfacial tension between brine and oil was obtained when the brine salinity was 40,000 ppm TDS. They concluded that the increase in the interfacial tension with increased in brine salinity was the result of a decrease in the level of solubility of oleic acid in brine.

2.9.6 IFT Reduction

Ultra low interfacial tensions e.g. $< 10^{-2}$ mN/m have been shown to be favorable to extract residual oil (Hirasaki et al., 2008). Earlier literature addressed the issue of nonionic surfactants failure to achieve ultralow interfacial tension, and whether they could be used effectively to recover residual oil (Garcias et al., 1982).

Hirasaki et al. (2008) also found that oil-water interfacial tension had to be reduced from 20-30 mN/m to values in the range of 0.001 to 0.01 mN/m to obtain low values (less than 0.05) of residual oil saturation.

Wang et al. (2001) introduced a new type of surfactant by synthesizing the anionic and nonionic surfactants for field use. Their proposed surfactant reduced the interfacial tension to ultralow values (3.36×10^{-3} - 8.39×10^{-3} mN/m) even in high salinity (88,540 - 195,000 ppm TDS) formations.

2.9.7 Wettability of Rock and Wettability Alteration by Surfactants

Boneau and Clappitt (1977) conducted coreflood experiments both in oil-wet and water-wet sandstones with similar permeability and porosity and found that tertiary oil recoveries ranged from 55 - 65% in oil-wet sandstones and 90 - 95% in water-wet sandstones. Since there was three to five times more sulfonate adsorption (surfactant loss) on the oil-wet sandstone than on the water-wet sandstone, this led to a lower amount of oil extraction from the oil-wet system.

Hirasaki and Zhang (2004) reported that sodium carbonate as the alkali and anionic surfactant altered the wettability of their carbonate sample from oil-wet to intermediate-wet or water-wet, which resulted in higher oil recovery in spontaneous imbibitions.

Rao et al., (2006) investigated the effect of surfactant on wettability and relative permeability in coreflood experiments. The high oil recovery (90%) as well as the gradual shifts to the right in relative permeability curves confirm the mixed wettability development due to the nonionic surfactants. The very low residual oil saturations at higher nonionic surfactant concentrations also indicate the development of mixed wettability as the nonionic surfactant concentration is increased.

2.9.8 Thermal Stability

Foam flooding at temperatures above 80°C requires careful design due to the sensitivity of foam stability to temperature. A benefit of formations at high temperature is that the adsorption of

surfactant in the formation will be lower (Ziegler and Handy, 1981). Surfactant solubility in brine will decrease with increased formation temperature. Zhang and Austad, 2005 reported some surfactants successfully used in field applications including ORS-41 and AOS at low temperature (approx. 45°C), and surfactants that can be used in high temperature applications including Stepanflo30, SuntechIV, Dow, Neoden 14-16 and Neoden 16-18 (Shell).

2.10 Foam Field Applications

Eson and Cooke (1989) were the first to review field applications of EOR foams, and later Hanssen et al. (1995) published more advanced EOR foam reviews.

Typical field applications include aqueous foams for improving steam drive and CO₂-flood performance, gelled foams for plugging high permeability channels, foams for prevention or delay of gas or water coning, and SAG processes for cleanup of aquifers. All of these methods have been tested in the laboratory and the field.

Approximately two-thirds of gas foam projects used the SAG injection mode and one-third used co-injection of gas and surfactant (Sheng, 2013).

The first foam field application was conducted in Siggins field, located near Casey, Illinois, from 1964 to 1967 by using air as the gas phase and a surfactant named O.K. Liquid (modified ammonium lauryl sulfate) which was selected between 100 surfactant candidates. The mobility of the surfactant solution was reduced to 35% of its original value because of a reduction in water saturation during foam propagation in SAG injection. The mobility of the injected air was reduced by 50% which mitigated the channeling of air through high permeability zones (Holm, 1970).

The second foam field application was performed in the Wilmington field, located in southern California in 1984. Eight cycles of SAG with 1.0 wt% of Alipal CD-128 surfactant solution and CO₂/N₂ gas were injected in order to divert the flow into the low permeability zones. An increase of 42% of injected gas in the low permeability zones was observed. The mobility of gas was also reduced by propagation of stable foams and the channeling of injected fluids was mitigated effectively (Holm and Garrison, 1988).

The third field application of foam-assisted EOR was performed in the Midway Sunset field, located in the San Joaquin Valley, California, in 1985. AOS-1618TM surfactant solution and nitrogen with steam were injected simultaneously for 40 months. After three years of the start of foam injection the surfactant concentration was reduced from 0.51 wt% to 0.24 wt% to test foam efficiency at lower concentration which was followed by a gradual reduction in oil production. The total incremental oil production was estimated to be 6% of OOIP (Mohammadi and Tenzer, 1990).

Another well-known SAG process was operated in the North Ward-Estes, Texas in 1990. Four cycles of SAG was performed by using Chaser CD-1040, an alpha-olefin sulfonate, as the surfactant solution injection and CO₂ as the gas phase. This foam treatment reduced CO₂ injectivity by 40 – 85% for 1 – 6 months. Based on the injection and production responses foam successfully diverted CO₂ from the thief zone to unswept regions (Chou et al., 1992).

The Snorre field operated by Statoil was the world's largest application of foam in the oil industry, with injection of 2000 tons of commercial grade alpha olefin sulfonate (AOS) surfactant and consisting of three injectivity tests, one full scale SAG test and one full scale co-injection test (Sheng, 2013). The objectives of the field trial of Snorre SAG project were to 1)

increase sweep efficiency during gas injection, 2) increase the storage of gas in the reservoir, 3) reduce the producing GOR in production well P-39. The project was started in 1997 in the central fault block of the Snorre field but because of the fracturing and gas leakages the injection area was moved to the western fault block (Spirov et al., 2012). It was estimated that the SAG treatment could contribute approximately 250,000 Sm³ of oil (\$ 117,933,948 USD at \$ 75 USD/bbl) and the cost of the treatment in the western fault block was approximately \$ 1 M USD (Sheng, 2013).

3. EXPERIMENTAL APPARATUS AND PROCEDURE

Coreflood experiments using Berea sandstone were performed to evaluate and optimize several factors in surfactant-alternating-gas injection using nonionic surfactants and nitrogen gas as the gas phase to generate foam in-situ in all experiments. Hibernia crude oil (33.9 °API) was used as the oil phase. Two levels of brine salinity, two types of surfactant with two levels of concentration were used; furthermore, different injection schemes 1) water-gas-surfactant-gas (WGSG) and 2) water-surfactant-gas-surfactant (WSGS) and the addition of a sacrificial adsorption agent to the secondary waterflooding cycle have been used and compared to evaluate their performance in improving oil recovery, foam generation, IFT reduction and contact angle change.

3.1 Experimental Fluids

According to the US Geological Survey (Perlman, 2014), moderately saline water is roughly about 3000 to 10,000 ppm TDS, and highly saline water is in the range of 10,000 to 35,000 ppm TDS; therefore, two levels of brine salinity (7000 ppm TDS and 21000 ppm TDS) were selected to examine the effect of salinity on oil recovery. The compositions of the two synthetic brines used in the tests are shown in Table 3.1. Deionized water was used to prepare the synthetic brine and surfactant solutions. The surfactant types with their corresponding CMC value, verified by Zubair et al. (2013), and sodium lignosulfonate as the sacrificial adsorption agent (SLS) properties are listed in Table 3.2. The properties of the Berea sandstone used in the experiments are shown in Table 3.3.

Table 3.1 Brine compositions

Composition	Low Salinity Concentration (ppm)	High Salinity Concentration (ppm)
NaCl	5000	15000
Na ₂ SO ₄	500	1500
NaHCO ₃	500	1500
CaCl ₂	500	1500
KI	500	1500
Total Salinity (TDS)	7000 ppm	21000 ppm

Table 3.2 Surfactants and SLS properties

Chemical	CMC (wt%)	Density (g/cm³)
Ivey-sol 108	0.021	1.030
Triton X-100	0.016	1.065
SLS	-	0.5 apparent

Table 3.3 Berea sandstone properties

Dimension	Measured Porosity* (%)	Measured Permeability** (mD)
12'' L * 1.5'' D 30.5 cm L * 3.8 cm D	18.7	58.5 – Brine

* Refer to Appendix B-1

** Refer to Appendix B-2

3.2 Experimental Methods

There are various laboratory tests used to measure the foaming tendency of fluids. These tests (outlined in Table 3.4) include static tests such as pouring, shaking, beating, rotational and stirring and dynamic tests that include: air injection and circulation.

Table 3.4 Foaming assessment methods

Principle	Classification	Method	Standard
Static Methods	Pouring	Ross & Miles Test	ASTM standard D 1173-53
		Modified Ross & Miles Test	ISO standard 696-1975(E)
	Shaking	Bottle Test	ASTM standard D 3601-88
	Beating	Perforated Disk Test	DIN standard 53902 part 1
	Stirring	Blender Test	ASTM standard D 3519-88
Dynamic Methods	Air injection	Diffuser Stone Test	ASTM standard D 892-92
			ASTM standard D 1881-86
		Gas Bubble Separation Test	ASTM standard D 3427-86
	Circulation	Recycling and Fall Test	AFNOR draft T73-421

Abbreviation: ASTM, American Society of Testing and Materials; ISO, International Standardization Organization; DIN, Deutsches Institut für Normung; AFNOR, Association Frances Normalization (Zhang and Austad, 2005).

In this study shaking and air injection tests were used to examine the foaming ability and foam stability of two surfactants at two concentrations.

3.2.1 Dynamic Test (Air Injection)

The air injection method is a common test to determine the foaming tendency of a hydraulic fluid (ASTM D 892). A simplified version of this test was used to measure the foaming properties of the surfactant solutions. The schematic of the set-up is shown in Figure 3.1. It consists of a 1000 cm³ graduated cylinder (meeting specification E1272 class B tolerance

requirement of $\pm 6 \text{ cm}^3$ and at least graduations of 10 cm^3) held in position when placed in the bath, such as fitted with a heavy ring or clamp assembly to overcome the buoyancy, and an air-inlet tube, to the bottom of which is fastened a gas diffuser. The gas diffuser can be either a 25.4 mm (1") diameter spherical gas diffuser stone made of fused crystalline alumina grain, or a cylindrical metal diffuser made of sintered five micron porous stainless steel. The cylinder had a diameter such that the distance from the inside bottom to the 1000 cm^3 graduation mark is $360 \pm 25 \text{ mm}$. It was circular at the top and fitted with stopper. The test bath was a glass cylinder, large enough to permit the immersion of the cylinder at least to the 900 cm^3 mark and capable of being maintained at constant temperature (Figure 3.2). The Neslab RTE-100 water bath was used to maintain a constant temperature in the glass bath cylinder (Figure 3.3). Bath and water shall be clear enough to permit observation of the graduations on the cylinder. Air was injected using an ISCO 500D pump at a constant flow rate (Figure 3.4).

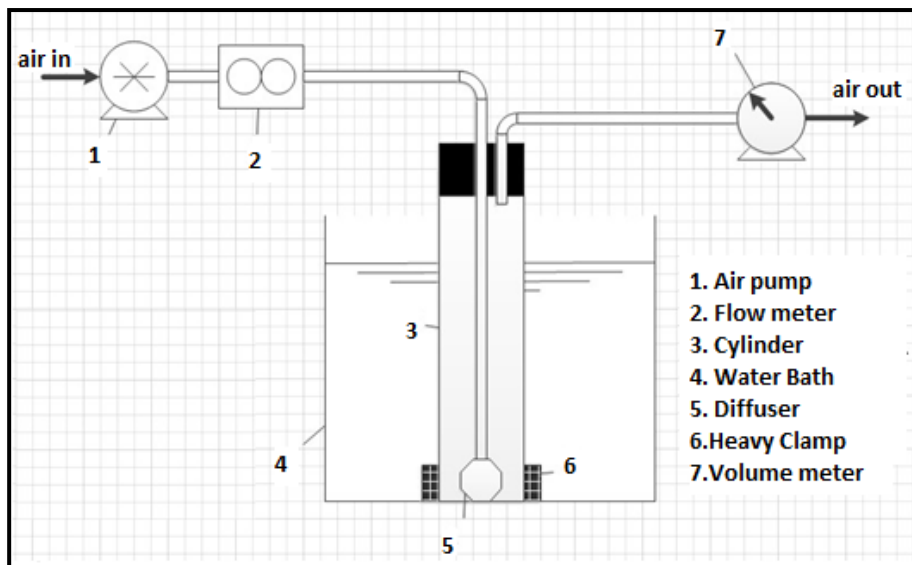


Figure 3.1 Schematic of the air injection foam assessment apparatus



Figure 3.2 Air injection apparatus in the glass bath cylinder



Figure 3.3 Neslab RTE-100 water bath

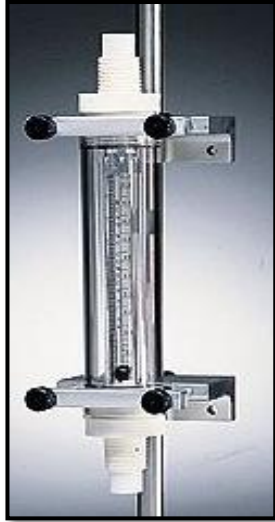


Figure 3.4 Gilmont GF-2160 flow meter

A solution (150 cm^3) was poured into the graduated cylinder and the cylinder was fixed in the glass water bath, then the water bath was filled with distilled water set to the specific test temperature (20°C or 80°C). After reaching the set point temperature in the water bath, air was injected at a constant flow rate of $95 \text{ cm}^3/\text{min}$ according to the ASTM 892 for five minutes. After 15 minutes, the injection was stopped and in the absence of oil foam height/volume was recorded every two minutes and in the presence of 10 vol% oil foam initial height/volume and foam collapse time were recorded (refer to Appendix C-1 for raw data).

3.2.2 Static Test (Bottle Shake)

Bottle Specifications. Clear glass, 16-oz (500 cm^3) Boston round bottles with screw necks were used in the experiments. The 16-oz bottle is $6\text{-}5/8''$ (168 mm) tall and has a maximum diameter of three inches (73.5mm). The outside neck is $1/4''$ (7mm) and the shoulder radius is one inch

(25.4 mm) (see Figure 3.5). A transfer pipette was used to pour a specific volume of the solutions into the bottles and a ruler and stop watch were used to measure the height of foam versus time.



Figure 3.5 Boston Round Bottle

Two hundred cm^3 of each solution was poured into a bottle and the height was measured to the nearest 1 mm of the liquid/air interface. Vigorous shakes were applied to the test sample bottle (approximately 40 shakes in 10 seconds). The initial height of foam was immediately marked and read to the nearest one mm. The bottle was allowed to stand undisturbed and the height of foam was measured and recorded to the nearest one mm every 15 minutes (raw data is presented in Appendix C-1).

For the stability measurement in the presence of oil, as recommended by Zhong et al. (1998), 10% by volume of oil was added into the solution and the experiment was repeated like before but the height was recorded every two – three minutes (refer to Appendix C-1 for raw data).

3.2.3 Lessons Learned in Foam Test

It is essential to clean the test bottles, cylinder, gas diffuser and air-inlet tube after each experiment to remove any additive remaining from previous tests which can seriously interfere with results of subsequent tests. The criterion that the test cylinder is adequately clean is that the interior walls drain water cleanly, without drops forming. One suitable technique for cleaning the gas diffuser and air tube is to first clean the inside of the air tube (disassembled from the gas diffuser) with toluene and then connect them together and immerse the gas diffuser in about 300 cm³ of toluene. It is strongly recommended to flush a portion of the toluene back and forth through the gas diffuser at least five times with vacuum and compressed air.

3.2.4 Interfacial Tension and Contact Angle Measurement

The Vinci IFT 700 apparatus shown in Figure 3.6 can measure the IFT between 0.1 to 72 mN/m. The maximum operating pressure is 69 MPa (10,000 psi) and the maximum operating temperature is 180°C.

Bulk fluid is the fluid where the drop is released and drop fluid is the fluid of the drop; for instance, for a drop of oil inside water; the bulk fluid is the water and the drop fluid is the oil.

The main parts of the apparatus are illustrated in Figure 3.7. Two manual pumps equipped with the pressure gauges control the bulk fluid pressure (BULK) and the droplet fluid pressure (DROP). Temperature is controlled by a PT100 thermocouple sensor and an electrical heater, which is equipped with piezoelectric pressure transducer. The drop shape is detected by a CCD color camera with 1.4 Megapixel resolution and one LED for lighting. The image can be analyzed by the IFT software installed.



Figure 3.6 Vinci Interfacial Tension (IFT 700) apparatus

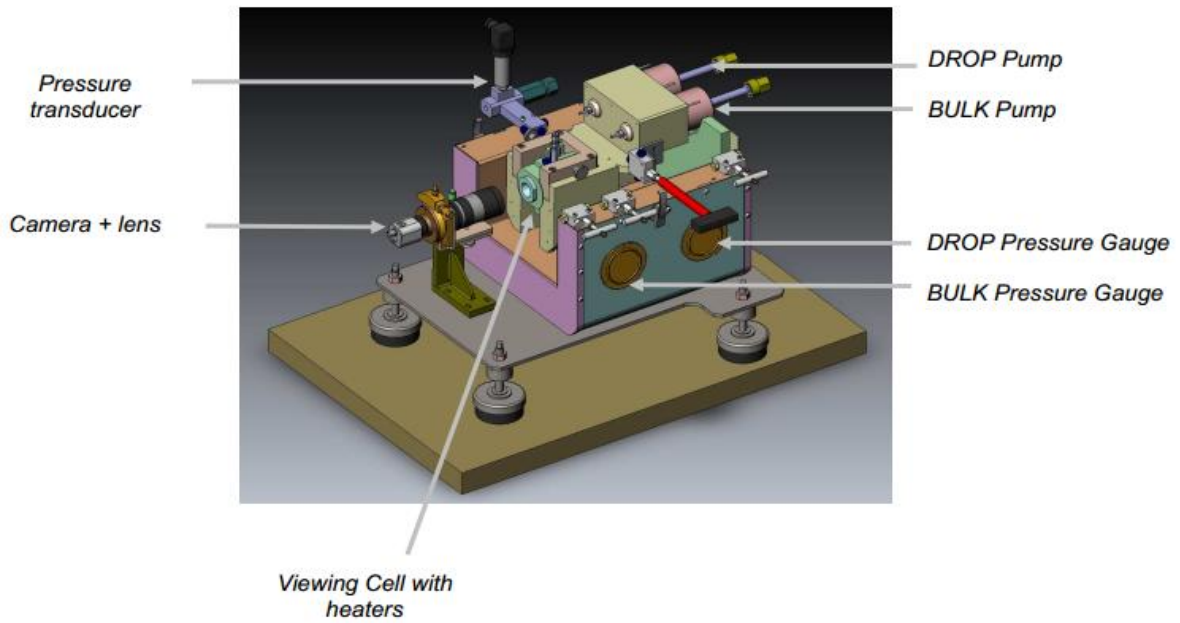


Figure 3.7 IFT apparatus schematic

The Vinci IFT 700 apparatus was used to determine the interfacial tension between liquid-liquid interfaces using the rising drop method as well as the contact angle between liquid and solid interfaces using the sessile up method. In the rising drop and sessile up methods, the drop fluid density is smaller than the bulk fluid density. It means the needle is on the bottom of the cell.

In IFT measurements, an oil drop is created in the presence of brine/surfactant solution as the bulk fluid in a cell at the condition of the coreflood experiments (25°C and 500 psi) and in contact angle measurements the drop is put in contact with the rock surface (raw data in Appendix C-2). A camera connected to a computer records the shape of the liquid drop to derive the interfacial and contact angle properties. The Drop Analysis System software allows the fast calculation of surface and interfacial tension of rising drop and contact angles of sessile drops. New optical calibration is required for the capillary needle each time the lens settings are modified. On the calibration tab of the software, the external diameter of the needle should be inserted.

The results of interfacial tension and contact angle measurements are presented in section 4.3. In both interfacial tension and contact angle tests, each measurement for a single or two drops in some cases was recorded several times for a period of time and based on the raw data presented in Appendix C-2, the mean value of each run was used as the best estimate of the true value (listed in Table 4.2). The standard deviation for each mean value was calculated according to the definitions (Appendix A). A sample calculation is provided in Appendix D-3. The capillary number corresponding to IFT and contact angle for each solution was calculated and listed in Table 4.2. The standard deviation for each capillary number was also calculated according to the error analysis method presented in Appendix A.

3.2.5 Lessons Learned in IFT and Wettability Measurement

The interfacial tension measurement is very sensitive. Incomplete cleaning, traces of any previous samples, dust, etc. would modify the results; therefore, the alternative use of solvent (toluene) and compressed air should be used for cleaning to ensure the IFT system is cleaned prior to sample loading in each run.

3.2.6 Core Cleaning

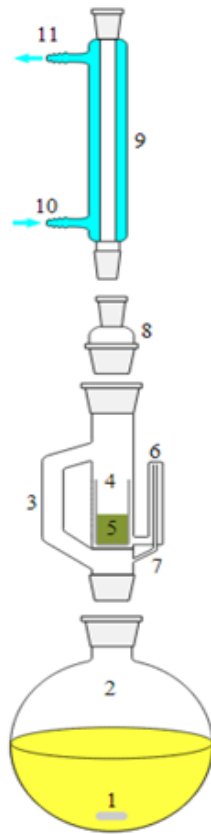
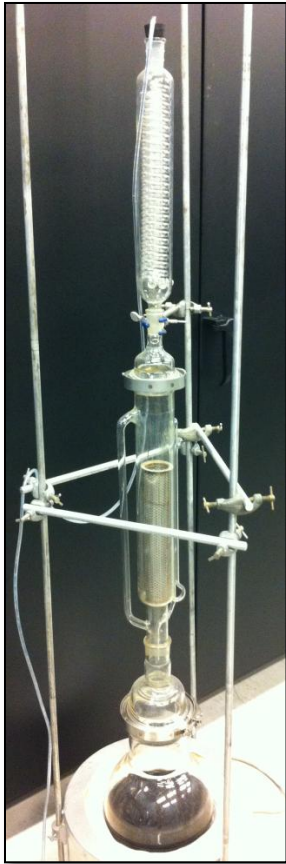
Different methods are used to clean cores and render them to strong water wettability. The most widely used methods are (1) distillation-extraction (Dean-Stark and Soxhlet, 1920), (2) flow-through, (3) centrifuge flushing, and (4) gas-driven solvent extraction (Gant and Anderson, 1986). For our experiments we used the distillation-extraction method.

Distillation-Extraction (Dean-Stark and Soxhlet): This is the most commonly used cleaning method. A schematic of a Soxhlet extractor is shown in Figure 3.8. The rock sample is placed in a soxhlet or Dean-Stark apparatus Figure 3.8(5). The solvent Figure 3.8(1) is heated to reflux. The solvent vapor travels up in the distillation path Figure 3.8(3), and floods into the chamber housing the rock Figure 3.8(5). The condenser ensures that any solvent vapor cools, and drips back down into the chamber. The chamber containing the rock sample slowly fills with the warm solvent. Some of the desired compound dissolves in the warm solvent. When the Soxhlet chamber is almost full, the chamber is drained by the siphon Figure 3.8(7). The solvent is returned to the still pot Figure 3.8(2). This cycle may be allowed to repeat many times, over hours or days until the color of solvent in the rock chamber is clear. The main drawback of this method is that solvent may not contact the entire core, especially the smaller pores. This is the

method that was used in the EOR laboratory to clean the cores after each coreflooding experiment. Core cleaning is mostly a trial-and error process where the selection of the best solvents to be used greatly depends on the experience with particular rocks. Common solvent mixtures are chloroform/methanol, toluene/methanol, toluene/ethanol, benzene, and carbon disulphide, among others. Some mixtures work better for different types of rocks and fluids. Sandstone is known to have a surface of acid type while limestone has a surface of basic type. Because of the surface types of this rock surfaces, acidic solvents tend to clean sandstone better, while basic solvents tend to clean limestone better (Cuiec, 1975). In this study, toluene was used to clean the Berea sandstone.

First, 2000 cm³ of toluene was prepared and placed in the still pot, and then the still pot with the solvent was placed on the heating mantle (Figure 3.9). The reflux core chamber was attached to the still pot. Then, the condenser was attached to the reflux core chamber. The cooling water source was connected to the lower part of the condenser and an outlet hose was connected to the upper part of the condenser.

The heating mantle was turned on in the appropriate setting (depending on the amount and type of solvent being used, here for 2000 cm³ toluene the heater was set on eight) and the reflux process was continued until no more color change was observed in the condensed solvent mixture (this took about three days). See Figure 3.10.



1: Stirrer bar

2: Still pot (the still pot should not be overfilled and the volume of solvent in the still pot should be 3 to 4 times the volume of the soxhlet chamber)

3: Distillation path

4: Thimble

5: Rock sample

6: Siphon top

7: Siphon exist

8: Expansion adapter

9: Condenser

10: Cooling water inlet

11: Cooling water outlet

Figure 3.8 Soxhlet apparatus schematic



Figure 3.9 Fresh toluene in still pot

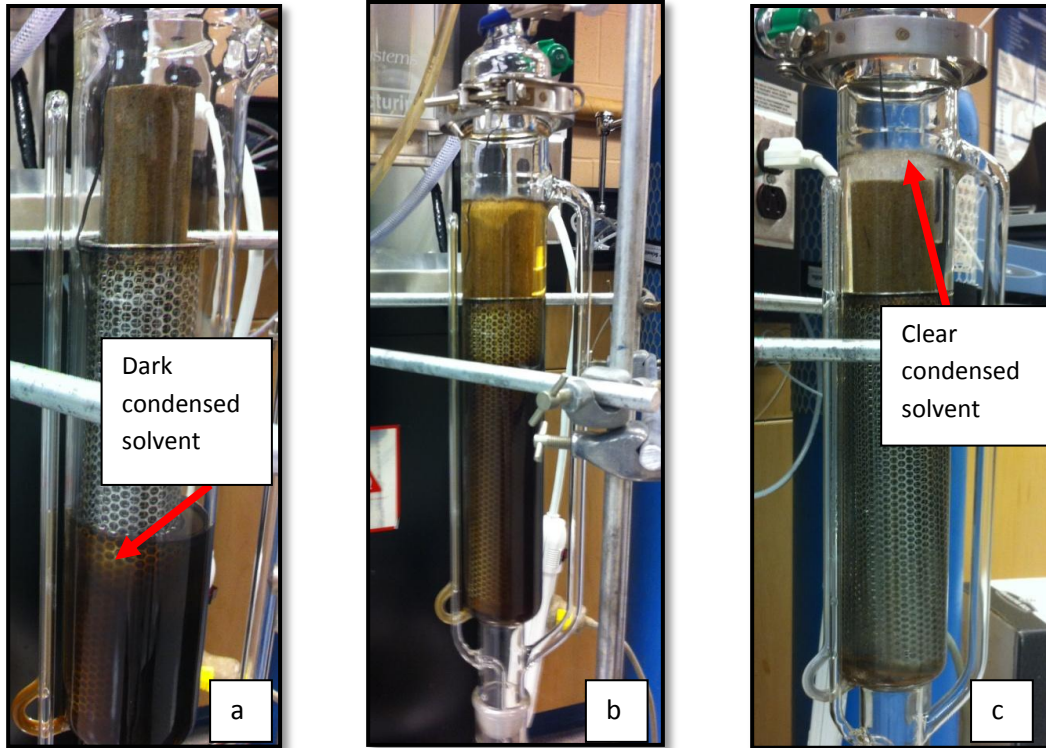


Figure 3.10 Distillation process (a) after 25 minutes, (b) after 45 minutes, (c) after three days

3.2.7 Low Pressure Coreflooding

The low pressure coreflood apparatus was setup to conduct coreflood experiments. A schematic of the apparatus is shown in Figure 3.11 and Figure 3.12 below. It consists of high pressure ISCO 500D pump (1) injection distilled water at desired flow rate or pressure to the bottom part of the custom made floating piston accumulators (2). The accumulators are filled with the fluid (brine/surfactant and oil) to be injected into the core held in a Vinci TRC coreholder (5). The exception was nitrogen, where the pump was used to directly inject gas to the core. Low pressure steel tubing (1/8" OD) carries the fluid and injects it into the core with the assistance of the distributor inlet cap of the coreholder. The overburden pressure was maintained constant by an Enerpac P-18 hand pump (4). The produced fluids were carried through the backpressure

regulator (7) into a burette three phase separator (8). The liquid phase was collected in the burette separator and the produced gas volume was measured through a gasmeter (9) connected to the top of the burette separator. The inlet and outlet pressures were measured using two Keller type pressure transducers (3). The type of gasmeter, pressure transducer, back pressure regulator and separator are shown in Figures 3.13 - 3.16 respectively.

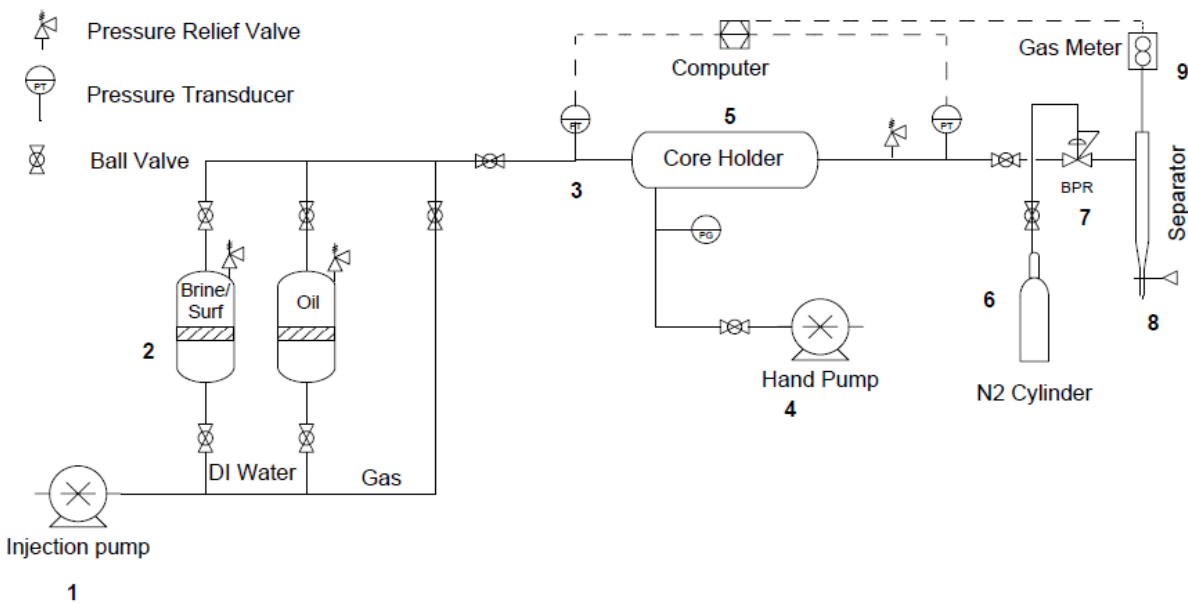
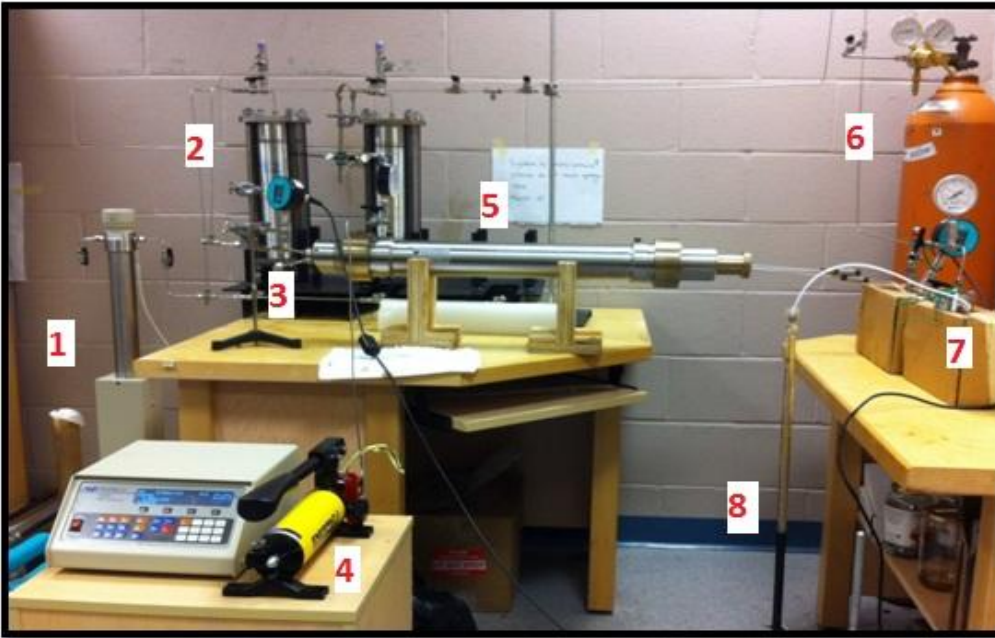


Figure 3.11 Schematic of the coreflooding apparatus



- 1: Injection Pump
- 2: Accumulators
- 3: Pressure Transducer
- 4: Hand Pump
- 5: Core Holder
- 6: N₂ Cylinder
- 7: BPR
- 8: Separator
- 9: Gas Meter

Figure 3.12 Low Pressure coreflooding setup



Figure 3.13 Coreflooding outlet section (8: phase separator, 9: Emdyne MK 2000 gasmeter)



Figure 3.14 Keller LEO3 pressure transducer



Figure 3.15 Equilibar back pressure regulator (model # EB1LF1)



Figure 3.16 Custom made three phase separator

The clean and dry sample was weighed. Then the core sample was saturated using synthetic brine and the weight of the core was measured after 20, 45, 60 and 120 minutes from the beginning of the saturating until no significant increase in the recorded weight was observed (refer to Appendix B-1). The actual pore volume of the core was calculated using the weight and density of the brine inside the core. After that the total volume of the core was measured by calculating the change in the height of 500 cm³ brine in a 1000 cm³ graduated cylinder after immersing the fully saturated sample into that. The porosity was calculated using the pore volume and the total volume of the core (refer to Appendix B-1). The errors in reading and measurements were calculated and used based on the rules in Appendix A to calculate the standard deviation in all the steps of coreflooding.

The fully saturated core was then flooded using synthetic brine to complete one pore volume (PV) at the flow rate of 0.1 cm³/min. Brine flooding was continued until a stable pressure drop was observed. The absolute permeability of the core to brine was calculated (refer to Appendix B-2). The absolute permeability, K, in Darcy was calculated using Darcy's law:

$$K = \frac{Q\mu L}{A\Delta P}, \quad (11)$$

where Q is flow rate in (cm³/s); μ is the viscosity of injected fluid in cP; L is the length in cm; A is the cross-sectional area in cm², and ΔP is pressure drop in atm.

The outlet dead volume of the coreflooding set-up was calculated and added to the actual pore volume and the new value was used as the pore volume (PV) to reduce errors in material balance calculation (Appendix D-1 and D-2).

The oil was filtered before transferring it to the oil accumulator and then injecting it into the core using an ISCO pump at a constant flow rate of $0.03 \text{ cm}^3/\text{min}$ for one pore volume (PV) or until no more water was produced. After that, the flow rate was changed to $0.08 \text{ cm}^3/\text{min}$ for one pore volume (PV) or until no more water was produced. The connate water saturation (S_{wc}) was calculated using material balance (refer to Appendix D-2 for sample calculation).

At this point, the core was at connate water saturation. The core was then flooded using synthetic brine (about one PV) with a flow rate of $0.05 \text{ cm}^3/\text{min}$ (at field rate of one ft/d the results are more representative for reservoir). The volume of brine and oil produced and the pressure drop were measured and recorded as a function of time (refer to Appendix C-3 for coreflooding raw data). The material balance was used to calculate the residual oil saturation S_{or} (refer to Appendix D-2 for sample calculation).

The core was then flooded with N_2 and surfactant solution alternately after the secondary brine flooding. In some experiments, it began with a gas cycle, whereas in others it began with surfactant solution. The flood was usually carried out at the flow rate of $0.05 \text{ cm}^3/\text{min}$. The slug size used for each cycle was 0.5 PV and tertiary flooding was continued to complete 1.5 PV. It was important to have similar pressures in both the surfactant and gas cylinders to prevent instabilities and early breakthrough during the flood. The brine, oil and gas volumes produced were measured using the separator and gas meter and tabulated as a function of time (raw data in Appendix C-3). The total oil recovery and the residual oil recovery for each experiment were calculated and listed in Table 4.4. A sample calculation is provided in the Appendix D-2. Due to time constraint the coreflooding experiments were not replicated but recovery from some cycles conducted at the same conditions (especially secondary floodings) were in good agreement.

3.2.8 Lessons Learned in Coreflooding Tests

- The hydraulic oil should be injected into the annulus of the core holder from the lower overburden pressure port so that air would be expelled from the upper port. Once the oil was seen coming out of the upper port, the annulus was full of hydraulic oil and the port was capped. The inlet and outlet fluid ports of the core holder were left open to ensure that the core sample was fitted properly between the end plugs. If sealing was not proper, the overburden fluid would leak through and come out of the ports and easily detected.
- In the case of using a pump for gas injection into core, the higher differential pressure, the greater the deviation from the constant rate. The error caused by using a pump for gas injection into a core is affected by the gas volume inside the pump cylinder. The less gas volume inside the cylinder, the less the error caused by using the pump for gas injection at constant rate into the core.
- During the experiment any significant delay in pressure buildup at the beginning of the injection or pressure drop during the experiment is a sign of leakage in the lines or valves which should be fixed to restore the pressure to reservoir pressure before proceeding further.
- Capillary end effects arise from the discontinuity of capillarity in the wetting phase at the outlet end of the core sample. In coreflooding experiments end effects can be minimized by using large core lengths (1 ft) and pore volume.

4. RESULTS AND DISCUSSION

The three main mechanisms enabling surfactant-alternating-gas injection to enhanced oil recovery are the presence of stable foam, the reduction in interfacial tension, and the alteration of wettability in porous media. The effects of different parameters that were evaluated in the coreflooding section are first examined in foam stability, interfacial tension and wettability measurement tests.

4.1 Dynamic Test Results and Discussion

Figures presented in this section show foam stability of different surfactant solutions in the absence and presence of oil.

Foam in the absence of oil. In the dynamic test, foam was generated by the injection of air into the surfactant solution for five minutes. After generation, the foam height decreased gradually (Figure 4.1). Slow liquid drainage is the reason for the foam thinning, which causes the foam to rupture. Foam collapses quickly when most of the liquid has drained out of plateau borders. Figure 4.2 shows the foam stability of the surfactant solutions studied. It is evident from Figure 4.2 showing foam height vs. time that there is a direct relationship between foam stability and surfactant concentration. An increase in surfactant concentration increased foaming ability and foam stability significantly. The surfactant molecules, which are located at the gas-solid interface, reduce the surface tension. Marangoni shear stress controls the decay rate of foam by acting on the plateau borders, which is because of surface active gradient generation. It is clear that foam was not generated in all of the solutions; Ivey-sol 108 at its CMC could not generate any foam both in low and high salinity brine. It can be seen that the most stable foam was produced when 0.3 wt% + CMC of Ivey-sol 108 was used in low salinity brine. The texture of

foam generated from Ivey-sol 108 at 0.3 wt% above its CMC in low salinity brine was very fine and coarsening rate was much slower than for TX-100 at 0.3 wt% above its CMC. Salts would be expected to reduce any electrostatic repulsion produced by charge buildup on bubble surfaces. Both TX-100 and Ivey-sol 108 at 0.3 wt% above their CMC values in low salinity brine showed a constant foam height initially, and then they started to decay. The initial decay rate is related to the stability of the thin lamellae films.

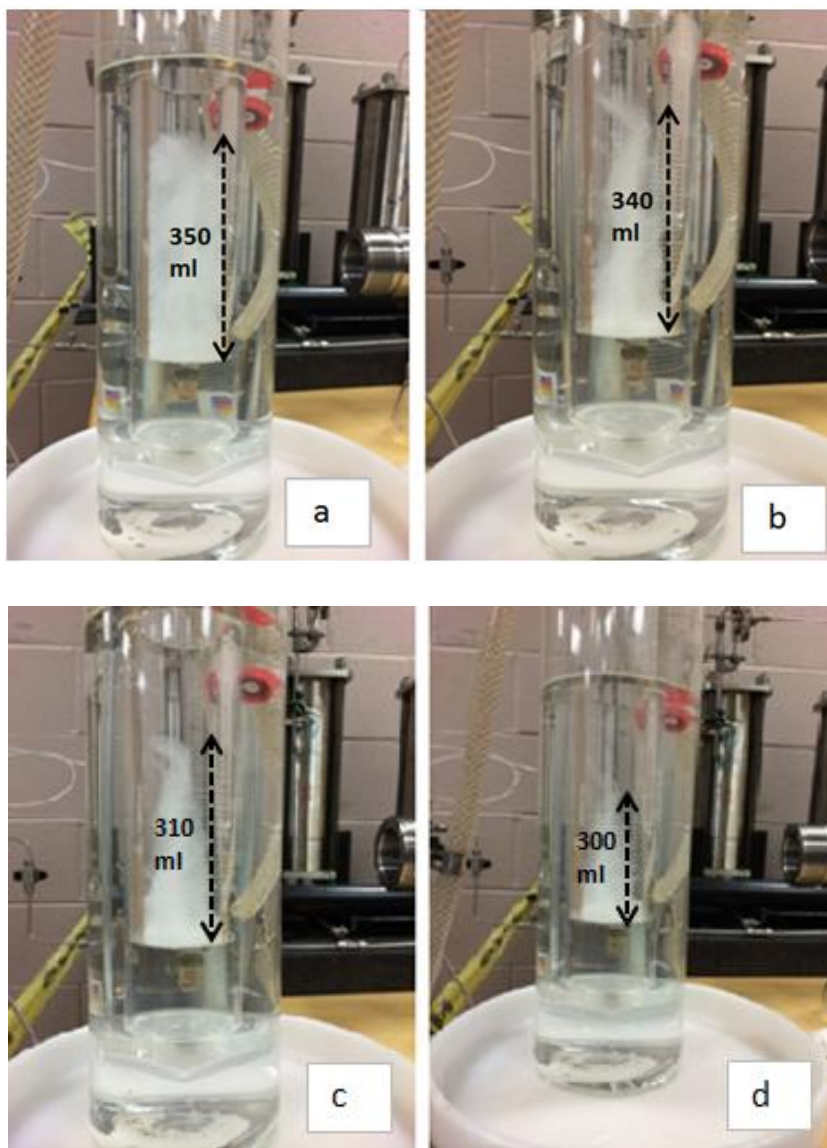


Figure 4.1 Collapse of Ivey-sol 108 foam, (a) $t = 5$ minutes, (b) $t = 7$ minutes, (c) $t = 10$ minutes, (d) $t = 15$ minutes

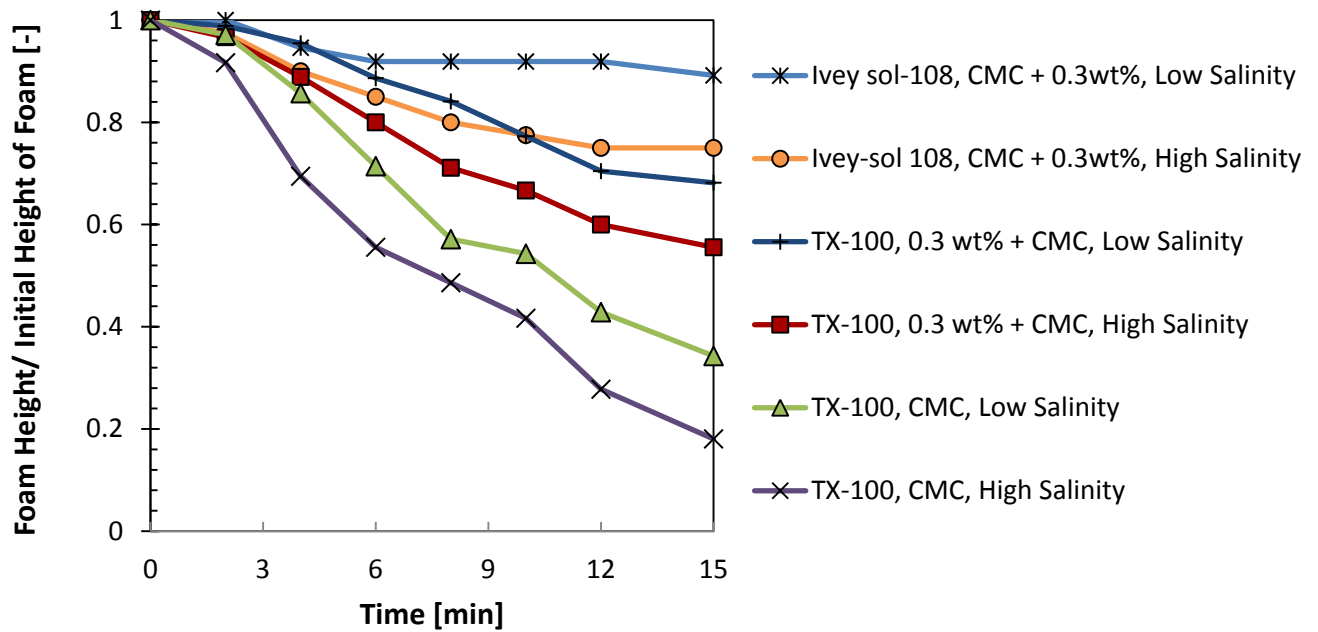


Figure 4.2 Dynamic foam test using different surfactant solutions in the absence of oil

Foam stability in the presence of oil. The effect of oil on the foam stability was investigated in order to find a surfactant solution that would generate a more stable foam. The underlying foam stability mechanism in the presence of oil has been discussed in terms of aqueous film thinning due to entry of oil drop, oil spreading on the gas-water interface, occurrence of an unstable bridge across the foam film, and stability of pseudoemulsion film, which is a thin aqueous film separating the approaching oil drop and gas-water interface. If the entry condition is favorable and the oil drop is able to exhibit a spreading behavior, the gas-water interface is expected to expand. The expansion results in thinning of the foam film and eventually the film ruptures. If there is no spreading and the oil drop forms a lens at the gas-water interface, the foam film may rupture once the oil drop enters both surfaces of the lamella. Under this condition, the oil drop spans the film by making an unstable bridge.

The results of the foam stability experiments in the presence of oil were observed at the one minute interval and are shown in Figure 4.3. The initial foam height was highest for TX-100, at above CMC in low salinity brine. For TX-100 the foam almost disappeared within 40 to 60 seconds at above CMC, 25 to 30 seconds at CMC and for Ivey-sol 108 it took 5 to 12 seconds at above CMC and no foam was generated at CMC. Foam generated from TX-100 at 0.3 wt% above its CMC in low and high salinity brine lasted longer.

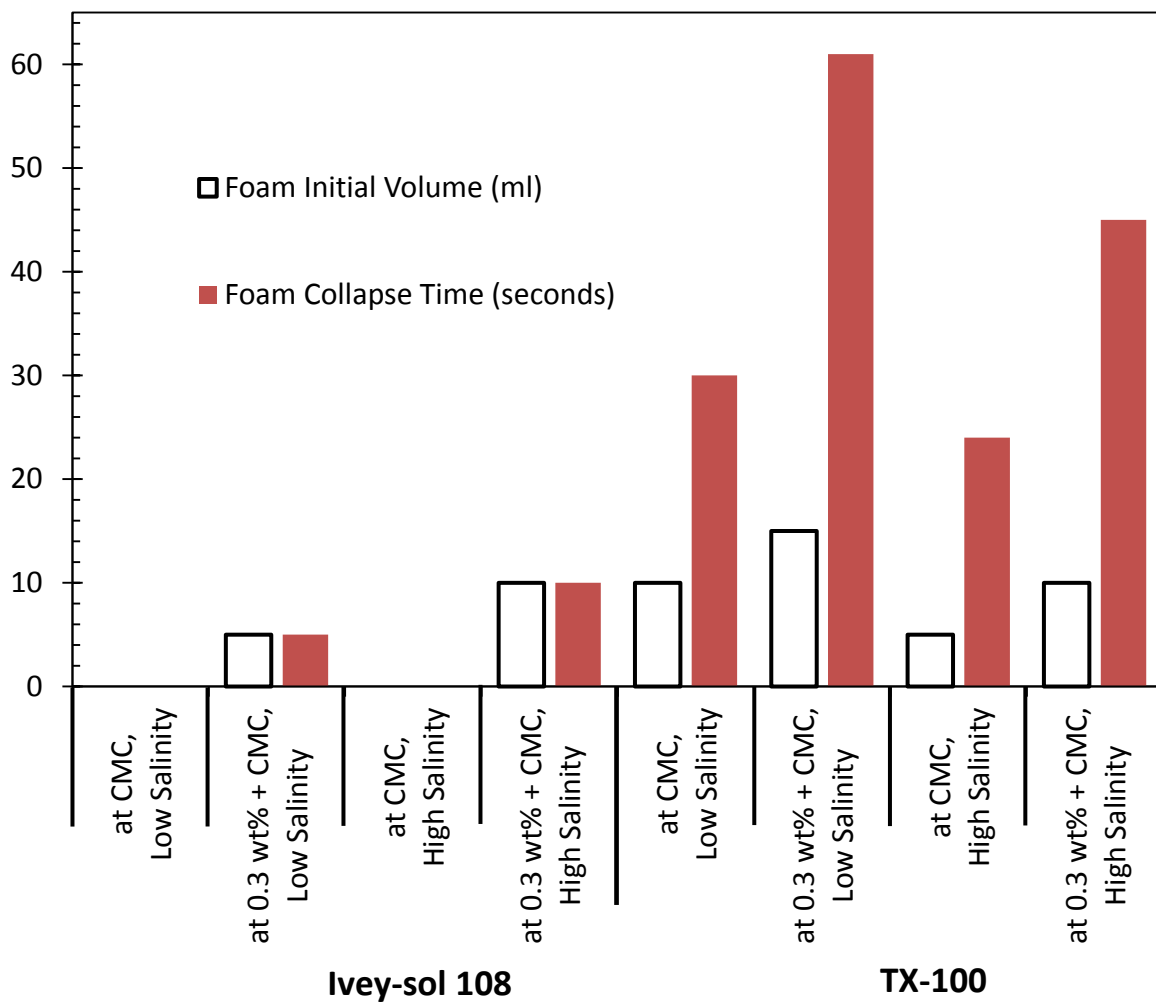


Figure 4.3 Initial foam volume and foam collapse time of different surfactant solutions in the presence of oil, using the air injection method

4.2 Static Test Results and Discussion

A series of bottle tests were conducted to compare the foaming ability and foam stability of different surfactant solutions, which are listed in Table 4.1. After shaking and foam generation, the height of foam decreased gradually. The foam height generated by all the solutions at zero time, one hour and four hours after shaking are shown in Figures 4.4 - 4.6 respectively.

Foam stability in the absence of oil. Figure 4.7 shows the relative height of foam in absence of oil for the studied solutions. The foam generated from TX-100 was more stable than Ivey-sol 108. Foam generation and stability increase with surfactant concentrations. The stability of foam for Ivey-sol 108 at 0.3 wt% above its CMC or at its CMC and at lower brine salinity was significantly higher compared to that at high salinity. TX-100 foam lasted longer simply because it was more stable and had a higher initial foam height.

Table 4.1 Solutions used in the bottle test

Salinity	Surfactant	Concentration	Symbol
Low 7000 ppm TDS	Triton X-100	0.3 wt% + CMC	T1
	Triton X-100	CMC	T3
	Ivey Sol-108	0.3 wt% + CMC	I1
	Ivey Sol-108	CMC	I3
High 21000 ppm TDS	Triton X-100	0.3 wt% + CMC	T2
	Triton X-100	CMC	T4
	Ivey Sol-108	0.3 wt% + CMC	I2
	Ivey Sol-108	CMC	I4



Figure 4.4 Foam height at 0 time generated by different solutions (solution from left to right in turn is: T1, T2, T3, T4, I1, I2, I3 and I4)



Figure 4.5 Foam height at 1 hour generated by different solutions (solution from left to right in turn is: T1, T2, T3, T4, I1, I2, I3, and I4)



Figure 4.6 Foam height at 4 hours generated by different solutions (solution from left to right in turn is: T1, T2, T3, T4, I1, I2, I3, and I4)

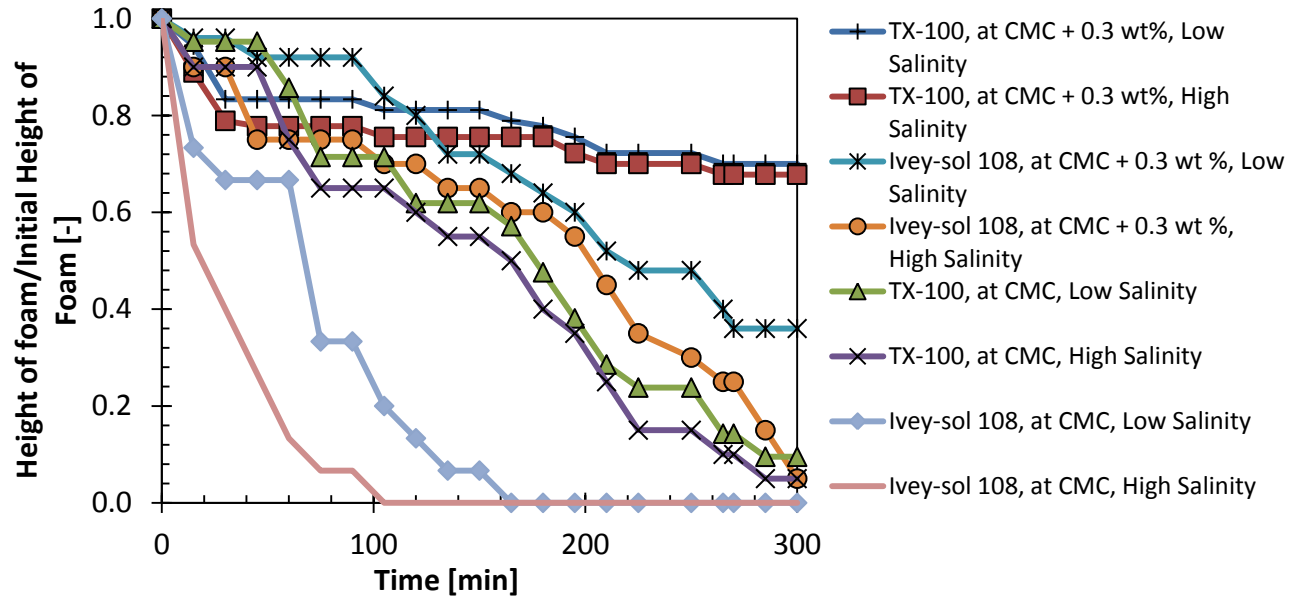


Figure 4.7 Foam stability of different surfactant solutions in the absence of oil

Foam stability in the presence of oil. Figure 4.8 shows the foam generated in the presence of oil after 5 minutes. The presence of oil significantly and detrimentally affects foam stability (Figure 4.9). Ivey-sol 108 and TX-100 at the concentration of 0.3 wt% above their CMC generated more stable foams compared to the solutions at their CMC values. The decay rate for Ivey-sol 108 at above CMC and in low salinity brine was smaller compared to the TX-100 solution, but the foam generated from TX-100 lasted longer again because of the initial foam volume. Figure 4.10 shows the comparison between the stability of foam in the absence and presence of oil in the static test for some selective solutions, which indicates that Ivey sol- 108 at 0.3 wt% above CMC in low salinity is the most stable solution both in the absence and presence of oil.



Figure 4.8 Condition of foam generated by different solutions after 5 minutes in the presence of 10 vol% oil (Solutions from left to right in turn are: T1, T2, T3, T4, I1, I2, I3, and I4)

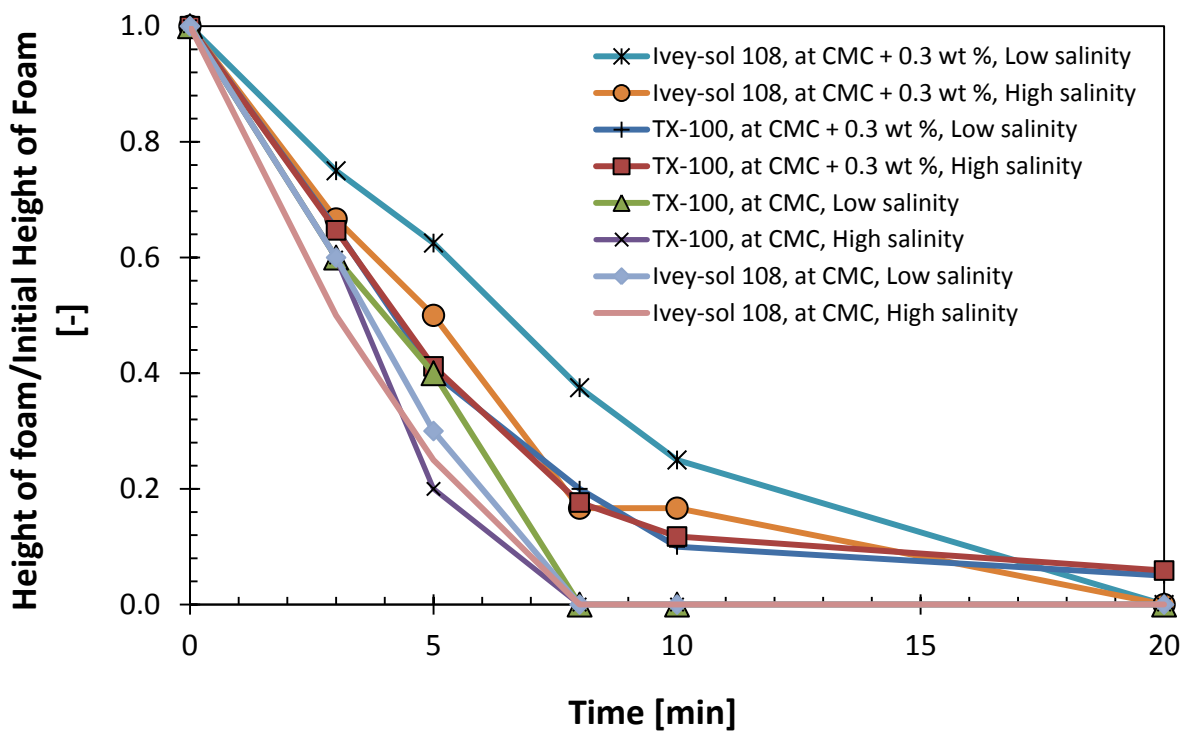


Figure 4.9 Foam stability of different surfactant solutions in the presence of oil

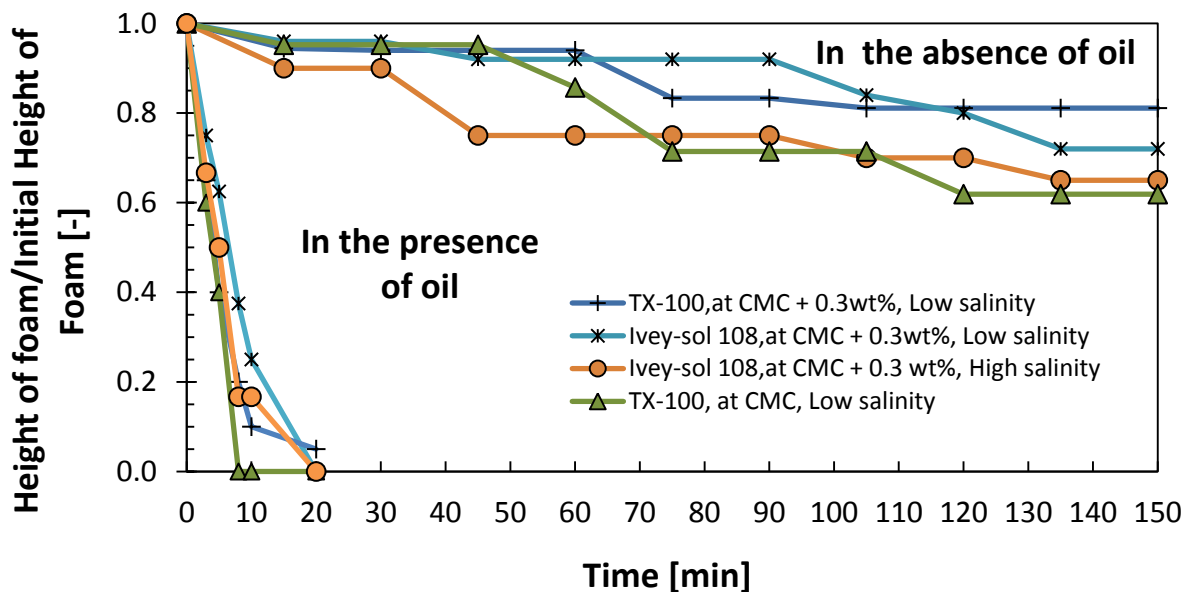


Figure 4.10 Comparison between the foam stability of different surfactant solutions in the presence and absence of oil

4.3 IFT and Contact Angle Results and Discussion

4.3.1 Effect of Surfactant Type and Concentration on IFT and Wettability

In both interfacial tension and contact angle tests, measurements for a single drop or in some cases for two drops were recorded several times for a period of time and based on the raw data presented in Appendix C-2, the mean value of each run was used as the best estimate of the true value (listed in Table 4.2). The standard deviation for each mean value was calculated according to the definitions (Appendix A). A sample calculation is provided in Appendix D-3.

Figure 4.11 shows the IFT (excluding standard deviation) between the oil and Ivey-sol 108 and TX-100 solutions in high salinity brine at various concentrations. The IFT decreased with increasing surfactant concentration. The IFT for TX-100 is almost eight times smaller than that

of Ivey-sol 108 at 0.3 wt% above their respective CMCs, which was verified by Zubair et al. (2013). The IFTs and contact angles for the solutions used in the coreflooding are listed in Table 4.2. Generally, higher surfactant concentration resulted in greater contact angle (less water-wet) and the contact angle measured for TX-100 solutions were greater compared to Ivey-sol 108. From the data listed in Table 4.2, it is clear that TX-100 at 0.3 wt% above CMC changed the wettability of the Berea sandstone toward intermediate-wet ($\theta = 90^\circ$).

Table 4.2 Interfacial tensions (IFT) and contact angles of different solutions

Solution	Salinity (ppm TDS)	IFT (mN/m)	Contact Angle (θ)	Capillary Number
Brine	7000	14.34 ± 0.36	34.4 ± 1.5	$2.98E-07 \pm 7.7E-09$
TX-100, at 0.3 wt% + CMC	7000	0.43 ± 0.01	71.2 ± 3.5	$4.79E-05 \pm 6.1E-06$
Ivey-108, at 0.3 wt% + CMC	7000	4.72 ± 0.22	41.3 ± 1.4	$9.89E-07 \pm 5.7E-08$
Brine	21000	17.94 ± 0.37	48.8 ± 2.3	$2.96E-07 \pm 1.6E-08$
TX-100, at CMC	21000	4.07 ± 0.15	61.3 ± 0.9	$1.79E-06 \pm 1.1E-07$
TX-100, at 0.3 wt% + CMC	21000	0.67 ± 0.02	88.8 ± 3.3	$2.61E-04 \pm 1.3E-05$
Ivey-108, at CMC	21000	13.75 ± 0.21	49.5 ± 2.5	$3.92E-07 \pm 1.7E-08$
Ivey-108, at 0.3 wt% + CMC	21000	5.33 ± 0.10	57.9 ± 0.3	$1.24E-06 \pm 1.1E-08$

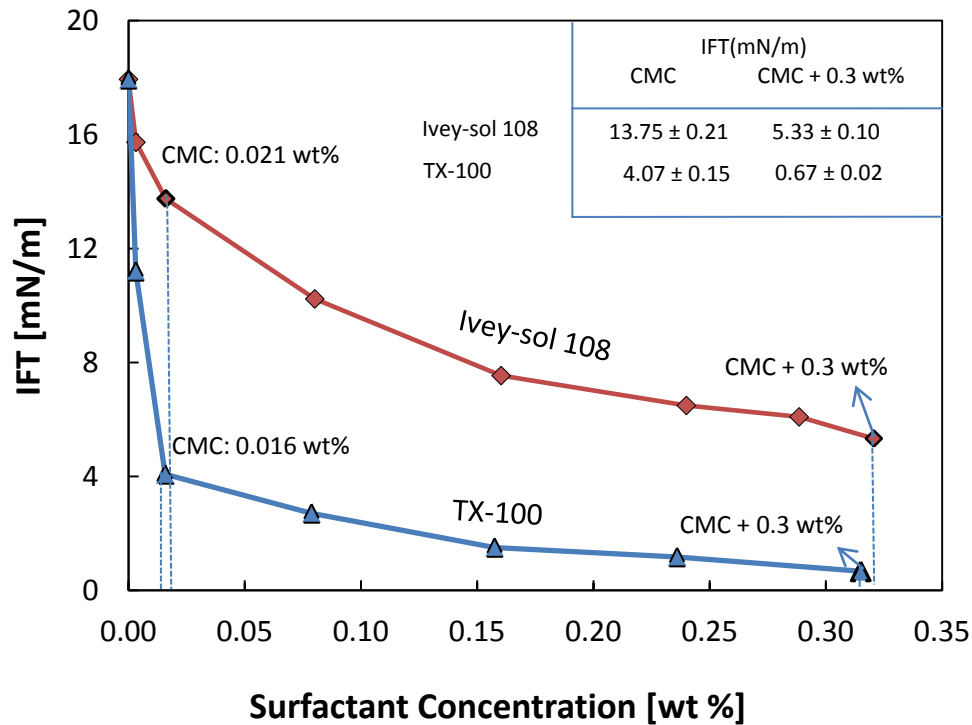


Figure 4.11 IFT at different surfactant concentrations.

4.3.2 Effect of Salinity on Interfacial Tension and Wettability

The results in Table 4.2 show the IFT between the oil phase and the surfactant solution and the contact angle between the oil droplet and the rock surface are greater when using high salinity brine (21000 ppm TDS) compared to low salinity (7000 ppm TDS), which indicates the ability of low salinity brine to alter the wettability of Berea rock to more water-wet. The same results were reported by Nasralla et al. (2013) when they used different levels of salinity from 0 to 174,000 mg/L to evaluate the effect of salinity on the Berea sandstone wettability. Figure 4.12 shows the oil drop shape in the presence of different brine and surfactant solutions.

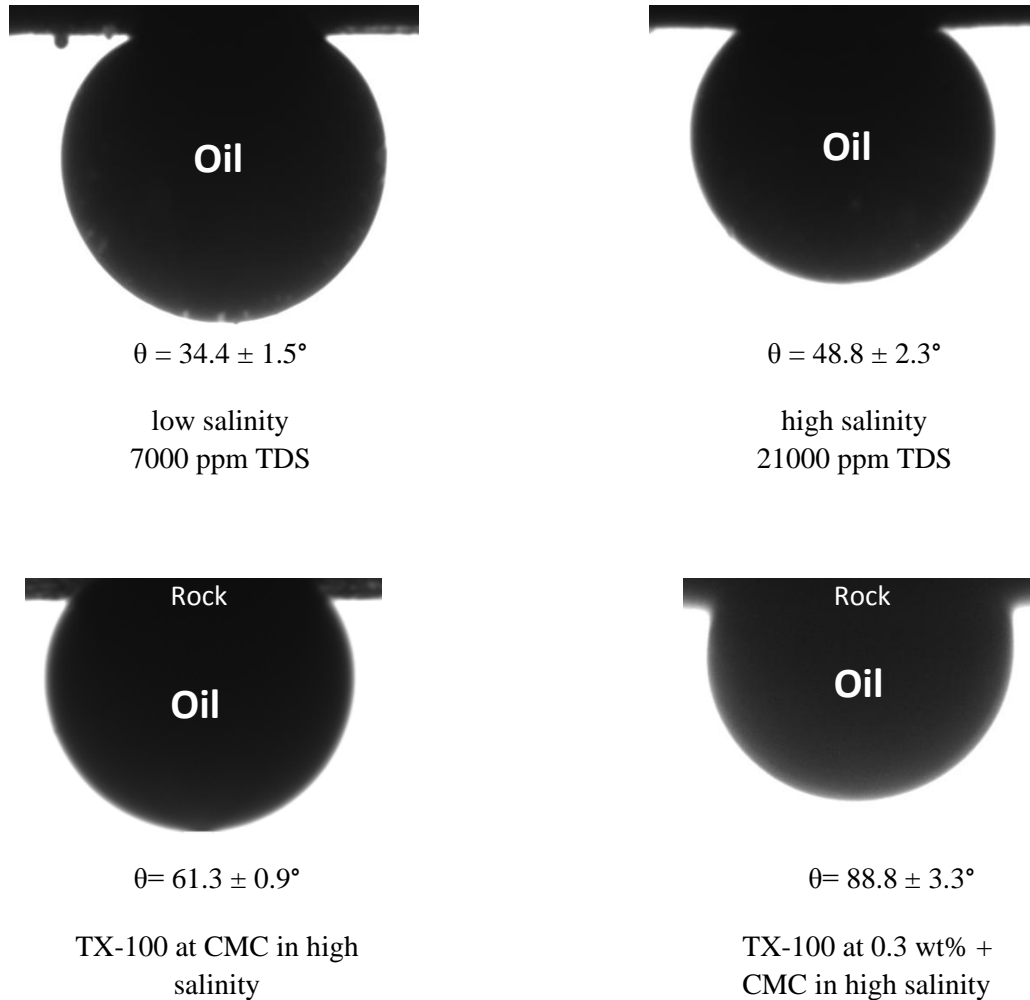


Figure 4.12 Contact angle of oil drop on Berea sandstone in bulk of different solutions: (a) 7000 ppm TDS brine, (b) 21,000 ppm TDS brine, (c) TX-100 at CMC with 21000 ppm TDS, (d) TX-100 at 0.3 wt% + CMC with 21000 ppm TDS

4.4 Coreflooding Test Results and Discussion

Nine coreflood experiments were carried out to evaluate the effect of different factors, such as surfactant type, surfactant concentration, brine salinity, injection scheme and the addition of a sacrificial adsorption agent, on the residual and total oil recovery. The connate water saturation,

residual oil saturation, waterflooding recovery, recovery of residual oil and total oil recovery for each experiment were calculated and listed in Table 4.4. From the results, it is clear that the connate water saturation (S_{wc}) is greater and residual oil saturation (S_{or}) is smaller for low salinity tests compared to high salinity because in low salinity systems the rock sample tends to be more water-wet. This will be further discussed later in section 4.4.3.

4.4.1 Errors in Coreflooding Experiments

The Coreflooding experiments were not replicated in their entirety. However, some secondary and tertiary cycles were carried out at the same conditions in different runs; i.e. according to the results reported in Table 4.3. Oil recoveries during secondary low salinity waterflooding in experiments 1, 2, and 3 are in good agreement and in the range of 62.6 – 64.2%, with an average oil recovery of $63.3 \pm 0.82\%$. Oil recoveries from high salinity secondary waterflooding, experiments 4, 5, 6, and 7 are in the range of 51.4 – 52.2% with an average of $52.1 \pm 0.5 \%$.

From Table 4.3, and as described above, there is good agreement in replication of oil recovery during different recovery cycles.

Table 4.3 Errors in Coreflooding Experiments

Exp. #	Part of Flooding	Salinity (ppm) TDS	Injected PV	Recovery [%]	Average	Standard deviation (\pm)
1	Secondary	7000	1	62.6	63.3	0.5
2	Secondary	7000	1	64.2	63.3	0.6
3	Secondary	7000	1	63.1	63.3	0.1
1	Tertiary	7000	0.5	19.4	19.3	0.1
2	Tertiary	7000	0.5	19.2	19.3	0.1
4	Secondary	21000	1	52.3	52.1	0.1
5	Secondary	21000	1	52.2	52.1	0.1
6	Secondary	21000	1	51.4	52.1	0.4
7	Secondary	21000	1	52.6	52.1	0.3

Table 4.4 Summary of the experimental runs

Exp. #	Injection Scheme	Brine Salinity (ppm) TDS	Surfactant Type	Surfactant Conc. (wt%)	S_{wc}	S_{or}	Waterflood Recovery [%OOIP]	Incremental Oil Recovery [%OOIP]	Total Recovery [%OOIP]	Residual Oil Recovery [%ROIP]
1	W-G-W-G	7000	-	-	0.31 ± 0.003	0.26 ± 0.003	62.6 ± 0.3	8.9 ± 0.5	71.5 ± 0.4	23.9 ± 0.6
2	W-G-S-G	7000	IV	0.321	0.36 ± 0.003	0.23 ± 0.003	64.2 ± 0.3	11.8 ± 0.5	76.1 ± 0.4	32.9 ± 0.6
3	W-S-G-S	7000	IV	0.321	0.32 ± 0.003	0.25 ± 0.003	63.1 ± 0.3	10.2 ± 0.5	73.3 ± 0.4	27.9 ± 0.6
4	W-S-G-S	21000	TX	0.016	0.21 ± 0.003	0.38 ± 0.003	52.3 ± 0.3	7.6 ± 0.5	59.9 ± 0.4	15.9 ± 0.6
5	W-S-G-S	21000	IV	0.021	0.25 ± 0.003	0.36 ± 0.003	52.2 ± 0.3	4.6 ± 0.5	56.8 ± 0.4	9.6 ± 0.6
6	W-S-G-S	21000	TX	0.316	0.27 ± 0.003	0.36 ± 0.003	51.4 ± 0.3	14.5 ± 0.5	65.8 ± 0.4	29.7 ± 0.6
7	W-S-G-S	21000	IV	0.321	0.23 ± 0.003	0.36 ± 0.003	52.6 ± 0.3	7.6 ± 0.5	60.3 ± 0.4	16.1 ± 0.6
8	SLS-S-G-S	21000	IV	0.321	0.25 ± 0.003	0.34 ± 0.003	54.2 ± 0.3	11.1 ± 0.5	65.2 ± 0.4	24.4 ± 0.6
9	SLS-G-S-G	7000	TX	0.316	0.33 ± 0.003	0.24 ± 0.003	63.9 ± 0.3	20.6 ± 0.5	84.5 ± 0.4	57.1 ± 0.6

4.4.2 Comparison of WAG and SAG injection

The effect of adding surfactant to the water cycle resulted in 9.0% more residual oil recovery comparing results from experiments 1 (WGWG, low salinity) and 2 (WGSG, Ivey sol-108 at 0.3 wt% + CMC in low salinity), shown in Figure 4.13. The pressure drop for each experiment is shown in Figure 4.14. The differential pressure in the last cycle of SAG injection is greater than the last cycle of WAG, which confirms the foam generation due to the presence of surfactant in the porous media, prior to gas injection in this cycle. Foam generated in-situ can improve recovery during the second gas injection by increasing viscosity and reducing the gas mobility.

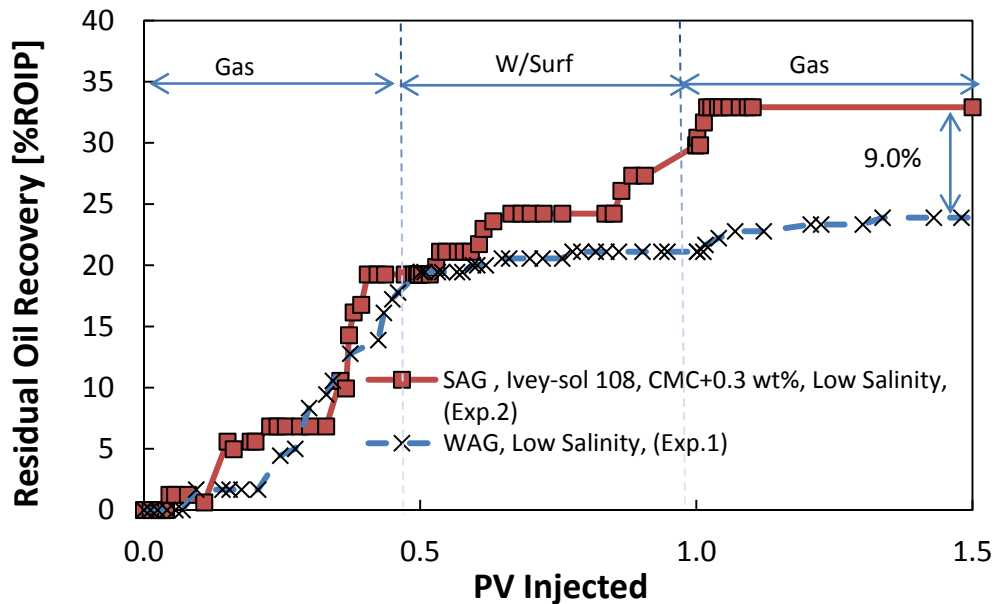


Figure 4.13 Comparison of WAG and SAG injection

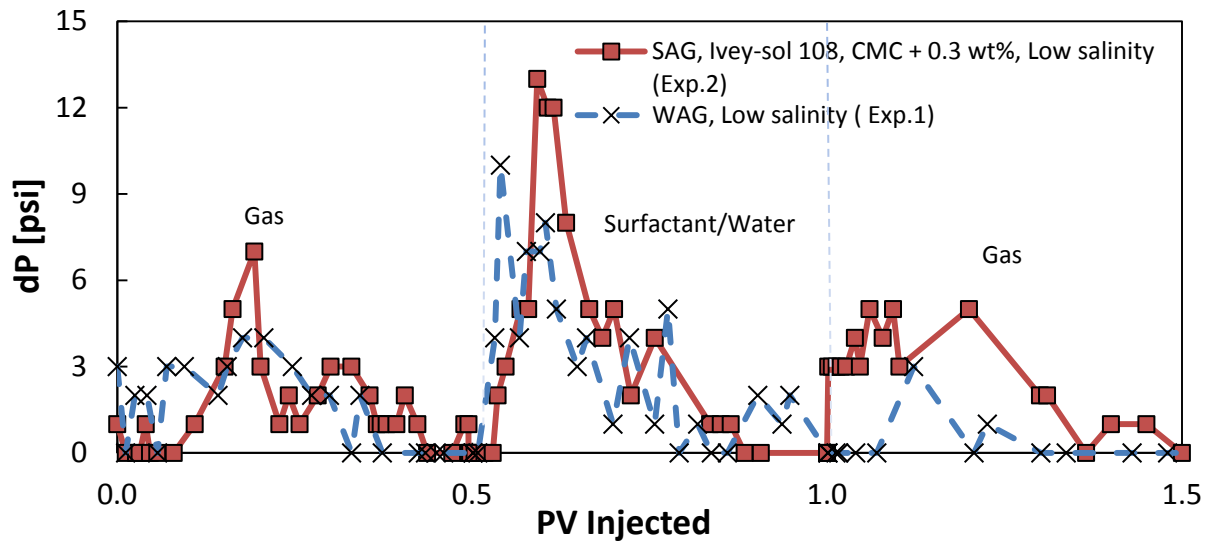


Figure 4.14 Pressure profile during WAG and SAG injection.

4.4.3 Effect of Surfactant Type and Concentration on Oil Recovery

Four experiments were conducted using high salinity brine and TX-100 or Ivey-sol 108 at either CMC or 0.3 wt% above their CMC. In Figure 4.15, the results show that residual oil recovery increases with surfactant concentration. At 0.3 wt% above CMC surfactant concentration, TX-100 yielded 13.6% higher residual oil recovery compared to Ivey-sol 108 whereas at CMC, TX-100 yielded 6.3% higher recovery. The largest reduction in interfacial tension of water-oil is caused by TX-100 at 0.3 wt% in low salinity brine (14.34 mN/m to 0.43 mN/m), which is two orders of magnitude. In order to improve the recovery of residual oil, a three to four orders of magnitude reduction in IFT would be required. Therefore, it is suggested that the increased recovery of residual oil observed in these experiments may be due to wettability alteration, from strongly water-wet to mixed-wet which is reported by Ayirala (2002) or to intermediate-wet, as reported by Moore and Slobod (1956), Kennedy et al. (1955), Li et al. (1997) and Jadhunandan and Morrow (1991).

The results of the wettability measurements in the previous section suggest that the TX-100 above CMC is able to alter the wettability of the rock toward the intermediate-wet condition ($\theta = 88.8^\circ$), which can explain the higher oil recovery during surfactant injection cycles using TX-100 at high concentration. Agbalaka et al. (2008) reported that the highest oil recovery is achieved when the reservoir is intermediately wet; i.e. not strongly oil-wet ($\theta = 180^\circ$) nor strongly water-wet ($\theta = 0^\circ$).

Another reason for the higher oil recovery when using TX-100 at 0.3 wt% above CMC compared to the other cases is the presence of a stronger foam in the gas cycle. The pressure profile in Figure 4.16 illustrates different cycles of these experiments, clearly showing that during the first surfactant injection cycle there is no noticeable difference in pressure drop. The pressure profiles for the gas injection after the first surfactant cycle show the highest differential pressure when using TX-100 at 0.3 wt% above its CMC, which indicates the presence of a stronger foam inside the core that leads to a higher oil recovery.

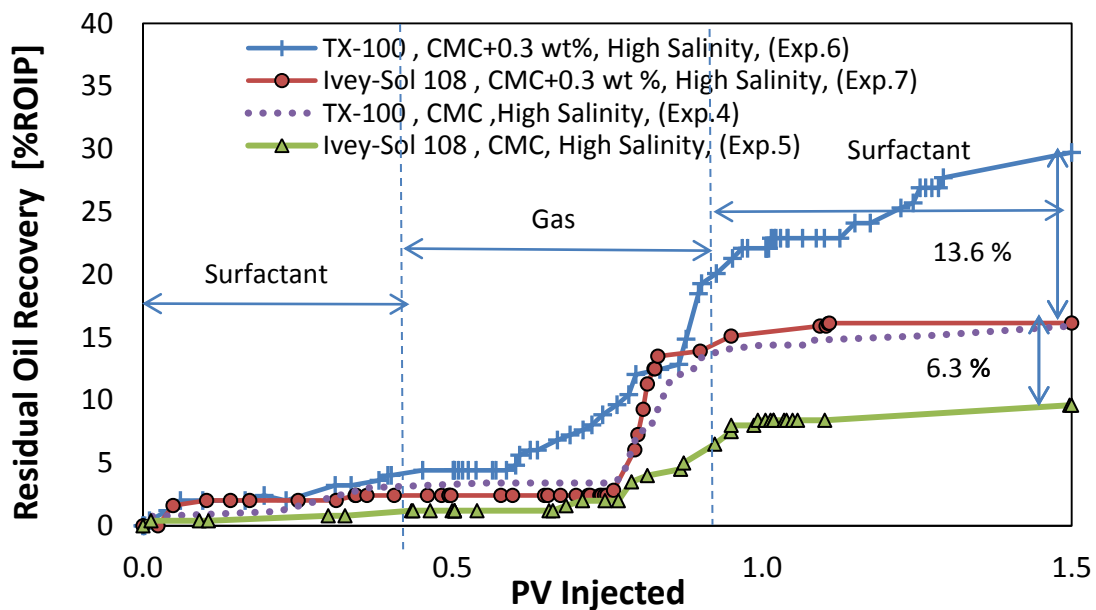


Figure 4.15 Effect of surfactant types and concentration on residual oil recovery

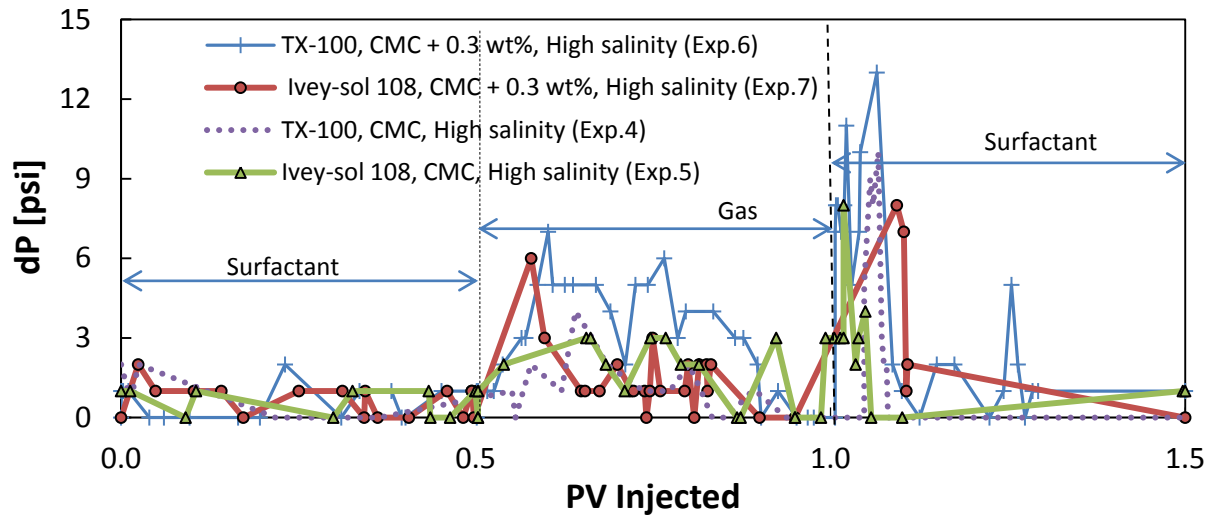


Figure 4.16 Pressure profile during SAG injection

4.4.4 Effect of Salinity on Oil Recovery

Ivey-sol 108 at 0.3 wt% above CMC in water with lower salinity was shown to increase oil recovery by 10.5% in secondary waterflooding and 13.0% in total oil recovery compared to flooding with higher salinity water (Figure 4.17). In sandstone reservoirs, lower water salinity has a great effect on enhancing oil recovery. The improved oil recovery in the secondary waterflooding cycle, when using low salinity brine, can be explained by three different mechanisms. The first mechanism is multicomponent ion exchange (MIE) process, which explains the release of oil components previously bonded to the rock surface by divalent ion bridging. Nasralla et al. (2013) explained that low salinity water injection results in a double layer expansion that makes the desorption of the oil bearing divalent ions from the rock surface possible. Tang and Morrow (1999) explained a second mechanism by describing a model in which pH increases as a result of mineral dissolution, which is the dominant mechanism for low salinity induced improved recovery. The third mechanism, also reported by Tang and Morrow

(1999), suggests that during low salinity water injection, fines may be washed away resulting in the exposure of primary surfaces that are more water-wet, but during high salinity water injection fines retain their oil-wet nature, resulting in lower sweep efficiency.

The pressure profile for each experiment is shown in Figure 4.18. The differential pressure during low salinity injection is almost the same as the high salinity injection.

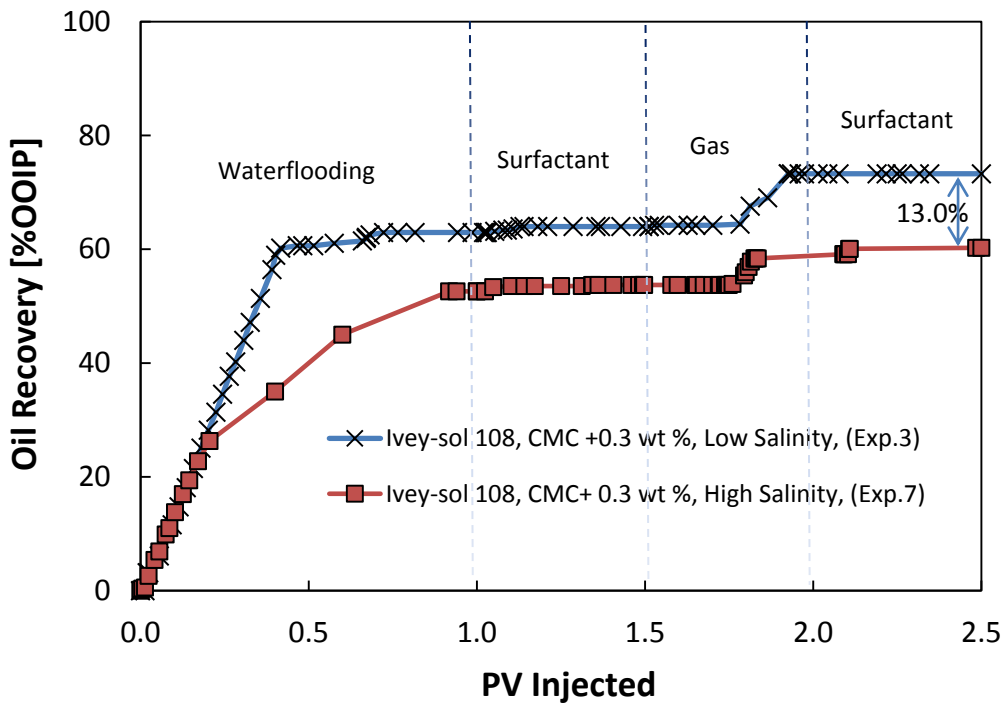


Figure 4.17 Effect of salinity on total oil recovery.

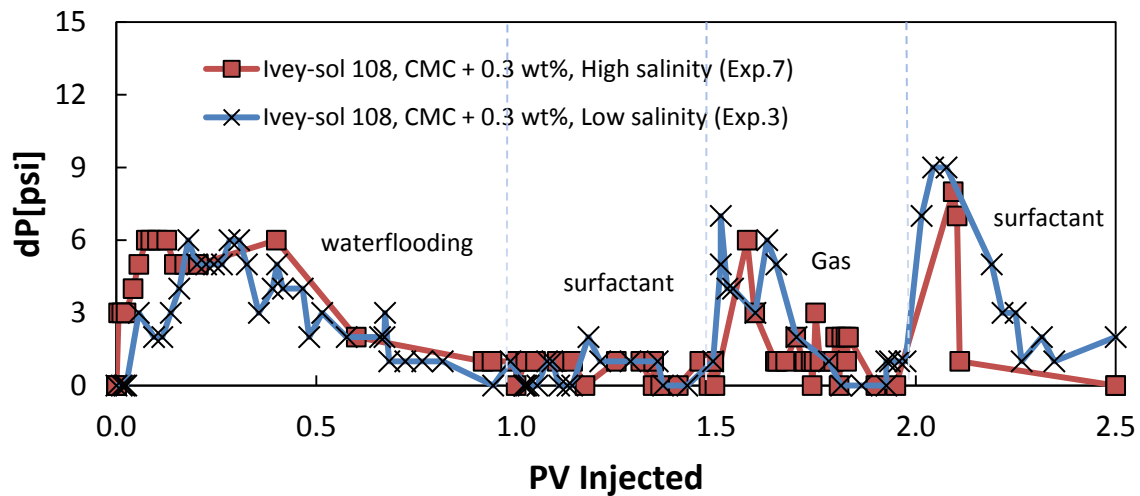


Figure 4.18 Pressure profile during SAG injection

4.4.5 Effect of Injection Scheme on Oil Recovery

The effect of starting with gas injection after secondary waterflooding was compared to beginning with surfactant injection in experiments 2 (WGS, Ivey-sol 108 at 0.3 wt% + CMC in low salinity) and 3 (WGS, Ivey-sol 108 at 0.3 wt% + CMC in low salinity). The results are shown in Figure 4.19. In the first cycle, gas was more effective than surfactant since the system was more water-wet (Table 4.2). This can be explained considering the hysteresis effect of drainage and imbibition processes. Residual oil is primarily trapped in large pores of water-wet rock after waterflooding (imbibition) whereas gas injection is a drainage process thereby better sweeping the residual oil from the larger pores assuming no other viscous or gravity effects. The pressure profiles are shown in Figure 4.20. The main difference in differential pressure is due to difference in injection scheme.

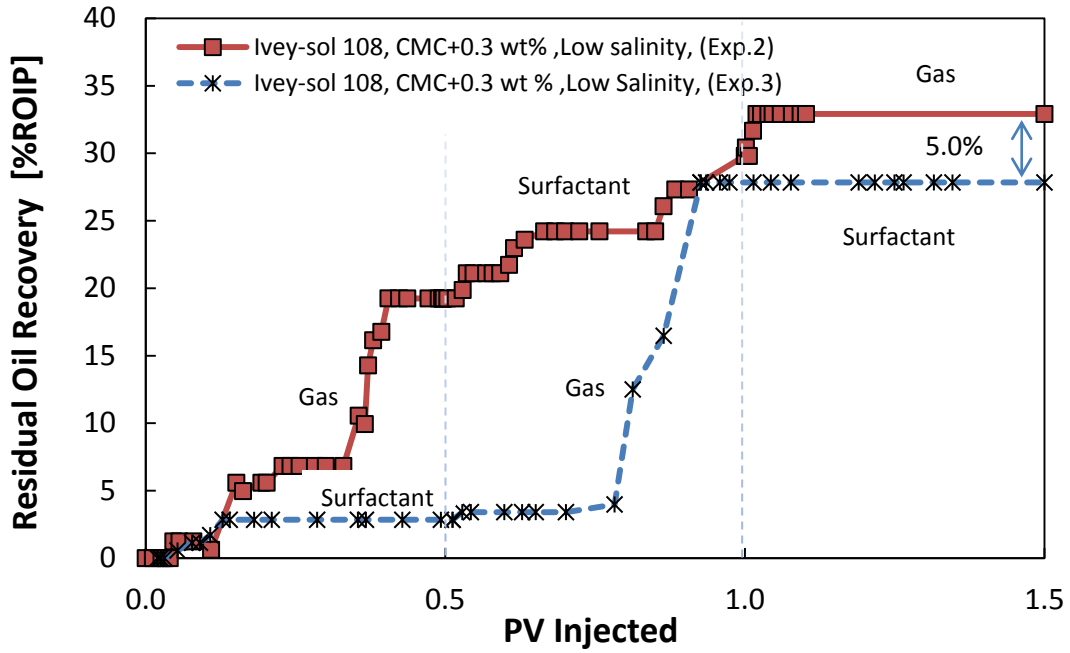


Figure 4.19 Effect of injection scheme (starting with gas or surfactant) after secondary water flooding

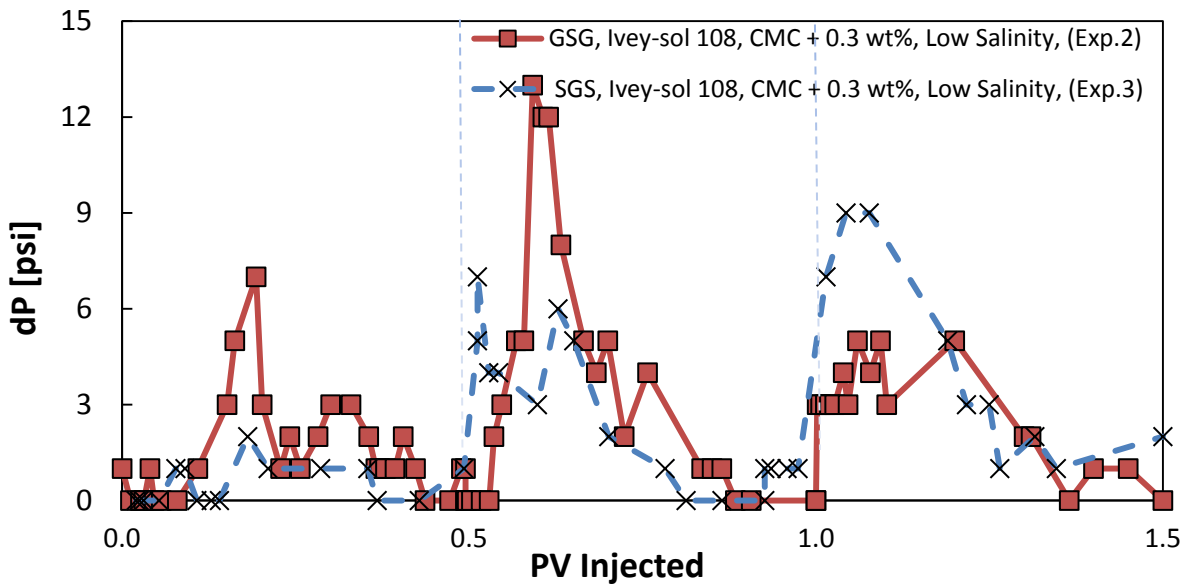


Figure 4.20 Pressure profile during two experiments with different injection schemes

4.4.6 Effect of Sacrificial Adsorption Agent on Oil Recovery

Based on the results of previous studies, which were outlined in the literature review, the interfacial tension of lignosulfonate solutions decreases with increasing lignosulfonate concentration, while the IFTs of surfactant and lignosulfonate mixtures increase with increasing lignosulfonate concentration. Thus, the effect of sodium lignosulfonate (SLS) was examined in SAG flooding experiments by adding 0.5 wt% of SLS to the secondary waterflooding rather than using the mixture of lignosulfonate and surfactant. In our experiments, the effluent was collected and based on the significant change in color (see Figure 4.21) of the water phase, it was concluded that the majority of SLS had been adsorbed to the rock surface preventing surfactant adsorption losses during the next cycles. Tsau et al. (2000) reported similar results when lignosulfonate and the surfactant CD1045 were injected into a Berea core in one cycle and the adsorption of surfactant was reduced by 24 - 60%.

This sacrificial additive prevented the surfactant adsorption on the rock surface during the surfactant injection cycle resulting in a better propagation of surfactant through the core leading to improved oil recovery by 4.9% compared to the case without SLS (Figure 4.22). The pressure profile for the aforementioned experiment is compared to the experiment without SLS in the secondary flooding shown in Figure 4.23 which indicates that differential pressure is almost the same for both experiments.

The sodium Lignosulfonate solution was very dark (close to oil color, Figure 4.21 b) therefore the camera was not able to distinguish the oil drop shape in the SLS solution and the IFT and contact angle measurement was not possible.



Figure 4.21 Color of 0.5 wt% SLS solutions (a) after production, (b) before injection

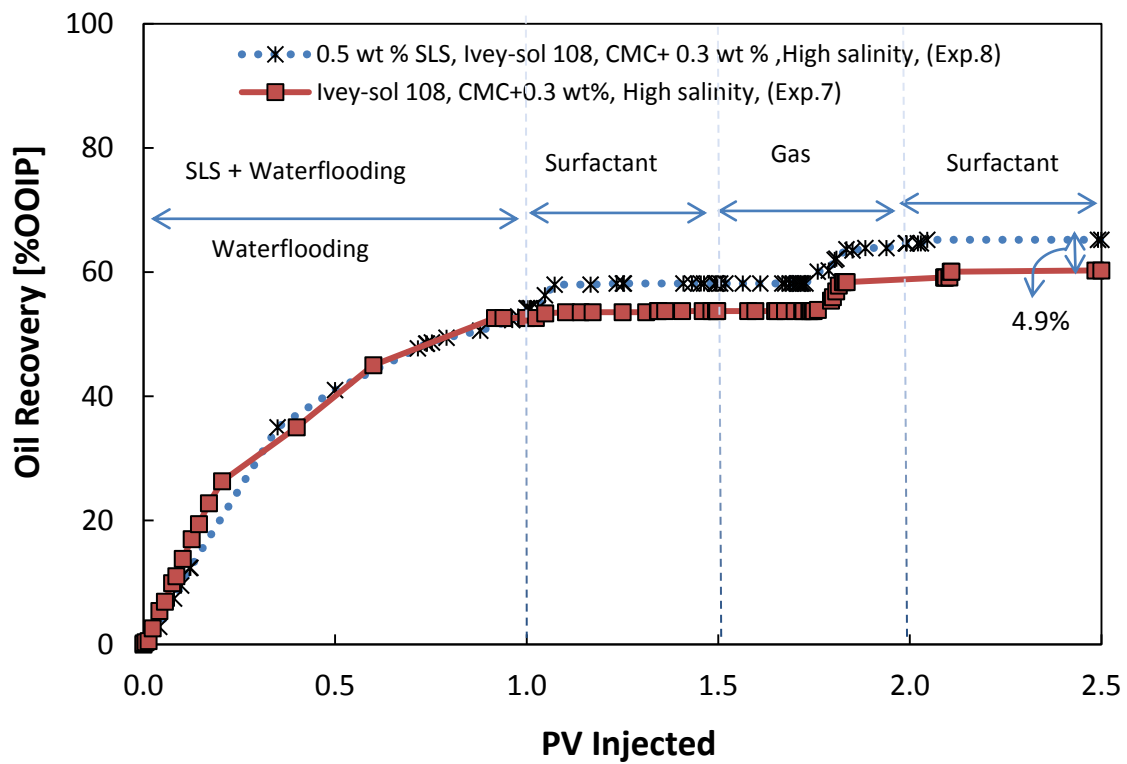


Figure 4.22 Effect of addition of SLS to the secondary waterflooding on total oil recovery

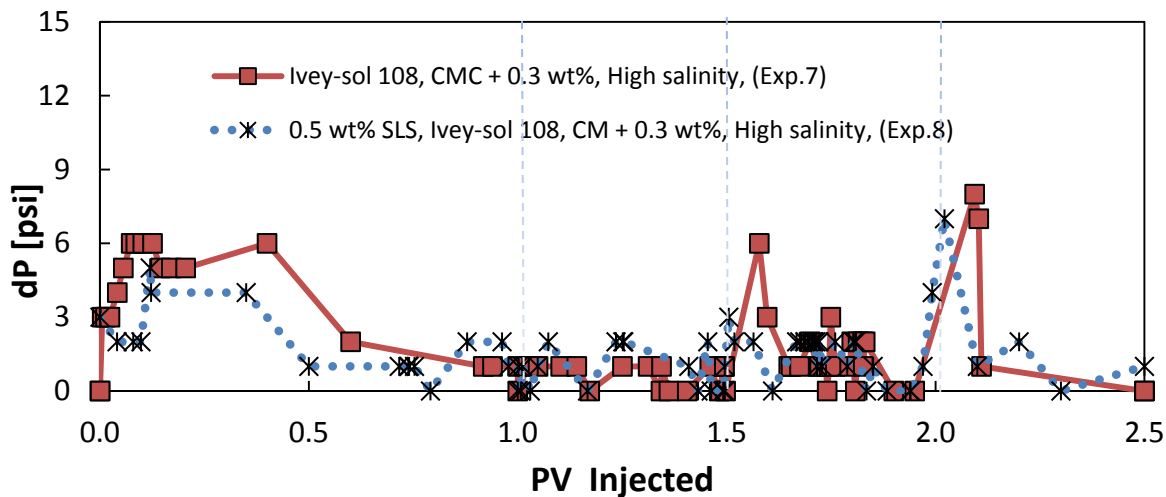


Figure 4.23 Pressure profile comparison in the absence and presence of sodium lignosulfonate in the secondary waterflooding.

4.4.7 Optimal Oil Recovery

Experiment 9 (TX-100 at 0.3 wt% + CMC in low salinity with the injection scheme of SLS-GSG) shows the optimal injection scheme based on the results previously described. The secondary waterflooding with the addition of 0.5 wt% SLS in low salinity brine was followed by a cycle of gas, and a cycle of TX-100 at 0.3 wt% + CMC surfactant concentration in low salinity brine, followed by a final gas cycle. The recovery curve is compared to previous experiments in Figure 4.24. As anticipated, the result showed the highest total oil recovery ($84.5 \pm 0.4\%$) compared to previous experiments. In this experiment, the major increase in oil recovery in the first cycle (one PV) is due to the effect of low salinity water which was discussed earlier. In the second cycle, gas injection improved the oil recovery compared to surfactant injection in experiment 8 (SLS-SGS, Ivey-sol 108 at 0.3 wt% + CMC in high salinity) and 6 (WSGS, TX-100 at 0.3 wt% + CMC in high salinity) due to water-wetness of the system prior to surfactant injection and wettability alteration. In the last gas injection cycle the improvement in oil recovery is due to foam generation when the rock is almost intermediate wet.

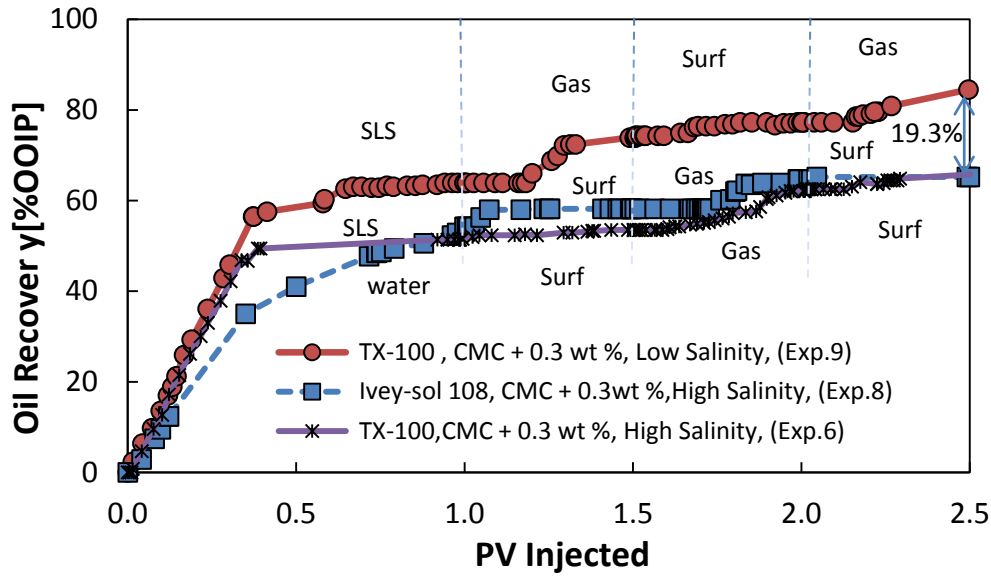


Figure 4.24 Optimization of experiments

Figure 4.25 shows the pressure profile for the optimized experiment. In the first cycle, there is no significant difference in pressure drops. For the experiment 9 (SLS-GSG, TX-100 at 0.3 wt% + CMC in low salinity) and 6 (WSGS, TX-100 at 0.3 wt% + CMC in high salinity) the main difference in differential pressure is due to difference in injection scheme.

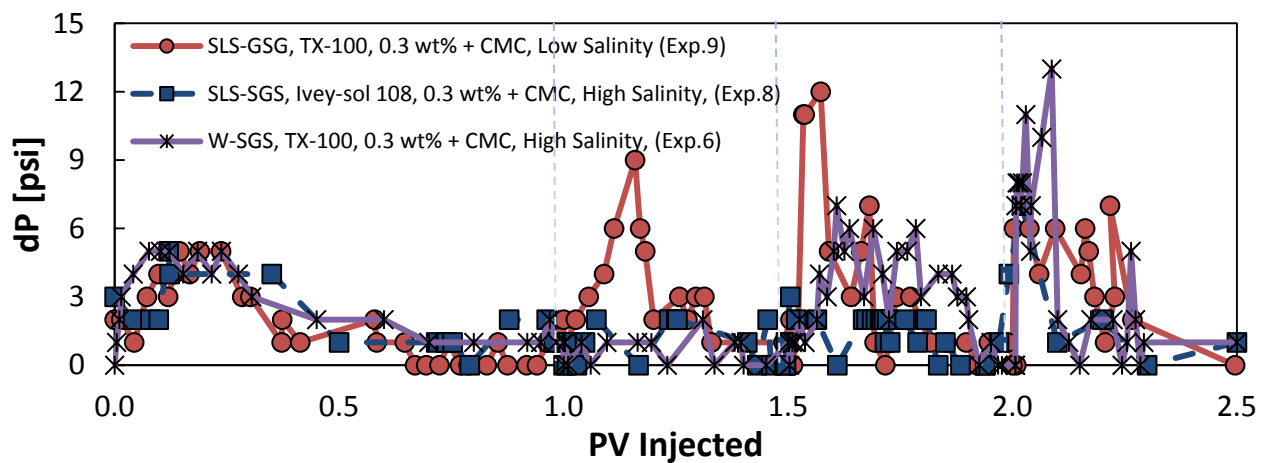


Figure 4.25 Pressure profile comparison

4.5 Considerations for Field Implementation

In SAG injection field applications, capital and operating costs for both gas and surfactant flooding should be considered. Capital and operating costs depend on rates and volumes predicted from a detailed simulation. For the gas injection, the capital costs include gas purchasing costs, compressors for reinjection of produced gas, injection gas recovery plants, gas injection facilities, pipelines for injected gas transmission, production facilities for handling increased amounts of produced gas, and separators and gas gathering surface facilities. Gas recovery plants can be the most expensive part of gas injection if one is not already nearby. Implementation of gas floods for offshore and deep water fields becomes even more expensive, mainly due to well costs and gas accessibility (Sheng, 2013).

Additional facilities (mixing tanks, storage tanks, pumps, pipes, etc.) are necessary to mix and process the chemical solutions at the field site; however these additional facilities are not very different from those used in routine oil field operations. Tubing and flow lines should be compatible with chemicals. In surfactant flooding, a large amount of water is required, and the quality of the water is the main factor to the success of surfactant flooding. Poor water quality may lead to less efficient surfactant injection and poor sweep efficiency. Each of the chemicals in the water should be identified because they may react with surfactants. Therefore, water treatment is required to filter suspended solids and to remove specific ionic parts such as the ferrous iron and divalent cations (Chang et al., 2013). Reverse osmosis and ion exchange units are commercially available and commonly used to remove specific cations to avoid interactions with chemicals. Surfactants are delivered to the field as high viscous liquids but they require being stored in insulated and heated tanks to maintain their viscosity suitable for pumping and efficient dilution (Sheng, 2013).

Offshore application of chemical EOR is limited to pilot activities due to several challenges such as remote locations, expensive wells and large well spacing, space and weight limitations on the deck, seawater as the source of injection water, and limited disposal options. All these challenges may not exist for a specific application; for instance, near shore projects may have some advantages over deepwater projects, particularly in disposal options and well costs. Also, produced emulsions from such projects may be pumped onshore for processing thereby reducing equipment weight and space requirements (Ibrahim et al., 2010).

Low salinity waterflooding is valuable when used for offshore because seawater reverse osmosis desalination equipment is very light and compact, which makes installation easy in small spaces. As suggested in our study, low salinity flooding can be used in combination with surfactant flooding.

Operating costs include labor, well servicing and workover, power, water disposal and injection and production facility maintenance costs. Workovers are typically a large percentage of field operating costs (Sheng, 2013).

The major potential environmental problems associated with chemical flooding are: (1) spills or leaks of chemical additives during transportation, storage and processing, (2) health hazards from dry chemicals and solutions to personnel operating the field; (3) leaks from surface storage and treatment ponds for produced brine; (4) leaks from high-pressure pipe transporting mixed chemicals to the wells; (5) underground leaks into shallow aquifers from damaged or corroded wells; (6) production into shallow aquifers from improperly plugged abandoned well (possible when the pressure of the oil reservoir is raised as a result of EOR activities); (7) subsidence along a fault plane caused by change of reservoir pressure.

4.6 Economic Analysis

When there are so many options an economic tool is needed to check the viability of projects before sanctioning one of them. The Net Present Value (NPV) is used and any project that has the highest NPV is favored. In this work, NPV value has been calculated for the experiment 1 (WAG injection, W-G-W-G, 7000 ppm TDS brine) and 9 (optimized SAG, SLS-G-S-G, 0.5 wt% SLS in secondary flooding, TX-100 at 0.3 wt% + CMC in 7000 ppm TDS brine) for a hypothetical reservoir with the characteristics listed in Table 4.5. Porosity, Permeability are assumed to be the same as the Berea core sample in coreflooding experiments. Connate water saturation and residual oil saturation are selected according to the corresponding values from experiment 1 and 9 (Table 4.4).

Table 4.5 Reservoir characteristics

OOIP (Sm³)	123,000,000
Porosity (%)	18.7
Permeability (mD)	58.5 Brine
Connate water saturation, S_{wc}	0.31- 0.33
Residual oil saturation, S_{or}	0.24 - 0.26

In carrying out this analysis, a number of assumptions were made which are as follow:

1. Total time to complete each scenario is 25 years;

Secondary flooding duration = 10 years

Each single cycle of water/surfactant/gas in WAG and SAG scenarios = 5 years

2. Oil price = \$ 75 USD/bbl
3. TX-100 price = \$ 74 USD/kg
4. SLS price = \$ 0.30 USD/kg
5. Total Facility cost of surfactant injection at the start of the project (before production) = \$ 8,850,000 USD (rough estimation from Warner ASP Flood project, Taber 2007)
6. Effective interest rate = 6%
7. The costs for the gas injection are considered to be identical in both cases and omitted from the calculations.

The results of economic analysis for the two scenarios are listed in Table 4.6. The detailed table of the economic analysis is presented in Appendix D. NPV at the end of each year is shown in Figure 4.26 for both scenarios. About \$ 2,728,000,000 USD higher NPV was achieved when SAG injection was used.

Table 4.6 Economic analysis of WAG and SAG injection

Exp. #	Injection Scheme	SLS Conc. (wt%)	Surfactant type, Conc. (wt%)	Total Recovery (%OOIP)	Revenue (\$ USD)	Capex (\$ USD)	Total NPV (\$ USD)
1	W-G-W-G	-	-	71.5 ± 0.1	3.3288E+10	0.0	3.3288E+10
9	SLS-G-S-G	0.5	TX-100, 0.316	84.5 ± 0.1	3.6025E+10	9.3810E+06	3.6016E+10

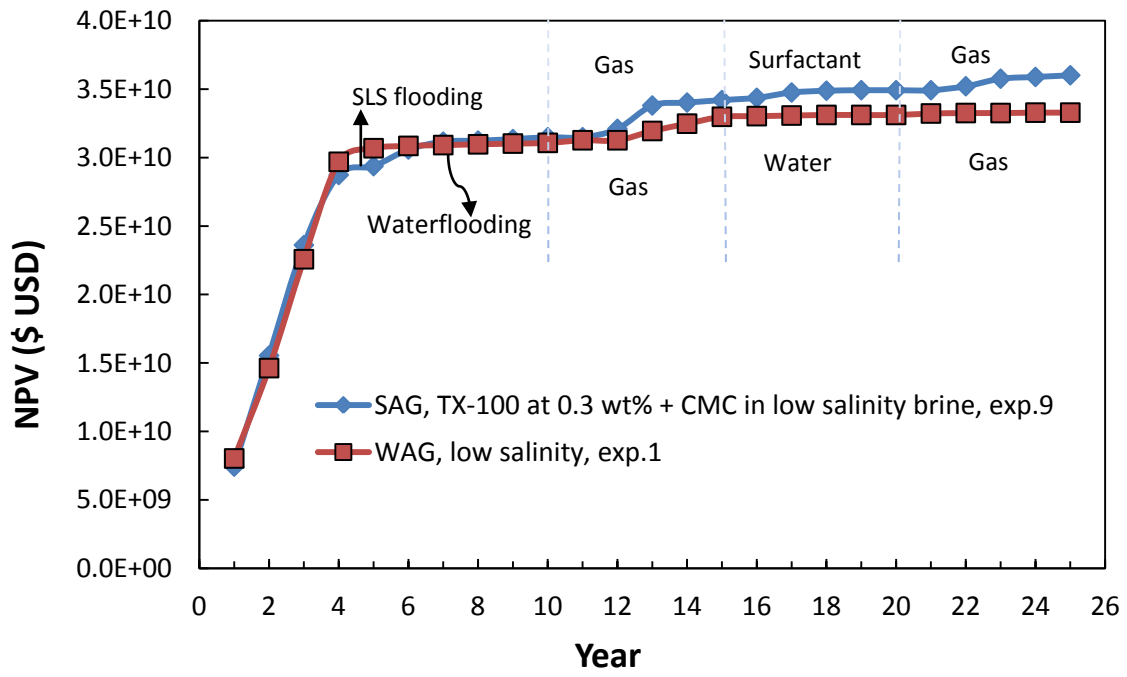


Figure 4.26 Net Present Value (NPV) for SAG and WAG injection

5. CONCLUSION AND RECOMMENDATIONS

5.1 Summary of Findings and Conclusions

Two nonionic surfactants (Ivey-Sol 108 and TX-100) were tested in a comparative laboratory study in a series of surfactant-alternating-gas tests to evaluate the effect of surfactant type, concentration, water salinity, injection scheme and presence of sodium lignosulfonate (as a sacrificial adsorption additive, prior to surfactant injection) on oil recovery. The interfacial tension between both of the surfactant solutions and the oil phase and wettability alteration in the presence of the surfactant solutions were measured, and foam generation and stability were investigated.

The salient effects of the aforementioned parameters on foam stability, interfacial tension, wettability and oil recovery are as follow:

1. Results from dynamic foam stability tests (air injection) and static tests (bottle shake) show that foam stability can be significantly improved by increasing surfactant concentration. In the absence of oil, foam generated using Ivey-sol 108 at 0.3 wt% above CMC was more stable in air injection method, while for bottle shake test, TX-100 was more stable. In the presence of oil, Ivey-sol 108 was more stable compared to TX-100. Foam generated from TX-100 solution lasted longer in both cases since it had a higher initial foam height.
2. From the results of air injection and bottle shake foam stability tests, it was found that foam is more stable in lower salinity brine; moreover, a lower interfacial tension and smaller contact angle were obtained when using lower salinity solutions.

3. The IFT decreased with an increase in surfactant concentration. At constant water salinity (21000 ppm TSD), the IFT for TX-100 is almost eight times smaller than that of Ivey-sol 108 at 0.3 wt% above their CMCs and 3.4 times less at their respective CMCs. A reduction of two orders of magnitude in oil-water interfacial tension was obtained with TX-100 surfactant, which is insufficient for enhancing the residual oil recovery. This clearly proves that wettability alteration is the predominant mechanism in improving oil recovery during surfactant injection. However, lower interfacial tension is favorable to generate stronger foam during the gas injection cycle which leads to higher oil recovery.
4. The results of contact angle measurements show that, generally, the contact angle will increase (the rock will become less water-wet) with increasing surfactant concentration. Measurements with and without TX-100 at 0.3 wt% > CMC, at 25°C and 500 psi indicate that the initially water-wet Berea sandstone sample was altered to intermediate wet by this surfactant, which leads to higher oil recovery.
5. Generally, TX-100 was superior to Ivey-sol 108 in improving recovery of residual oil. TX-100 was able to alter the wettability toward intermediate-wet, which is a more favorable condition compared to a strongly water-wet or oil-wet condition in enhancing oil recovery. Surfactants above their CMC values produced more stable foams, as observed by higher differential pressure, during gas injection, which led to higher oil recovery.
6. The injection of low salinity brine increased the recovery of oil by 13.0%. The major increase was observed during the secondary waterflooding section (10.5% improvement).
7. The injection scheme of gas-surfactant-gas was more efficient compared to surfactant-gas-surfactant. This can be explained considering the hysteresis effect of drainage and

imbibition processes. Residual oil is primarily trapped in large pores of water-wet rock after waterflooding (imbibition) whereas gas injection is a drainage process thereby better sweeping the residual oil from the larger pores assuming no other viscous or gravity effects.

8. The addition of 0.5 wt% sodium lignosulfonate (SLS) to the secondary waterflooding results in a major amount of adsorption to the rock surface. This was observed qualitatively by the significant color change of the produced water phase. This sacrificial additive prevented the surfactant adsorption on the rock surface during the surfactant injection cycle resulting in a better propagation of surfactant through the core leading to improved oil recovery by 4.9% compared to the case without SLS.
9. The total oil recovery increased by 13.0% when we used optimized injection scheme (SAG injection, with 0.5 wt% SLS in the secondary waterflooding, TX-100 at 0.3 wt% + CMC in low salinity water, experiment 9) compared to WAG (low salinity, experiment 1).

5.2 Recommendations and Future Work

1. Surfactant adsorption has a substantial negative impact on the performance and economics of foam. Batch equilibrium and circulating tests can be conducted to evaluate surfactant adsorption on the rock surface.
2. Foam stability must be tested for bubble sizes that are comparable to the rock pore sizes. It is possible that two surfactants produce foams with different droplets scales and the better foam eventually is the one where droplets are on the pore scale, so it would be useful to study the droplet size distributions of the foams.

3. The thin film pressure balance (TFPB) technique should be used to measure the equilibrium film thickness and disjoining pressure isotherms of foam films containing varying concentration of nonionic surfactant.
4. The findings from the experiments could be implemented in a chemical flooding simulator like UTCHEM for comparison of results and as a basis for economic analyses.
5. In future experiments, the Berea sandstone sample can be aged and some chemicals can be used to create a strongly oil-wet system, then the effect of the same surfactants on contact angle and oil recovery can be evaluated.
6. Foam thermal stability at high temperatures ($> 70 - 80$ °C) should be evaluated. Corefloods should be conducted with live reservoir fluids and formation rock sample and at reservoir conditions in order to enable collection of data for field-scale reservoir simulation studies and to facilitate field implementation of promising concepts and processes.

REFERENCES

- Abdel-Wali, A. A. (1996). Effect of Simple Polar Compounds and Salinity on Interfacial Tension and Wettability of Rock/Oil/Brine System. *Journal of King Saud University-Engineering Science*, 8(2), 153-163.
- Afsharpoor, A. (2009). *Mechanistic Foam Modeling and Simulations: Gas Injection During Surfactant- Alternating-Gas Processes Using Foam-Catastrophe Theory* (Master's thesis). Louisiana State University, U.S.A.
- Agbalaka, C., Dandekar, A. Y., Patil, S. L., Khataniar, S., Hemsath, J. R. (2008). The Effect of Wettability on Oil Recovery: A Review. *SPE Asia Pacific Oil & Gas Conference and Exhibition, Perth, Australia*, SPE 114496.
- Alkan, H., Goktekin, A., Satman, A. (1991). A Laboratory Study of CO₂-Foam Process for Bati Raman Field. *SPE Middle East Oil Show, Kingdom of Bahrain*, SPE 21409.
- Ayirala, S. (2002). *Surfactant-Induced Relative Permeability Modifications for Oil Recovery Enhancement* (Master's thesis). Louisiana State University, U.S.A.
- Bergeron, V. (1999). Forces and Structures in Thin Liquid Soap Films. *Journal of Physics: Condensed Matter*, 11, 215-238.
- Bond, D. C., and Holbrook O. C. (1958). *Gas Drive Oil Recovery Process*. U.S. Patent No.2866507.
- Boneau, D. F., and Clampitt, R. L. (1977). A Surfactant System for Oil-Wet Sandstone of the North Burbank Unit. *Journal of Petroleum Technology*, 29(5), 501-506.
- Boon, J. A. (1984). Chemistry in Enhanced Oil Recovery- An Overview. *Journal of Canadian Petroleum Technology*, 23(1).
- Cai, B., Yang, J., Guo, T. (1996). Interfacial Tension of Hydrocarbon + Water/Brine Systems under High Pressure. *Journal of Chemical Engineering*. 41(3), 493-496.
- Chang, H., Yanming, G., Wu, F., Huaye, H. (2013). Chemical Injection Facilities – From Pilot Test to Field-Wide Expansion. *SPE Enhanced Oil Recovery Conference held in Kuala Lumpur, Malaysia*, SPE 165308.
- Chatzis, Ioannis. Fundamentals of Petroleum Production ChE 514. University of Waterloo, Waterloo, ON. 2003. Class lecture.

- Chiwetelu, C., Neale, G., Hornof, V. (1980). Improving the Oil Recovery Efficiency of Lignosulfonate Solutions. *Canadian Petroleum Technology*, 19(3).
- Chou, S. I., Vasicek, S. L., Pizio, D. L., Jasek, D. E., Goodgame, J. A. (1992). CO₂ Foam Field Trial at North Ward-Estes. *SPE Annual Technical Conference and Exhibition, Washington, D. C.*, SPE-24643-MS.
- Cuiec, L. E. (1975). Restoration of the Natural State of Core Samples. *50th Annual Fall Meeting of the Society of Petroleum Engineers of AIME held in Dallas, Texas*, SPE 5634.
- Derjaguin, B. V. and Landau, L. D. (1941). *Acta Physicochem. USSR*, 14, 633.
- Donaldson, E. C., and Chilingarian, T. F. (1989). *Enhanced Oil Recovery, II: Processes and Operations*. Elsevier, 258-285.
- Eson, R. I., and Cooke, R. W. (1989). A Comprehensive Analysis of Steam Foam Diverters and Application Methods. *SPE California Regional Meeting, Bakersfield, California*, SPE 10785.
- Farajzadeh, R., Andrianov, A., Krastev, R., Hirasaki, G. J., Rossen, W. R. (2012). Foam-Oil Interaction in Porous Media: Implications for Foam Assisted Enhanced Oil Recovery. *SPE conference at Oil and Gas West Asia held in Muscat, Oman*, SPE 154197.
- Gant, P. L., and Anderson, W. G. (1986). Core Cleaning for Restoration of Native Wettability. *Rocky Mountains Regional Meeting of the Society of Petroleum Engineers, Billings, MT*, SPE 14875.
- Garcias, A., Fortney, L. N., Schechter, R. S., Wade, W. H., Yiv., S. (1982). Criteria for Structuring Surfactants to Maximize Solubilisation of Oil and Water: Part 1-Commercial Nonionics. *Society of Petroleum Engineers Journal*, 22(5), 743-749.
- Hanssen, J. E., Castanier, L. M., Surgucev, L. M., Dalland, R. F. (1995). Field Experiences with Foam Processes. A Critical Review. *16th Collaborative Project on Enhanced Oil Recovery Workshop and Symposium, Japan*.
- Heller, J. P. (1994). *CO₂ Foams in Enhanced Oil Recovery*. American Chemical Society, 242, 201-234.
- Hirasaki, G. J., Miller, C. A., Puerto, M. (2008). Recent Advances in Surfactant EOR. *SPE*, 16(04), 889-907.
- Hirasaki, G. J., and Zhang, D. L. (2004). Surface Chemistry of Oil Recovery from Fractured, Oil-Wet, Carbonate Formations. *SPE*, 9(2), 151-162.

- Holm, L. W. (1970). Foam Injection Test in the Siggins Field, Illinois. *Journal of Petroleum Technology*, SPE-2750-PA, 22 (12), 1499-1506.
- Holm, L. W., and Garrison, W. H. (1988). Diversion with Foam in an Immiscible CO₂ Field Project. *SPE Reservoir Engineering*, 3(1), 112-118.
- Hong, S. A., Bae, J. H., Lewis, G. R. (1987). An Evaluation of Lignosulfonate as a Sacrificial Adsorbate in Surfactant Flooding. *SPE Reservoir Engineering*, 2(1), 17-27.
- Ibrahim, K., Narayasami, D., Jaberi, M., Briers, J., Goh, K., and de Boer, F. (2010). Asset-Wide Reconciled Production Monitoring-a Key Enabler to Successful Real-Time Field Management. *SPE Intelligent Energy Conference and Exhibition, Utrecht, the Netherlands*, SPE 128654.
- Iyer, S. (2014). Rules for Identifying Significant Figures with Examples. Retrieved from <http://www.buzzle.com/articles/rules-for-identifying-significant-figures-with-examples.html>
- Jadhunandan, P. P., and Morrow, N. R. (1991). Effect of Wettability on Waterflood Recovery for Crude-Oil/Rock System. *66th Annual Technical Conference and Exhibition, Dallas, TX*, SPE 22597.
- Jiménez, A. I., and Radke, C. J. (1989). Dynamic Stability of Foam Lamellae Flowing Through Periodically Constricted Pore. *Oil-Field Chemistry*, 25, 460-479.
- Kalfoglou, G., Prieditis, J., Paulett, G. S. (1997). Lignosulfonate-acrylic acid graft copolymers as sacrificial agent for carbon dioxide foaming agents. Canadian Patent CA2185499 A1.
- Kam, S. I., and Rossen, W. R. (2002). A Model for Foam Generation in Homogeneous Media. *SPE Annual Technical Conference and Exhibition, San Antonio, TX*, SPE 77689.
- Kennedy, H. T., Burja, E. O., Boykin, R. S. (1955). An Investigation of the Effects of Wettability on the Recovery of Oil by Waterflooding. *Physical Chemistry*, 59(9), 867-869.
- Khatib, Z. I., and Hirasaki, G. J. (1988). Effects of Capillary Pressure on Coalescence and Phase mobilities in Foams Flowing through Porous Media. *SPE*, 3(3), 919-926.
- Kibodeaux, K. R., and Rossen, W. R. (1997). Coreflood Study of Surfactant-Alternating-Gas Foam Processes: Implications for Field Design., *SPE Western Regional Meeting held in Long Beach, California*, SPE 38318.
- Kopeliovich, D. (2013, June 1). Surfactants. Retrieved from <http://www.substech.com/dokuwiki/doku.php?id=surfactants>
- Kornev, K. G., Niemark, A. V., Rozhkov, A. N. (1999). Foam in Porous Media: Thermodynamic and Hydrodynamic Peculiarities. *Advance in Colloid and Interface Science*, 82, 127-187.

- Kovscek, A. R., and Radke, C. J. (1996). Gas Bubble Snap Off Under Pressure-Driven Flow in Constricted Noncircular Capillaries. *Colloids and Surface*, 117, 55-76.
- Kovscek, A. R., and Radke, C. J. (2003). Pressure-driven Capillary Snap-off Gas Bubbles at Low Wetting-Liquid content. *Colloids and Surface*, 212, 99-108.
- Kovscek A. R., and Radke, C. J. (1994). *Fundamentals of Foam Transport in Porous Media Foams: Fundamentals and Applications in the Petroleum Industry*. American Chemical Society, 242, 115-163.
- Kuhlman, M. I., Lau, H. C., Falls, A. H. (2000). Surfactant Criteria for Successful Carbon Dioxide Foam in Sandstone Reservoirs. *SPE Reservoir Evaluation & Engineering*, 3(1), 35-41.
- Lager, A., Webb, K. J., Black, C. J., Singleton, M., Sorbie, K. S. (2006). Low Salinity Oil Recovery-An Experimental Investigation. *International Symposium of the Society of Core Analysts, Norway*, SCA2006-36.
- Lawson, J. B. (1978). The adsorption of Nonionic Surfactants on Sandstone and Carbonate. *SPE Symposium on Improved Methods for Oil Recovery, Tulsa, Oklahoma*, SPE 7052.
- Li, K., Lenormand, R., Robin, M., Codreanu, B. D. (1997). Numerical Evaluation of the Combined Effect of Wettability and Heterogeneity on Waterflood Performance. *International Energy Agency, Copenhagen DK*.
- Liave, F. M., and Olsen, D. K. (1994). Use of Mixed Surfactants to Generate Foams for Mobility Control in Chemical Flooding. *SPE Reservoir Engineering*, 9(12), 125-132.
- Liu, Y., Grigg, R. B., Bai, B. (2005). Salinity, pH, and Surfactant Concentration Effects on CO₂-Foam. *SPE International Symposium on Oilfield Chemistry, Woodlands, Texas, USA*. SPE 93095.
- Marsden, S. S., Eerligh, J. P., Albrecht, R. A., David, A. (1967). Use of Foam in Petroleum Operations. *7th World Petroleum Congress, Mexico*.
- Mohammadi, S. S., and Tenzer, J. R. (1990). Steam-Foam Pilot Project at Dome-Tumbador, Midway Sunset Field: Part 2. *SPE/DOE Enhanced Oil Recovery Symposium, Tulsa, Oklahoma*, SPE-20201-MS.
- Moradi-Araghi, A., Johnston, E. L., Zornes, D. R., Harpole, K. J. (1997). Laboratory Evaluation of Surfactants for CO₂-Foam Applications at the South Cowden Unit. *SPE International Symposium on Oilfield Chemistry held in Houston, Texas*, SPE 37218, 16-21.

- Moore, T. F., and Slobod, R. L. (1956). Effect of Viscosity and Capillarity on Displacement of Oil by Water. *Producers Monthly*, 20, 20-30.
- Moroi, Y., (1992). *Micelles: Theoretical and Applied Aspects*. Springer Science & Business Media, 47.
- Mysels, K. J., Shinoda, K., and Frankel, S. (1959). *Soap Films: Studies of Their Thinning*. London, UK, Pergamon Press.
- Nasralla, R. A., Bataweel, M. A., Nasr-El-Din, H. A. (2013). Investigation of Wettability Alteration and Oil-Recovery Improvement by Low-Salinity Water in Sandstone Rock. *SPE Offshore Europe Oil and Gas Conference and Exhibition*, SPE 146322.
- Perlman, H. (2014, Apr 30). Saline Water. Retrieved from <http://water.usgs.gov/edu/saline.html>
- Ransohoff, T. C., and Radke, C. J. (1988). Mechanisms of Foam Generation in Glass-Bead Packs. *SPE Reservoir Engineering*, 3(2) 573-585.
- Rao, D. N., Ayirala, S. C., Abe, A. A., Xu, W. (2006). Impact of Low-Cost Dilute Surfactants on Wettability and Relative Permeability. *SPE/DOE Symposium on Improved Oil Recovery held in Tulsa, Oklahoma*, SPE 99609.
- Rateman, K. T. (1989). An Investigation of Oil Destabilization of Nitrogen Foams in Porous Media. *SPE Annual Technical Conference and Exhibition, Texas*, SPE 19692.
- Rossen, W. R., and Gauglitz, P. A. (1990). Percolation Theory of Creation and Mobilization of Foams in Porous Media. *AIChEJ*, 36, 1176-1188.
- Safarzadeh, M. A., and Nejad, S. A. (2011). Experimental Investigation of the Effect of Calcium Lignosulfonate on Adsorption Phenomenon in Surfactant Alternative Gas Injection. *Journal of Chemical and Petroleum Engineering, University of Tehran*, 45(2), 141-151.
- Salathiel, R. A. (1973). Oil Recovery by Surface Film Drainage in Mixed-Wettability Rocks. *Journal of Petroleum Technology*, 1216-1224.
- Schimdt, R. L. (1990). Thermal Enhanced Oil Recovery-Current Status and Future Needs. *Chemical Engineering Progress*, 47-59.
- Schramm, L. L., and Wassmuth, F. (1994). *Foams: Fundamentals and Application in the Petroleum Industry*. Washington: American Chemical Society.
- Shafian, S. R., Bahrim, R. Z., Hamid, P. A., Manap, A. A., Darman, N., Sedaralit, M. F., Bhd, C. S., Tewari, R. D. (2013). Enhancing the Efficiency of Immiscible Water Alternating Gas (WAG)

Injection in a Matured, High Temperature and High CO₂ Solution Gas Reservoir- A Laboratory Study. *Enhanced Oil Recovery Conference held in Kuala Lumpur, Malaysia*, SPE 165303.

Sharma, M. K., Brigham, W. E., Shah, D. O. (1986). Effect of Mixed-Chain-Length Surfactants on Fluid Displacement in Porous Media by In-Situ Foaming Process. *SPE Reservoir Engineering*, 1(3), 253-260.

Sheng, J. (2011). *Modern Chemical Enhanced Oil Recovery, Theory and Practice*. Burlington, MA, USA: Gulf Professional Publishing.

Sheng, J. (2013). *Enhanced Oil Recovery Field Case Studies*. Gulf Professional Publishing, 2013, 11, 265-276.

Shi, J. X., and Rossen, W. R. (1998). Improved Surfactant-Alternating-Gas Foam Process to Control Gravity Override. *SPE/DOE Improved Oil Recovery Symposium, Tulsa*, SPE 39653.

Skjæveland, S. M., and Kleppe, J. (1992). Recent Advances in Improved Oil Recovery Methods for North Sea Sandstone Reservoirs. SPOR monograph, 1.

Spirov, P., Rudyk, S. N., Khan, A. A. (2012). Foam Assisted WAG, Snorre Revisit with New Foam Screening Model. *North Africa Technical Conference and Exhibition in Cairo, Egypt*, SPE-150829-MS.

Syahputra, A. E., Tsau, J. S., Grigg, R. B. (2000). Laboratory Evaluation of Using Lignosulfonate and Surfactant Mixture in CO₂ Flooding. *SPE/DOE Improved Oil Recovery Symposium held in Tulsa, Oklahoma*, SPE 59368.

Taber, J. J., Martin, F. D., Seright, R. S. (1997). EOR Screening Criteria Revisited-Part 1: Introduction to Screening Criteria and Enhanced Recovery Field Projects. *SPE/DOE Improved Oil Recovery Symposium, Tulsa*, SPE 35385.

Taber, S. (2007). Warner ASP Flood, Annual Report, June 28, 2007. Retrieved from www.energy.gov.ab.ca

Tang, G. Q., and Morrow, N. R. (1999). Influence of Brine Composition and Fines Migration on Crude Oil Brine Rock Interactions and Oil Recovery. *Journal of Petroleum Science & Engineering*, 24, 99-111.

Taylor, J. R. (1982). *An Introduction to Error Analysis*. University Science Books, Mill Valley, California.

The EOR Alliance. (2014, June 12). Gas Foam. Retrieved from <http://www.eor-alliance.com/solutions/foam>

Tsau, J., Syahputra, A. E., Grigg, R. B. (2000). Economic Evaluation of Surfactant Adsorption in CO₂ Foam Application. *SPE/DOE Improved Oil Recovery Symposium, Tulsa*, SPE 59365.

Turta, A. T., and Singhal, A. K. (2002). Field Foam Applications in Enhanced Oil Recovery Projects: Screening and Design Aspects. *Canadian Petroleum Technology*, 41(10).

Verkruyse, L. A., and Salter S. J. (1985). Potential Use of Nonionic Surfactants in Micellar Flooding., *SPE International Symposium on Oilfield and Geothermal Chemistry, Arizona*, SPE 13574.

Verwey, E. J. W., and Overbeek, J. Th. G. (1948). Theory of Stability of Liophobic colloids, *Elsevier, Amesterdam*.

Wang, Y., Wang, L., Li, J. (2001). Surfactant Oil Displacement System in High Salinity Formations: Research and Application. *SPE Permian Basin Oil and Gas Recovery Conference, Midland, TX*, SPE70047.

Wassmuth, F. R., Green, K. A., Randall, L. (2001). Details of In-Situ Foam Propagation Exposed with Magnetic Resonance Imaging. *SPE Reservoir Engineering*, 135-1459.

Swagelok Web Catalog. (2014, August) Stainless Steel Tubing, Valve and Fittings. Retrieved from www.swagelok.com

Wenxiang, W., and Jianhua, P. (2010). Study on the Foamability and its Influencing Factors of Foaming Agents in Foam-Combined Flooding. *Power and Energy Engineering Conference (APPEEC), Asia-Pacific*.

Xu, Q., and Rossen, W. R. (2003). Experimental Study of Gas Injection in Surfactant-Alternating-Gas Foam Process., *SPE Annual Technical Conference and Exhibition held in Denver, USA*, SPE 84183.

Zhang, P., and Austad, T., (2005). The Relative Effects of Acid Number and Temperature on Chalk Wettability. *SPE International Symposium on Oilfield Chemistry, Houston*, SPE 92999.

Zheng, Y. (2012). *Effect of Surfactants and Brine Salinity and Composition on Spreading, Wettability and Flow Behavior in Gas-Condensate Reservoirs* (Doctoral dissertation). Louisiana State University, U.S.A.

Zhong, L., Siddiqui, S., El-Hardalo, S., and Islam, M. R. (1998). A Rapid Standard Test for Screening Foam-Forming Surfactants. *8th International Petroleum Exhibition and Conference in Abu Dhabi, U.A.E.*, SPE 49559.

Ziegler, V. M., and Handy, L. L. (1981). Effect of Temperature on Surfactant Adsorption in Porous Media. *SPE*, 21(2), 218-228.

Zubair, A., James, L. A., and Hawboldt, K. (2013). Screening of non-ionic surfactants for Bunker C contaminated soil washing. *36th AMOP Technical Seminar on Environmental Contamination and Response. Halifax, Canada*, 871-887.

APPENDIX

APPENDIX A: Error Analysis

1. Reading Errors:

A rule of thumb for evaluating the reading error on measuring devices, such as ruler is $\pm 1/2$ of the smallest division, and for many digital instruments, it is assumed that the reading error is $\pm 1/2$ of the last digit displayed; e.g. in our case that the mass of the dry core was measured 743.2831 (g) using a mass balance, the error can be assumed to be ± 0.00005 (g).

In the coreflooding experiments, a 50 ml burette with the 0.1 ml graduation level was used for measuring produced fluids volume. The level of water and oil is read to the nearest 0.1 ml; therefore, a reasonable estimate of the uncertainty in this case would be ± 0.05 ml.

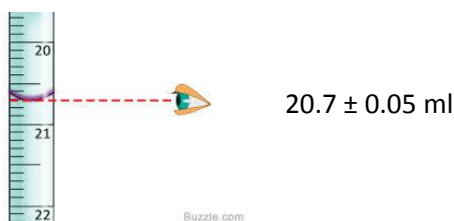


Figure A.1 Burette reading (Iyer, 2014)

2. Mean Value and Standard Deviation:

The best estimate of a quantity x measured n times (interfacial tension or contact angle in our case), is assumed to be the average or mean value of x (Taylor, 1982):

$$\bar{x} = \frac{1}{n} \sum_1^n x_i$$

The standard deviation of x is given by

$$\sigma = \sqrt{\frac{\sum_1^n (x_i - \bar{x})^2}{n-1}}$$

3. Propagation of Errors:

Suppose we have measured the value of x_1 and x_2 with uncertainty Δx_1 and Δx_2 respectively. If

$$y = f(x_1, x_2)$$

A simple error calculation is:

$$\Delta y \approx \frac{df}{dx_1} \Delta x_1 + \frac{df}{dx_2} \Delta x_2$$

3-1) Calculation of Δy According to the Standard Deviation:

Rule 1: If two mutually independent quantities are being added or subtracted:

$$y = x_1 + x_2 \quad \text{or} \quad y = x_1 - x_2$$

then,

$$\Delta y = \sqrt{(\Delta x_1)^2 + (\Delta x_2)^2}$$

Rule 2: If two mutually independent quantities are being multiplied or divided:

$$y = x_1 x_2 \quad \text{or} \quad y = \frac{x_1}{x_2}$$

then,

$$\frac{\Delta y}{y} = \sqrt{\left(\frac{\Delta x_1}{x_1}\right)^2 + \left(\frac{\Delta x_2}{x_2}\right)^2}$$

Rule 3: If a quantity is raised to a power:

$$y = x^n$$

then,

$$\frac{\Delta y}{y} = n \frac{\Delta x}{x}$$

APPENDIX B: Porosity and Absolute Permeability Measurement

B-1: Porosity Measurement and Pore Volume Calculation

1. Mass of dry core = $M_{\text{dry}} = 743.2831 \pm 0.00005$ (g)
2. Mass of wet core after 20 minutes saturating = $M_{\text{wet, 20 mins}} = 805.7021 \pm 0.00005$ (g)
3. Mass of wet core after 45 minutes saturating = $M_{\text{wet, 45 mins}} = 808.4362 \pm 0.00005$ (g)
4. Mass of wet core after 60 minutes = $M_{\text{wet, 60 mins}} = 808.6651 \pm 0.00005$ (g)
5. Mass of wet core after 2 hours = $M_{\text{wet, 2 hours}} = 808.6952 \pm 0.00005$ (g)
6. Total volume of core = $V_{\text{total}} = 350 \pm 0.5$ (cm³)
7. $\Delta M = M_{\text{wet, 2 hours}} - M_{\text{dry}} = (808.6952 \pm 0.00005) - (743.2831 \pm 0.00005) = 65.4121 \pm 0.00007$ (g)
8. Water density = $\rho = 0.9982$ (g/cm³)

Porosity =

$$\Phi = \frac{\Delta M(\text{g}) / \rho (\text{g} / \text{cm}^3)}{V_{\text{total}}(\text{cm}^3)} = \frac{(65.4121 \pm 0.00007 (\text{g})) / 0.9982(\text{g} / \text{cm}^3)}{350 \pm 0.5 (\text{cm}^3)} = 0.1872 \pm 0.0001$$

9. Pore Volume (PV) = $V_{\text{total}} \times \Phi = (350 \pm 0.5 (\text{cm}^3)) \times (0.1872 \pm 0.0001) = 65.4 \pm 0.1 (\text{cm}^3)$

B-2: Absolute Permeability Measurement:

Table B.1 Primary water flooding

Exp # 1: Primary water flooding				
Flow rate (cm ³ /min)	Time	Pin (psi)	Pump volume (cm ³)	Pout (psi)
0.100	14:33	522	389.14	519
	14:59	512	386.58	510
	15:10	505	385.45	503
	15:17	525	384.81	524
	16:40	516	376.53	515
	17:00	516	374.56	515

Using Darcy's law:

$$K = \frac{Q \cdot \mu \cdot L}{A \cdot \Delta P}$$

$$Q = 0.100 \pm 0.0005 \text{ (cm}^3\text{/min)} = 0.0017 \pm 0.00001 \text{ (cm}^3\text{/s)}$$

$$\mu = 0.89 \text{ (cP)}$$

$$L = 30.5 \text{ (cm)}$$

$$A = 11.39 \text{ (cm}^2\text{)}$$

$$\Delta P = 1 \pm 0.5 \text{ psi} = 0.07 \pm 0.03 \text{ (atm)}$$

$$K = \frac{(0.0017 \pm 0.00001) \times 0.89 \times (30.5 \pm 0.05)}{11.39 \times (0.07 \pm 0.03)} = 0.058 \pm 0.025 \text{ (Darcy)} = 58.5 \pm 25.0 \text{ (mD)}$$

APPENDIX C: Raw Data

C-1: Foam Stability Test Raw Data

Table C.1 Foam stability dynamic test in the absence of oil

		Time (min)	0	2	4	6	8	10	12	15
Surfactant Type	Salinity (ppm TDS)	Concentration (wt%)	Foam Height (cm³)							
Ivey-sol 108	7000	CMC	0	0	0	0	0	0	0	0
	7000	0.3 + CMC	370	370	350	340	340	340	340	330
	21000	CMC	0	0	0	0	0	0	0	0
	21000	0.3 + CMC	400	390	360	340	320	310	300	300
TX-100	7000	CMC	350	340	300	250	200	190	150	120
	7000	0.3 + CMC	440	435	420	390	370	340	310	300
	21000	CMC	360	330	250	200	175	150	100	65
	21000	0.3 + CMC	450	435	400	360	320	300	270	250

Table C.2 Foam stability dynamic test in the presence of oil

Surfactant Type	Salinity (ppm TDS)	Concentration (wt%)	Foam Initial Volume (cm³)	Foam Collapse Time (seconds)
Ivey-sol 108	7000	CMC	0	0
	7000	0.3 + CMC	5	5
	21000	CMC	0	0
	21000	0.3 + CMC	10	10
TX-100	7000	CMC	10	30
	7000	0.3 + CMC	15	61
	21000	CMC	5	24
	21000	0.3 + CMC	10	45

Table C.3 Foam stability static test in the absence of oil

		Time (min)	0	15	30	45	60	75	90	105	120	135	150
Surfactant type	Salinity (ppm TDS)	Conc. (wt %)	Foam Height (mm)										
TX-100	7000	0.3 + CMC	90	85	75	75	75	75	75	73	73	73	73
	21000	0.3 + CMC	90	80	71	70	70	70	70	68	68	68	68
	7000	CMC	21	20	20	20	18	15	15	15	13	13	13
	21000	CMC	20	18	18	18	15	13	13	13	12	11	11
Ivey-sol 108	7000	0.3 + CMC	25	24	24	23	23	23	23	21	20	18	18
	21000	0.3 + CMC	20	18	18	15	15	15	15	14	14	13	13
	7000	CMC	15	11	10	10	10	5	5	3	2	1	1
	21000	CMC	15	8	6	4	2	1	1	0	0	0	0

Table C.4 Foam stability static test in the absence of oil

		Time (min)	165	180	195	210	225	250	265	270	285	300
Surfactant type	Salinity (ppm TDS)	Conc. (wt%)	Foam Height (mm)									
TX-100	7000	0.3 + CMC	71	70	68	65	65	65	63	63	63	63
	21000	0.3 + CMC	68	68	65	63	63	63	61	61	61	61
	7000	CMC	12	10	8	6	5	5	3	3	2	2
	21000	CMC	10	8	7	5	3	3	2	2	1	1
Ivey-sol 108	7000	0.3 + CMC	17	16	15	13	12	12	10	9	9	9
	21000	0.3 + CMC	12	12	11	9	7	6	5	5	3	1
	7000	CMC	0	0	0	0	0	0	0	0	0	0
	21000	CMC	0	0	0	0	0	0	0	0	0	0

Table C.5 Foam stability static test in the presence of oil

		Time (min)	0	3	5	8	10	20
Surfactant Type	Salinity (ppm TDS)	Conc. (wt%)	Foam Height (mm)					
TX-100	7000	0.3 + CMC	20	13	8	4	2	1
	21000	0.3 + CMC	17	11	7	3	2	1
	7000	CMC	5	3	2	0	0	0
	21000	CMC	5	3	1	0	0	0
Ivey-sol 108	7000	0.3 + CMC	8	6	5	3	2	0
	21000	0.3 + CMC	6	4	3	1	1	0
	7000	CMC	5	3	2	0	0	0
	21000	CMC	4	2	1	0	0	0

C-2: IFT and Contact Angle Raw Data

Table C.6 IFT and contact angle results, crude oil – brine 21000 ppm TDS

IFT															
DateTime	Pressure [Temperat	Drop dens	Bulk dens	De[mm]	V[mm ³]	IFT[mN/m	Bond	Left Angle	Right Angl	Drop	Deth	SurfaceD	SurfaceG	SurfaceTh
12:05:14	49.9	30.6	0.85	1	3.0309	16.2802	17.65	0.6822	0	0	Rising	3.02882	4.11032	4.09779	4.110137
12:05:24	50.2	30.6	0.85	1	3.0309	16.2811	17.97	0.6818	0	0	Rising	3.02881	4.11014	4.09767	4.102605
12:05:34	50.2	30.6	0.85	1	3.0309	16.2796	17.65	0.6822	0	0	Rising	3.02882	4.11111	4.10013	4.112159
12:05:44	50.2	30.6	0.85	1	3.0309	16.2707	17.97	0.6818	0	0	Rising	3.02881	4.10935	4.0994	4.102605
12:05:54	50.1	30.6	0.85	1	3.0309	16.3129	17.65	0.6822	0	0	Rising	3.02882	4.11666	4.0943	4.112159
12:06:04	50.1	30.6	0.85	1	3.0309	16.2785	17.65	0.6822	0	0	Rising	3.02882	4.11159	4.10011	4.112159
12:06:14	50	30.5	0.85	1	3.037	16.3604	17.97	0.6805	0	0	Rising	3.03485	4.12287	4.09126	4.12019
12:06:24	50	30.6	0.85	1	3.0309	16.2918	17.65	0.6822	0	0	Rising	3.02882	4.11333	4.10046	4.112159
12:06:34	49.9	30.5	0.85	1	3.0309	16.3034	17.65	0.6822	0	0	Rising	3.02882	4.11528	4.09936	4.112159
12:06:44	49.9	30.5	0.85	1	3.0309	16.2977	17.65	0.6822	0	0	Rising	3.02882	4.11455	4.10263	4.112159
12:06:54	49.9	30.5	0.85	1	3.0792	17.0723	18.32	0.6714	0	0	Rising	3.07709	4.23878	4.22258	4.234568
12:07:04	49.8	30.5	0.85	1	3.0974	17.3999	18.66	0.6673	0	0	Rising	3.09518	4.29059	4.25639	4.280622
12:07:53	49.6	30.5	0.85	1	2.9847	15.5817	17.03	0.6929	0	0	Rising	2.98264	3.98716	3.95461	3.983962
12:08:03	50.8	30.5	0.85	1	3.1942	19.2585	18.33	0.6488	0	0	Rising	3.19202	4.64379	4.61423	4.639693
12:08:13	50	30.5	0.85	1	3.1942	19.3563	18.13	0.6491	0	0	Rising	3.19203	4.66547	4.61802	4.652538
12:08:23	49.8	30.5	0.85	1	3.1942	19.3676	17.85	0.6494	0	0	Rising	3.19205	4.68074	4.63273	4.67723
12:08:33	49.8	30.5	0.85	1	3.1942	19.3683	17.85	0.6494	0	0	Rising	3.19205	4.68521	4.63467	4.679086
12:08:43	49.8	30.5	0.85	1	3.1942	19.3873	17.85	0.6494	0	0	Rising	3.19205	4.68849	4.63767	4.679086
12:08:53	49.7	30.5	0.85	1	3.1709	19.0252	17.53	0.6543	0	0	Rising	3.1688	4.62724	4.57096	4.613079
12:09:03	49.7	30.5	0.85	1	3.1709	18.9617	17.53	0.6543	0	0	Rising	3.1688	4.62108	4.58501	4.616772
12:09:13	49.6	30.5	0.85	1	3.1709	18.9616	17.53	0.6543	0	0	Rising	3.1688	4.62175	4.58774	4.616772

Contact Angle															
DateTime	Pressure [Temperat	Drop dens	Bulk dens	De[mm]	V[mm ³]	IFT[mN/m	Bond	Left Angle	Right Angl	Drop	Deth	SurfaceD	SurfaceG	SurfaceTh
14:57:32	48.1	24	0.85	1	3.2386	10.5728	-1	-1	48.8	48.8	Sessile Up	0.69153	89941.38	127023.3	116321.5
14:57:42	48.1	24	0.85	1	3.2441	10.3743	-1	-1	47.6	49.3	Sessile Up	0.69153	88855.88	127844.4	115296.1
14:57:52	48.1	24	0.85	1	3.2386	11.7336	-1	-1	42.5	50.5	Sessile Up	0.69153	95566	122654.9	116280.9
14:58:02	48.2	24	0.85	1	3.2386	10.7106	-1	-1	45.2	49.6	Sessile Up	0.69153	90224.38	126988.8	115827.8
14:58:12	48.2	24	0.85	1	3.2331	11.4295	-1	-1	45.5	50.6	Sessile Up	0.69153	94145.5	124064.8	115732.1
14:58:27	48.2	24	0.85	1	3.2331	10.7062	-1	-1	49.1	47.7	Sessile Up	0.69153	90265.13	126297.1	116221.9
14:58:32	48.2	24	0.85	1	3.2276	11.3626	-1	-1	48.5	49.3	Sessile Up	0.69153	93081	123268.5	116084.4
14:58:42	48.2	24	0.85	1	3.2276	11.1619	-1	-1	49.6	49.9	Sessile Up	0.69153	92027	123996	116435.6
14:58:52	48.2	24	0.85	1	3.2276	11.0051	-1	-1	49.5	50.2	Sessile Up	0.69153	91283.5	124509.5	116978
14:59:02	48.2	24	0.85	1	3.2221	11.3705	-1	-1	50.3	49.4	Sessile Up	0.69153	92703.88	122673.8	116061.5
14:59:12	48.2	24	0.85	1	3.2166	11.092	-1	-1	52.3	51.5	Sessile Up	0.69153	92126	124065	118552.9
14:59:22	48.2	24	0.85	1	3.2166	12.6592	-1	-1	51.3	51	Sessile Up	0.69153	98721	116948.8	116107.1
14:59:32	48.2	24	0.85	1	3.2166	11.2414	-1	-1	52.1	52.1	Sessile Up	0.69153	92620.88	122974.9	117305.3

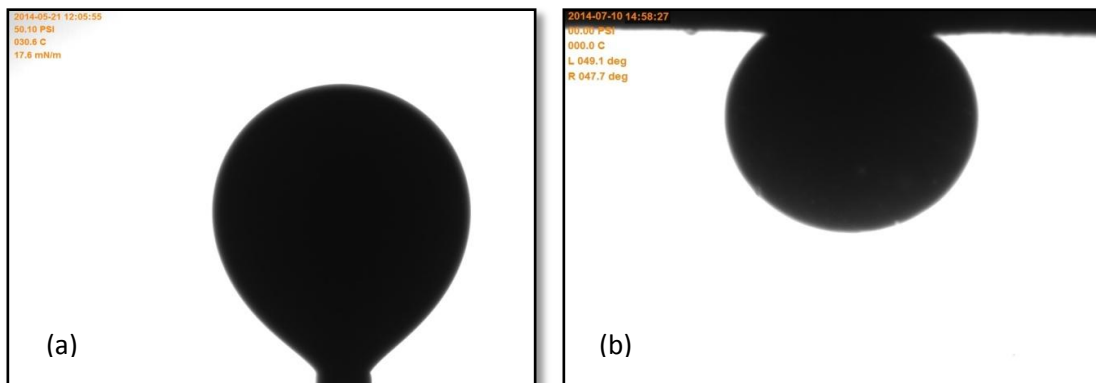


Figure C.1 (a) IFT, (b) contact angle, crude oil – brine 21000 ppm TDS

Table C.7 IFT and contact angle results, crude oil – brine 7000 ppm TDS

IFT															
DateTime	Pressure	Temperat	Drop dens	Bulk dens	De[mm]	V[mm3]	IFT[mN/m	Bond	Left Angle	Right Angl	Drop	Deth	SurfaceD	SurfaceG	SurfaceTh
22:29:34	47.9	20.9	0.85	1	2.5363	9.3281	14.88	0.8107	0	0	Rising	2.53443	2.79488	2.79176	2.78782
22:29:44	47.9	20.9	0.85	1	2.5363	9.3283	14.88	0.8107	0	0	Rising	2.53443	2.79566	2.79208	2.78782
22:29:54	47.9	20.9	0.85	1	2.5539	9.5526	14.86	0.8054	0	0	Rising	2.55203	2.84181	2.82828	2.832882
22:30:04	47.8	20.9	0.85	1	2.5128	9.098	14.26	0.8188	0	0	Rising	2.51097	2.74879	2.73624	2.742118
22:30:24	47.8	20.9	0.85	1	2.683	11.2556	14.51	0.7695	0	0	Rising	2.68113	3.19258	3.1761	3.180056
22:30:34	47.9	20.9	0.85	1	2.8181	13.1274	14.87	0.7344	0	0	Rising	2.81611	3.56272	3.54647	3.556498
22:30:44	47.8	20.9	0.85	1	2.8415	13.4799	14.89	0.7287	0	0	Rising	2.8396	3.63415	3.62365	3.628335
22:30:54	47.8	20.9	0.85	1	2.8181	13.1814	14.33	0.7353	0	0	Rising	2.81615	3.57834	3.56429	3.57609
22:31:04	47.8	20.9	0.85	1	2.8181	13.1953	14.33	0.7353	0	0	Rising	2.81615	3.58055	3.56093	3.57609
22:31:14	47.7	20.9	0.85	1	2.8181	13.1953	14.33	0.7353	0	0	Rising	2.81615	3.58055	3.56093	3.57609
22:31:25	47.8	20.9	0.85	1	2.8181	13.1953	14.33	0.7353	0	0	Rising	2.81615	3.58055	3.56093	3.57609
22:31:36	47.7	20.9	0.85	1	2.8181	13.1953	14.33	0.7353	0	0	Rising	2.81615	3.58055	3.56093	3.57609

Contact Angle															
DateTime	Pressure	Temperat	Drop dens	Bulk dens	De[mm]	V[mm3]	IFT[mN/m	Bond	Left Angle	Right Angl	Drop	Deth	SurfaceD	SurfaceG	SurfaceTh
20:13:08	53.3	24.4	0.85	1	2.16	0.7571	-1	-1	37.5	35.3	Sessile Up	0.56813	55358.25	250607.8	0.127749
20:13:18	53.3	24.3	0.85	1	2.16	0.7514	-1	-1	35.3	34.6	Sessile Up	0.56813	55122	250940	0.127749
20:13:28	53.3	24.4	0.85	1	2.1633	0.76	-1	-1	36.9	35.1	Sessile Up	0.56813	55484.63	250791.3	0.127749
20:13:38	53.3	24.4	0.85	1	2.1633	0.7687	-1	-1	37.1	35.3	Sessile Up	0.56813	55849	250585.6	0.127749
20:13:48	53.4	24.3	0.85	1	2.1667	0.7715	-1	-1	37.3	34.4	Sessile Up	0.56813	55970.5	250751.9	0.127749
20:13:58	53.4	24.4	0.85	1	2.1667	0.7743	-1	-1	34.1	34.8	Sessile Up	0.56813	56083.75	250871.3	0.127749
20:14:08	53.4	24.4	0.85	1	2.1667	0.7765	-1	-1	35.9	34.5	Sessile Up	0.56813	56176	251033.3	0.127749
20:14:18	53.4	24.4	0.85	1	2.17	0.7798	-1	-1	33.5	34.6	Sessile Up	0.56813	56309.5	251166.9	0.127749
20:14:28	53.5	24.3	0.85	1	2.1733	0.7815	-1	-1	34.5	34.6	Sessile Up	0.56813	56372.25	251303.5	0.127749

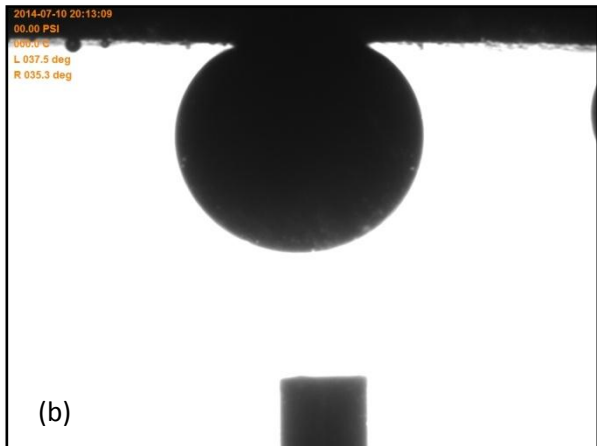


Figure C.2 (a) IFT, (b) contact angle, crude oil – brine 7000 ppm TDS

Table C.8 IFT and contact angle results, crude oil – TX-100, 0.3 wt% + CMC, 21000 ppm TDS

IFT															
DateTime	Pressure	Temperat	Drop dens	Bulk dens	De[mm]	V[mm ³]	IFT[mN/m Bond]		Left Angle	Right Angl	Drop	Deth	SurfaceD	SurfaceG	SurfaceTh
18:45:06	52.1	21.1	0.85	1	0.7778	0.2993	0.7	2.7183	0	0	Rising	0.77757	0.28867	0.28815	0.288205
18:45:16	52.1	21.1	0.85	1	0.7877	0.3118	0.7	2.6888	0	0	Rising	0.78743	0.30058	0.30301	0.302138
18:45:26	52.1	21.1	0.85	1	0.7877	0.3163	0.68	2.6913	0	0	Rising	0.78744	0.3034	0.30218	0.303364
18:45:36	52.1	21.1	0.85	1	0.768	0.2887	0.67	2.7564	0	0	Rising	0.76774	0.28359	0.285	0.284317
18:45:46	52.1	21.1	0.85	1	0.7352	0.2447	0.66	2.8659	0	0	Rising	0.73488	0.24918	0.24984	0.250304
18:45:56	52.1	21.1	0.85	1	0.6925	0.1974	0.67	3.0226	0	0	Rising	0.69215	0.2125	0.21373	0.212938
18:46:06	52.1	21.1	0.85	1	0.6531	0.1604	0.67	3.1893	0	0	Rising	0.65273	0.18199	0.18267	0.183177
18:46:16	52.1	21.1	0.85	1	0.6137	0.132	0.64	3.3846	0	0	Rising	0.61335	0.15807	0.15925	0.15821
18:46:26	52.1	21.1	0.85	1	0.6137	0.1295	0.66	3.3807	0	0	Rising	0.61334	0.15595	0.15751	0.157439

Contact Angle															
DateTime	Pressure	Temperat	Drop dens	Bulk dens	De[mm]	V[mm ³]	IFT[mN/m Bond]		Left Angle	Right Angl	Drop	Deth	SurfaceD	SurfaceG	SurfaceTh
17:25:07	34.9	24.4	0.85	1	0.7141	0.1141	-1	-1	85.4	85.2	Sessile Up	0.45577	1543.5	6960.25	0.235142
17:25:17	34.9	24.4	0.85	1	0.7102	0.1108	-1	-1	89.1	82.1	Sessile Up	0.39992	2368.625	7252	0.190161
17:25:27	34.4	24.4	0.85	1	0.722	0.1	-1	-1	90	88.5	Sessile Up	0.38024	7049.5	8923.875	0.178353
17:25:37	34.4	24.4	0.85	1	0.7141	0.1141	-1	-1	84.8	86.3	Sessile Up	0.39993	6801.75	9317.75	0.191377
17:25:47	34.1	24.4	0.85	1	0.7102	0.1131	-1	-1	85.3	87.9	Sessile Up	0.50178	7111.75	9790.625	0.275895
17:26:07	33.5	24.4	0.85	1	0.718	0.106	-1	-1	89.1	82.1	Sessile Up	0.49193	7295	8496.5	0.269056
17:26:27	33.0	24.4	0.85	1	0.7141	0.1128	-1	-1	88.5	84.9	Sessile Up	0.38353	6721	8147.5	0.181675
17:26:37	32.2	24.4	0.85	1	0.7102	0.1149	-1	-1	85.4	88.8	Sessile Up	0.53465	6964.75	8914.875	0.311707
17:27:22	32.1	24.4	0.85	1	1.3268	0.0003	-1	-1	88.9	86.4	Sessile Up	0.38682	7070.25	8821	0.185033

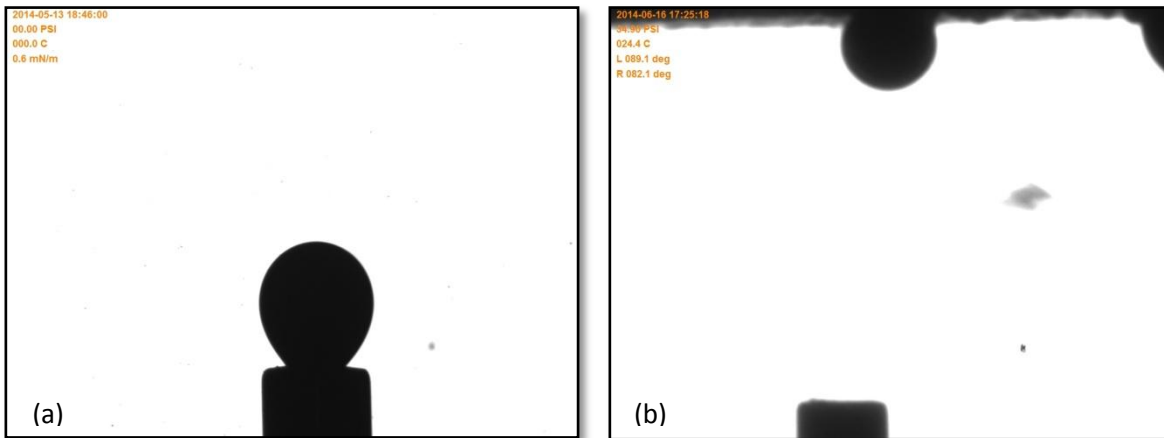


Figure C.3 (a) IFT, (b) contact angle, crude oil – TX-100, 0.3 wt% + CMC, 21000 ppm

Table C.9 IFT and contact angle results, crude oil – TX-100, CMC, 21000 ppm TDS

IFT															
DateTime	Pressure	Temperat	Drop dens	Bulk dens	De[mm]	V[mm ³]	IFT[mN/m]	Bond	Left Angle	Right Angl	Drop	Deth	SurfaceD	SurfaceG	SurfaceTh
21:06:44	50.2	30.1	0.85	1	1.6356	2.6175	4.32	1.2722	0	0	Rising	1.63453	1.22682	1.24543	1.226928
21:06:54	50.2	30.2	0.85	1	1.6356	2.6326	4.21	1.2735	0	0	Rising	1.63456	1.23245	1.24887	1.232117
21:07:04	50.1	30.1	0.85	1	1.6356	2.6359	4.21	1.2735	0	0	Rising	1.63456	1.23438	1.25244	1.232919
21:07:14	50.1	30.2	0.85	1	1.6356	2.6387	4.19	1.2738	0	0	Rising	1.63457	1.23575	1.25617	1.234651
21:07:24	50.1	30.2	0.85	1	1.6356	2.6397	4.16	1.2741	0	0	Rising	1.63457	1.23765	1.25707	1.237197
21:07:34	50.1	30.2	0.85	1	1.6356	2.6384	4.11	1.2747	0	0	Rising	1.63459	1.23796	1.25918	1.239883
21:07:44	50.1	30.1	0.85	1	1.632	2.6387	4.09	1.2777	0	0	Rising	1.63103	1.23752	1.2515	1.235086
21:07:54	50	30.2	0.85	1	1.632	2.6274	4.09	1.2777	0	0	Rising	1.63103	1.2345	1.24879	1.235086
21:08:04	50.1	30.2	0.85	1	1.6284	2.6084	4.06	1.2806	0	0	Rising	1.62748	1.22984	1.24994	1.231134
21:08:14	50	30.2	0.85	1	1.6249	2.6004	4.03	1.2835	0	0	Rising	1.62393	1.22621	1.24121	1.225541
21:08:24	50	30.1	0.85	1	1.6178	2.5678	3.79	1.2922	0	0	Rising	1.61689	1.21688	1.23007	1.226192
21:08:34	50	30.1	0.85	1	1.6142	2.5494	3.97	1.2921	0	0	Rising	1.61328	1.21101	1.2314	1.210378
21:08:44	49.9	30.2	0.85	1	1.6142	2.5593	3.92	1.2928	0	0	Rising	1.61329	1.21363	1.22502	1.21225
21:08:54	49.9	30.2	0.85	1	1.6036	2.5096	3.86	1.3015	0	0	Rising	1.60263	1.19743	1.21034	1.196332
21:09:04	49.9	30.2	0.85	1	1.6	2.4731	3.9	1.3036	0	0	Rising	1.59906	1.1862	1.2343	1.188055
21:09:14	49.8	30.2	0.85	1	1.6	2.4145	4.2	1.2996	0	0	Rising	1.59899	1.16808	1.20129	1.174119
21:09:24	49.8	30.1	0.85	1	1.5893	2.4347	3.89	1.3118	0	0	Rising	1.58839	1.17199	1.18694	1.168882
21:09:34	49.8	30.2	0.85	1	1.5858	2.4042	3.88	1.3145	0	0	Rising	1.58483	1.16295	1.18496	1.163342

Contact Angle															
DateTime	Pressure	Temperat	Drop dens	Bulk dens	De[mm]	V[mm ³]	IFT[mN/m]	Bond	Left Angle	Right Angl	Drop	Deth	SurfaceD	SurfaceG	SurfaceTh
20:54:39	51.5	24.5	0.85	1	2.4523	5.5947	-1	-1	62.3	61.5	Sessile Up	0.62163	48111	50890.63	0.115489
20:54:49	51.5	24.5	0.85	1	2.4523	5.5982	-1	-1	62.6	61.9	Sessile Up	0.62163	47726.5	50831.63	0.115489
20:54:59	51.5	24.5	0.85	1	2.4523	5.6047	-1	-1	62.8	62.4	Sessile Up	0.62163	47773.25	50829.75	0.115489
20:55:09	51.5	24.5	0.85	1	2.4523	5.6053	-1	-1	62.3	62	Sessile Up	0.62163	47657.25	49954.75	0.115489
20:55:45	51.5	24.5	0.85	1	2.4523	5.5036	-1	-1	60.1	62.1	Sessile Up	0.62163	47063	49754.38	0.115489
20:55:55	51.5	24.5	0.85	1	2.4582	5.554	-1	-1	60.3	61.7	Sessile Up	0.62163	47252.75	49458.63	0.115489
20:56:05	51.5	24.5	0.85	1	2.4582	5.5751	-1	-1	60.6	61.7	Sessile Up	0.62163	47380.75	49402.25	0.115489
20:56:15	51.5	24.5	0.85	1	2.4523	5.5344	-1	-1	60	62.2	Sessile Up	0.62163	47190	49577.13	0.115489
20:56:25	51.4	24.5	0.85	1	2.4582	5.5371	-1	-1	60.8	62.1	Sessile Up	0.62163	47183.25	49281.5	0.115489
20:56:35	51.4	24.5	0.85	1	2.4523	5.5274	-1	-1	61.3	61.3	Sessile Up	0.62163	47126.88	49384	0.115489
20:56:45	51.4	24.5	0.85	1	2.4582	5.5307	-1	-1	60.7	61.6	Sessile Up	0.62163	47119.63	49393	0.115489
20:56:55	51.4	24.5	0.85	1	2.4523	5.5438	-1	-1	60.4	62.4	Sessile Up	0.62163	47167.5	49323.63	0.115489
20:57:05	51.4	24.5	0.85	1	2.4523	5.5484	-1	-1	60.1	61.7	Sessile Up	0.62163	47119.63	49308	0.115489
20:57:15	51.4	24.5	0.85	1	2.4523	5.5432	-1	-1	60.4	62	Sessile Up	0.62163	47086.63	49395.63	0.115489
20:57:25	51.4	24.5	0.85	1	2.4523	5.5093	-1	-1	60.5	61.7	Sessile Up	0.62163	46897.25	49544.63	0.115489

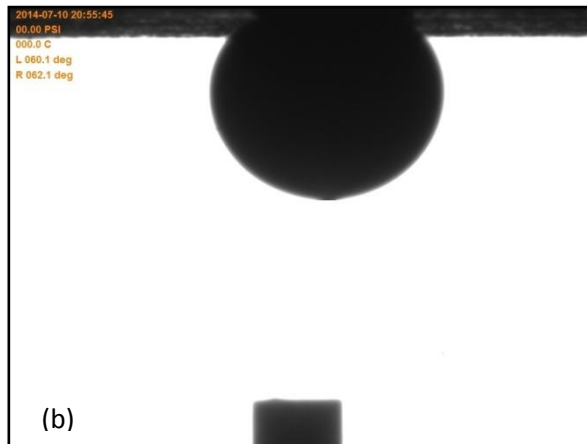


Figure C.4 (a) IFT, (b) contact angle, crude oil – TX-100, CMC, 21000 ppm TDS

Table C.10 IFT and contact angle results, crude oil – Ivey-sol 108, 0.3 wt% + CMC, 21000 ppm TDS

IFT															
12:55:46	49.9	30	0.85	1	2.0555	5.4693	5.42	1.0228	0	0	Rising	2.05456	2.06711	2.06025	2.07354
12:55:56	49.9	30	0.85	1	2.0555	5.4652	5.45	1.0225	0	0	Rising	2.05455	2.06887	2.06449	2.074146
12:56:06	49.9	30	0.85	1	2.0555	5.4608	5.48	1.0222	0	0	Rising	2.05454	2.06831	2.06684	2.071927
12:56:16	49.9	30	0.85	1	2.0508	5.4901	5.28	1.0262	0	0	Rising	2.04993	2.07738	2.068195	2.07966
12:56:26	49.8	30	0.85	1	2.0555	5.4705	5.42	1.0228	0	0	Rising	2.05456	2.07498	2.07015	2.082042
12:56:36	49.9	30	0.85	1	2.0508	5.4854	5.28	1.0262	0	0	Rising	2.04993	2.07947	2.06807	2.083992
12:56:46	49.9	30	0.85	1	2.0508	5.4833	5.25	1.0265	0	0	Rising	2.04994	2.08021	2.06823	2.087776
12:56:56	49.8	30	0.85	1	2.0508	5.486	5.28	1.0262	0	0	Rising	2.04993	2.08234	2.06873	2.086882
12:57:06	49.8	30	0.85	1	2.0508	5.4856	5.28	1.0262	0	0	Rising	2.04993	2.08383	2.07103	2.088311
12:57:16	49.8	30	0.85	1	2.0508	5.4799	5.31	1.0259	0	0	Rising	2.04992	2.08491	2.07477	2.088754
12:57:26	49.8	30.1	0.85	1	2.0508	5.4874	5.31	1.0259	0	0	Rising	2.04992	2.08907	2.07703	2.091578
12:57:36	49.8	30	0.85	1	2.0508	5.4773	5.31	1.0259	0	0	Rising	2.04992	2.08931	2.08106	2.094399

Contact Angle																
DateTime	Pressure	Temperat	Drop dens	Bulk dens	De[mm]	V[mm ³]	IFT[mN/m]	Bond	Left Angle	Right Angl	Drop	Deth	SurfaceD	SurfaceG	SurfaceTh	
18:23:19	53.2	20.1	0.85	1	2.2514	5.1793	-1	-1	57.9	57.8	Sessile Up	0.62163	47562.5	47091.75	0.115489	
18:23:29	53.2	20.1	0.85	1	2.2455	5.1381	-1	-1	58	57.7	Sessile Up	0.62163	47365.5	47259.75	0.115489	
18:23:39	53.2	20.1	0.85	1	2.2455	5.1365	-1	-1	58.2	58	Sessile Up	0.62163	47349.5	47224.75	0.115489	
18:23:49	53.2	20.1	0.85	1	2.2455	5.154	-1	-1	58.3	57.7	Sessile Up	0.62163	47428.88	47137.13	0.115489	
18:23:59	53.2	20.1	0.85	1	2.2455	5.1589	-1	-1	57.8	57.8	Sessile Up	0.62163	47463	47093.88	0.115489	
18:24:09	52.9	20.1	0.85	1	2.2455	5.1236	-1	-1	57.3	57.9	Sessile Up	0.62163	47290.5	47251.25	0.115489	
18:24:19	52.9	20.1	0.85	1	2.2455	5.1241	-1	-1	58	57.8	Sessile Up	0.62163	47297.5	47233.25	0.115489	
18:24:29	51.7	20.1	0.85	1	2.2455	5.187	-1	-1	58.3	57.5	Sessile Up	0.62163	47602	46947.25	0.115489	
18:24:39	51.7	20.1	0.85	1	2.2455	4.9747	-1	-1	58.2	57.7	Sessile Up	0.62163	46566.5	47982.75	0.115489	
18:24:49	51.7	20.3	0.85	1	2.2455	4.1902	-1	-1	58	57.9	Sessile Up	0.62163	42546.5	52067.13	0.115489	
18:24:59	51.7	20.3	0.85	1	2.2455	4.3001	-1	-1	58.3	57.7	Sessile Up	0.62163	43134.5	51418.25	0.115489	
18:25:09	51.7	20.3	0.85	1	2.2455	4.3837	-1	-1	58.3	57.9	Sessile Up	0.62163	43578.25	50986.75	0.115489	
18:25:19	51.7	20.3	0.85	1	2.2455	4.3823	-1	-1	58.1	57.5	Sessile Up	0.62163	43564.88	50976.25	0.115489	
18:25:29	51.7	20.3	0.85	1	2.2455	4.3523	-1	-1	58.3	58.6	Sessile Up	0.62163	43406.88	51137	0.115489	
18:25:39	51.7	20.3	0.85	1	2.2455	4.3277	-1	-1	58.3	58	Sessile Up	0.62163	43276.63	51276.75	0.115489	
18:25:49	51.7	20.3	0.85	1	2.2455	4.209	-1	-1	57.8	57.7	Sessile Up	0.62163	42635.5	51879.25	0.115489	
18:25:59	51.7	20.3	0.85	1	2.2455	4.2913	-1	-1	58.5	58.2	Sessile Up	0.62163	43074.5	51529	0.115489	
18:26:09	51.7	20.3	0.85	1	2.2455	4.3192	-1	-1	58.3	57.9	Sessile Up	0.62163	43223.25	51584.38	0.115489	
18:26:19	51.7	20.3	0.85	1	2.2455	4.4019	-1	-1	58	57.7	Sessile Up	0.62163	43663.25	51228	0.115489	
18:26:29	51.7	20.3	0.85	1	2.2455	4.4283	-1	-1	57.3	58.3	Sessile Up	0.62163	43796	50683	0.115489	
18:26:39	51.7	20.3	0.85	1	2.2455	4.0653	-1	-1	58	58.4	Sessile Up	0.62163	41853.75	52635.38	0.115489	



Figure C.5 (a) IFT, (b) contact angle, crude oil – Ivey-sol 108, 0.3 wt% + CMC, 21000 ppm TDS

Table C.11 IFT and contact angle results, crude oil – Ivey-sol 108, CMC, 21000 ppm TDS

IFT															
DateTime	Pressure	Temperat	Drop dens	Bulk dens	De[mm]	V[mm3]	IFT[mN/m	Bond	Left Angle	Right Angl	Drop	Deth	SurfaceD	SurfaceG	SurfaceTh
19:36:27	49.7	29.9	0.85	1	2.8467	13.7639	13.95	0.7292	0	0	Rising	2.84479	3.71683	3.70242	3.710116
19:36:37	49.7	29.9	0.85	1	2.8467	13.7576	13.68	0.7297	0	0	Rising	2.84482	3.71732	3.70069	3.719532
19:36:47	49.7	29.9	0.85	1	2.8467	13.7555	13.68	0.7297	0	0	Rising	2.84482	3.71688	3.70322	3.721699
19:36:57	49.6	29.9	0.85	1	2.8467	13.7334	13.86	0.7293	0	0	Rising	2.8448	3.71372	3.70108	3.713239
19:37:07	49.6	29.9	0.85	1	2.8467	13.7235	13.86	0.7293	0	0	Rising	2.8448	3.71208	3.70071	3.713239
19:37:17	49.6	30	0.85	1	2.8467	13.7241	13.95	0.7292	0	0	Rising	2.84479	3.71327	3.70352	3.712186
19:37:27	49.6	29.9	0.85	1	2.8533	13.7649	14.25	0.727	0	0	Rising	2.85143	3.71658	3.69058	3.715349
19:37:37	49.6	29.9	0.85	1	2.8467	13.7404	13.95	0.7292	0	0	Rising	2.84479	3.71515	3.70279	3.712186
19:37:47	49.5	30	0.85	1	2.8467	13.7168	13.95	0.7292	0	0	Rising	2.84479	3.71151	3.70359	3.712186
19:37:57	49.5	30	0.85	1	2.8467	13.7291	13.95	0.7292	0	0	Rising	2.84479	3.71462	3.70174	3.712186
19:38:07	49.5	29.9	0.85	1	2.8467	13.7209	13.95	0.7292	0	0	Rising	2.84479	3.7123	3.70216	3.712186
19:38:17	50.4	29.9	0.85	1	2.8467	13.7067	13.95	0.7292	0	0	Rising	2.84479	3.70947	3.69686	3.712186
19:38:27	50.3	30	0.85	1	2.8467	13.7637	13.95	0.7292	0	0	Rising	2.84479	3.71773	3.68839	3.710116
19:38:37	49.8	29.9	0.85	1	2.8467	13.7835	13.68	0.7297	0	0	Rising	2.84482	3.72311	3.6984	3.721699
19:38:47	50.2	29.9	0.85	1	2.8467	13.797	13.68	0.7297	0	0	Rising	2.84482	3.72573	3.69313	3.721699
19:38:57	49.9	30	0.85	1	2.8467	13.7656	13.68	0.7297	0	0	Rising	2.84482	3.72174	3.70259	3.723857
19:39:07	49.7	29.9	0.85	1	2.8533	13.7658	14.25	0.727	0	0	Rising	2.85143	3.72156	3.70467	3.719473
19:39:17	50	30	0.85	1	2.8467	13.7362	13.77	0.7295	0	0	Rising	2.84481	3.71684	3.70339	3.718542
19:39:27	50.1	30	0.85	1	2.8467	13.746	13.77	0.7295	0	0	Rising	2.84481	3.71857	3.70602	3.720648
19:39:37	50	30	0.85	1	2.8467	13.7267	13.86	0.7293	0	0	Rising	2.8448	3.71557	3.7029	3.71536

Contact Angle															
DateTime	Pressure	Temperat	Drop dens	Bulk dens	De[mm]	V[mm3]	IFT[mN/m	Bond	Left Angle	Right Angl	Drop	Deth	SurfaceD	SurfaceG	SurfaceTh
22:25:14	50.1	28.7	0.85	1	2.5245	7.4971	-1	-1	52.5	45.8	Sessile Up	0.53077	62051.5	61437	0.121458
22:25:24	50.1	28.7	0.85	1	2.5245	7.4208	-1	-1	53.4	45.9	Sessile Up	0.53077	61646.13	62040.75	0.121458
22:25:34	50.1	28.7	0.85	1	2.5245	7.3574	-1	-1	52.4	45.3	Sessile Up	0.53077	61195	62124	0.121458
22:25:44	50.1	28.7	0.85	1	2.5245	7.4221	-1	-1	52.8	46	Sessile Up	0.53077	61590.88	62018.75	0.121458
22:25:54	50.1	28.9	0.85	1	2.5245	7.3891	-1	-1	53.3	45.9	Sessile Up	0.53077	61326.75	62135.5	0.121458
22:26:18	50.1	28.9	0.85	1	2.5245	7.5091	-1	-1	49.2	48.9	Sessile Up	0.53077	62243.75	61372.75	0.121458
22:26:28	50.1	28.9	0.85	1	2.5245	7.4438	-1	-1	48.9	48.8	Sessile Up	0.53077	61832.25	61680.25	0.121458
22:26:38	50.1	28.9	0.85	1	2.5186	7.3837	-1	-1	49.1	47.7	Sessile Up	0.53077	61522.25	61985	0.121458
22:26:48	50.1	28.9	0.85	1	2.5186	7.3438	-1	-1	49.1	47.7	Sessile Up	0.53077	61342.75	62161	0.121458
22:26:58	50.1	28.8	0.85	1	2.5186	7.3089	-1	-1	49.1	50.1	Sessile Up	0.53077	61189.25	62328	0.121458
22:27:08	50.1	28.8	0.85	1	2.5186	7.4054	-1	-1	48.7	51.1	Sessile Up	0.53077	61695.63	61972	0.121458
22:27:18	50.1	28.8	0.85	1	2.5186	7.4151	-1	-1	48.7	47.6	Sessile Up	0.53077	61827.25	61905.75	0.121458

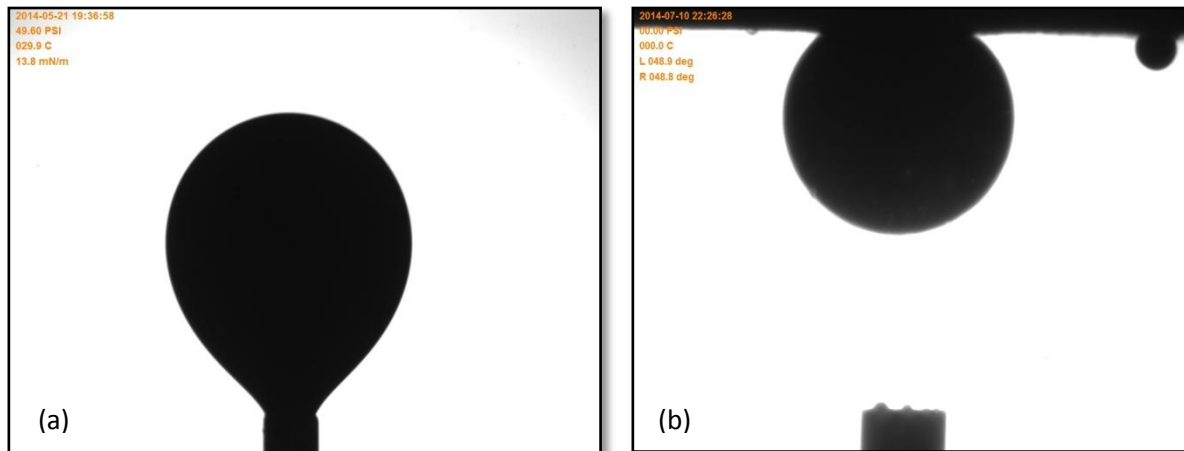


Figure C.6 (a) IFT, (b) contact angle, crude oil – Ivey-sol 108, CMC, 21000 ppm TDS

Table C.12 IFT and contact angle results, crude oil – TX-100, 0.3 wt% + CMC, 7000 ppm TDS

IFT															
DateTime	Pressure	Temperat	Drop dens	Bulk dens	De[mm]	V[mm3]	IFT[mN/m Bond		Left Angle	Right Angl	Drop	Deth	SurfaceD	SurfaceG	SurfaceTh
16:16:24	51.2	28.9	0.85	1	0.7866	0.3639	0.41	2.8249	0	0	Rising	0.78613	0.32924	0.34213	0.336917
16:17:07	51.2	28.9	0.85	1	0.7866	0.3124	0.43	2.795	0	0	Rising	0.78624	0.28299	0.28276	0.28364
16:17:17	51.2	28.9	0.85	1	0.7866	0.3159	0.43	2.7967	0	0	Rising	0.78623	0.28584	0.29228	0.288677
16:17:27	51.2	28.9	0.85	1	0.7866	0.3183	0.43	2.7982	0	0	Rising	0.78623	0.28778	0.29424	0.290398
16:17:37	51.2	28.9	0.85	1	0.7866	0.317	0.43	2.7967	0	0	Rising	0.78623	0.28653	0.28649	0.285382

Contact Angle															
DateTime	Pressure	Temperat	Drop dens	Bulk dens	De[mm]	V[mm3]	IFT[mN/m Bond		Left Angle	Right Angl	Drop	Deth	SurfaceD	SurfaceG	SurfaceTh
16:46:28	49.2	29.9	0.85	1	1.5475	1.2153	-1	-1	72.6	75.5	Sessile Up	0.43644	20906.63	21096.5	0.213138
16:46:38	49.2	29.9	0.85	1	1.5424	1.2219	-1	-1	70.7	76.2	Sessile Up	0.43644	20572	20750	0.213138
16:46:48	49.2	29.9	0.85	1	1.5424	1.23	-1	-1	71.6	72.4	Sessile Up	0.43644	20814.5	20833.25	0.213138
16:46:58	49.2	29.8	0.85	1	1.5475	1.2173	-1	-1	71.3	75.8	Sessile Up	0.43644	20526.5	20899	0.213138
16:47:08	49.2	29.8	0.85	1	1.5424	1.2071	-1	-1	70.3	72.4	Sessile Up	0.43644	20663.5	20813.25	0.213138
16:47:18	49.2	29.8	0.85	1	1.5475	1.2277	-1	-1	70.7	72.6	Sessile Up	0.43644	20878	20639.75	0.213138
16:47:28	49.2	29.8	0.85	1	1.5424	1.2172	-1	-1	70.6	72.5	Sessile Up	0.43644	20574.5	20881.5	0.213138
16:47:38	49.2	29.8	0.85	1	1.5527	1.1598	-1	-1	70.6	76	Sessile Up	0.43644	20173.38	21375.63	0.213138
16:47:48	49.2	29.8	0.85	1	1.5424	1.2337	-1	-1	69.4	76.9	Sessile Up	0.43644	21136	20677.38	0.213138
16:47:58	49.2	29.8	0.85	1	1.5424	1.2137	-1	-1	70.9	76.4	Sessile Up	0.43644	21047.75	20913.25	0.213138
16:48:08	49.2	29.8	0.85	1	1.5424	1.2508	-1	-1	69.4	72.4	Sessile Up	0.43644	21426	20502.5	0.213138
16:49:37	49.2	29.8	0.85	1	1.5578	1.1996	-1	-1	62.9	70.5	Sessile Up	0.43644	20357.5	20689.38	0.213138
16:49:47	49.2	29.8	0.85	1	1.5527	1.2304	-1	-1	63.2	69.5	Sessile Up	0.43644	20801.5	20462.25	0.213138

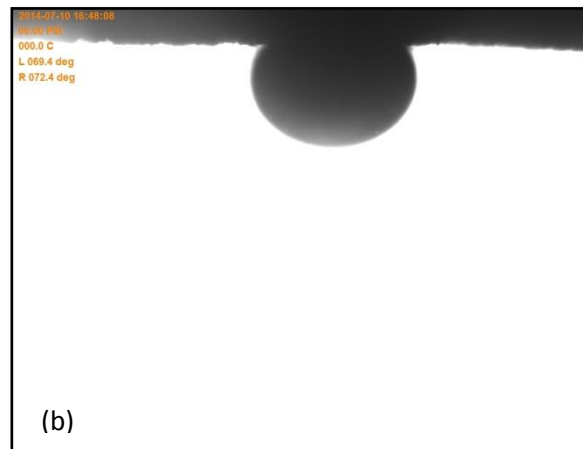


Figure C.7 (a) IFT, (b) contact angle, crude oil – TX-100, 0.3 wt% + CMC, 7000 ppm TDS

Table C.13 IFT and contact angle results, crude oil – Ivey-sol 108, 0.3 wt% + CMC, 7000 ppm TDS

IFT															
18:19:01	0	0	0.85	1	1.7333	3.1011	4.84	1.2006	0	0	Rising	1.73225	1.35288	1.34868	1.350298
18:19:11	0	0	0.85	1	1.7285	3.0955	4.72	1.2048	0	0	Rising	1.72746	1.35008	1.33815	1.345269
18:19:21	0	0	0.85	1	1.7285	3.0884	4.72	1.2048	0	0	Rising	1.72746	1.34816	1.3359	1.345269
18:19:31	0	0	0.85	1	1.7237	3.0468	4.75	1.2076	0	0	Rising	1.72264	1.3371	1.33515	1.336574
18:19:41	0	0	0.85	1	1.7189	3.046	4.71	1.2111	0	0	Rising	1.71783	1.33479	1.32164	1.328185
18:19:51	0	0	0.85	1	1.7189	3.0402	4.71	1.2111	0	0	Rising	1.71783	1.33321	1.32005	1.328185
18:20:01	0	0	0.85	1	1.7141	3.0073	4.8	1.2143	0	0	Rising	1.71301	1.32428	1.31999	1.320452
18:20:11	0	0	0.85	1	1.7141	2.9868	4.82	1.2132	0	0	Rising	1.71299	1.31762	1.31406	1.316217
18:20:21	0	0	0.85	1	1.7093	2.988	4.7	1.2175	0	0	Rising	1.7082	1.31674	1.30445	1.311225
18:20:31	0	0	0.85	1	1.7093	2.9695	4.74	1.2172	0	0	Rising	1.70819	1.31075	1.29867	1.308793

Contact Angle															
DateTime	Pressure [Temperat	Drop dens	Bulk dens	De[mm]	V[mm ³]	IFT[mN/m	Bond	Left Angle	Right Angl	Drop	Deth	SurfaceD	SurfaceG	SurfaceTh
21:38:39	52.2	28.9	0.85	1	3.0693	11.7772	-1	-1	38.4	41.1	Sessile Up	1.70337	99856.25	92897.5	1.30113
21:38:49	52.2	28.9	0.85	1	3.0693	11.6018	-1	-1	38.8	41.3	Sessile Up	1.70337	99054.75	93690	1.30113
21:38:59	52.2	28.9	0.85	1	3.0693	10.9197	-1	-1	38.5	41.3	Sessile Up	1.70337	95906.25	96957.13	1.30113
21:39:09	52.2	28.9	0.85	1	3.0693	11.0501	-1	-1	38.5	41.6	Sessile Up	1.70337	96674.25	95997.25	1.30113
21:39:19	52.5	28.9	0.85	1	3.0693	11.1576	-1	-1	38.8	41.3	Sessile Up	1.70337	96981.25	95590.75	1.30113
21:39:29	52.5	28.9	0.85	1	3.0693	11.0552	-1	-1	39.1	41	Sessile Up	1.70337	96162.25	95526.88	1.30113
21:39:39	52.5	28.8	0.85	1	3.0693	11.1463	-1	-1	38.6	41.3	Sessile Up	1.70337	96898.75	95141.75	1.30113
21:40:59	52.5	28.8	0.85	1	3.0693	11.163	-1	-1	39.1	41.8	Sessile Up	1.70337	96628.75	94721.88	1.30113
21:41:09	52.5	28.8	0.85	1	3.0693	10.6226	-1	-1	38.9	41.5	Sessile Up	1.70337	94095.75	97748.25	1.30113
21:45:23	52.5	28.8	0.85	1	3.0693	9.4809	-1	-1	41.9	41	Sessile Up	1.70337	88880	102941	1.30113
21:45:33	52.5	28.8	0.85	1	3.0693	10.8619	-1	-1	41.4	41	Sessile Up	1.70337	95514	96624.25	1.30113
21:46:19	52.2	28.8	0.85	1	3.0693	10.8372	-1	-1	41.9	41.3	Sessile Up	1.70337	95051	96341.38	1.30113
21:46:29	52.5	28.8	0.85	1	3.0642	10.6954	-1	-1	41.3	41.1	Sessile Up	1.70337	94498.75	96027.75	1.30113
21:46:39	52.2	28.8	0.85	1	3.0642	10.9405	-1	-1	41.1	40.8	Sessile Up	1.70337	95641.38	95519.13	1.30113
21:46:49	52.5	28.8	0.85	1	3.0642	10.894	-1	-1	41.2	40.8	Sessile Up	1.70337	95414	95719.38	1.30113
21:46:53	52.5	28.9	0.85	1	3.0642	10.7879	-1	-1	40.7	41.1	Sessile Up	1.70337	94888.5	95777	1.30113
21:46:03	52.5	28.9	0.85	1	3.059	11.0532	-1	-1	43	40.5	Sessile Up	1.70337	96356.5	95795.88	1.30113

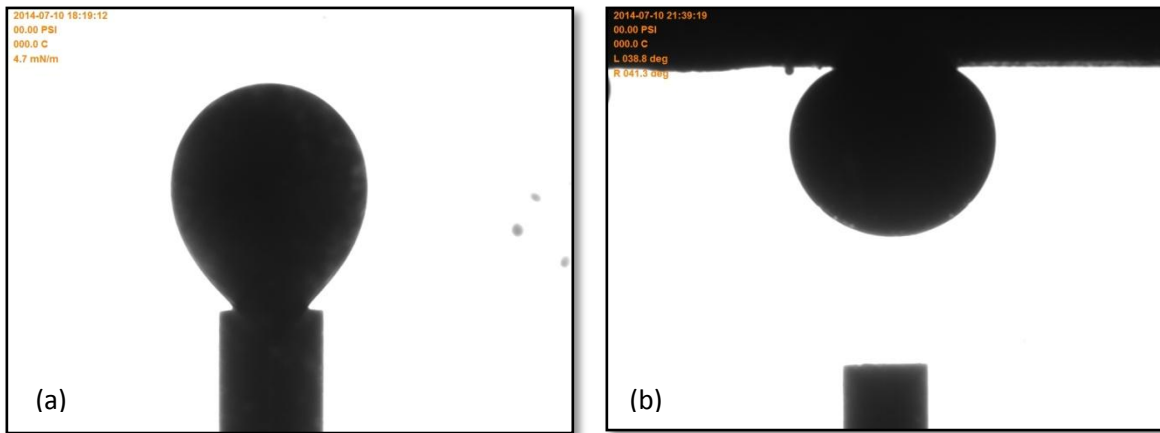


Figure C.8 (a) IFT, (b) contact angle, crude oil – Ivey-sol 108, 0.3 wt% + CMC, 7000 ppm TDS

C-3: Coreflooding Raw Data

Table C.14 Experiment # 1, W-G-W-G, 7000 ppm TDS, oil flooding

Exp #1: Oil flooding						
Flow (cm ³ /min)	Time	P _{in} (Psi)	Pump Volume (cm ³)	P _{out} (Psi)	Water level in burette (cm ³)	Oil Level in burette (cm ³)
0.030	17:36	431	442.93	432	50.0	50.0
	18:38	535	441.07	535	50.0	50.0
	19:06	502	440.23	502	49.9	49.9
	19:38	538	439.26	538	49.9	49.9
	20:34	444	437.59	444	46.9	46.9
	20:42	444	437.35	444	46.7	46.7
	6:55	439	418.95	439	27.3	27.3
	8:02	437	416.95	437	25.1	25.1
	8:54	438	415.38	437	23.5	23.5
	9:30	438	414.31	438	22.1	22.1
	10:36	441	412.33	439	20.0	20.0
	11:31	439	410.6	438	18.2	18.2
	11:58	437	409.86	437	17.3	17.3
	12:56	432	408.12	431	15.3	15.3
	13:51	432	406.48	431	13.8	13.8
	14:15	432	405.75	432	13.0	13.0
15:03	434	404.33	432	11.7	11.7	
15:24	435	403.7	434	10.9	10.9	
16:26	434	401.83	432	9.2	9.2	
17:16	463	400.33	461	8.2	8.2	
17:30	466	399.9	463	7.2	7.2	
burette	17:33	466	399.8	466	50.0	50.0
	18:09	467	398.72	466	49.5	48.8
	18:36	474	397.93	474	49.5	48.0
	20:05	484	395.32	483	49.4	38.4
	22:03	484	391.71	483	49.4	42.0
	9:50	468	370.51	467	48.6	20.6
0.08	10:02	471	369.79	468	48.6	20.0
	11:00	463	365.15	457	48.4	15.5
	11:26	464	363.03	457	48.4	13.1
	11:44	463	361.56	458	47.9	11.8
	11:58	466	360.47	463	47.8	10.7
burette	12:39	463	357.16	460	50.0	48.1

	14:07	466	350.18	463	49.8	44.4
	14:42	466	347.4	463	49.8	38.1
	15:28	464	343.7	461	49.7	34.6
	16:13	455	340.1	453	49.6	30.7
	17:09	454	335.56	450	49.6	26.1
	18:53	453	327.25	450	49.6	8.3
0.5	10:28		327.01			
burette	10:34	497	324.73	484	50.0	50.0
	10:36	502	323.74	486	49.0	49.0
	10:56	503	313.74	484	49.8	39.6
	11:04	499	309.81	484	49.8	35.5
	11:25	500	299.41	484	49.5	25.4
	11:47	502	288.25	484	49.3	14.2
0.8	11:51	512	286.17	484	49.3	12.3
	12:03	512	276.58	484	48.8	2.9
	12:17	511	265.65	484	48.5	0.0
burette					50.0	50.0
	12:41	511	245.74	483	49.6	28.6
1.25	13:06	511	226.76	483	49.6	9.6
burette	14:28	516	225.85	480	50.0	50.0
	14:38	522	215.81	480	49.7	39.5
	14:57	522	192.99	483	49.5	15.2
burette	15:15	529	185.13	473	50.0	49.5
	15:34	542	148.23	480	49.8	12.0
	15:39	542	137.2	480	49.6	1.7
	15:22	420	95.77	415	50.0	15.0

Table C.15 Experiment # 1, W-G-W-G, 7000 ppm TDS, secondary flooding

Exp # 1 : Secondary flooding					
Time	Pump volume (cm ³)	Water level in burette (cm ³)	Oil level in burette (cm ³)	P _{in} (psi)	P _{out} (psi)
10:15	473.6	49.9	49.9	479	479
10:56	471.53	49.8	47.8	480	477
11:40	469.31	49.8	45.3	482	479
12:14	467.63	49.7	43.6	476	474
12:47	465.96	49.7	41.7	476	474
13:18	464.41	49.7	40.2	476	473
13:53	462.65	49.7	38.4	476	474
14:21	461.28	49.7	37.0	474	471
14:31	460.74	49.7	36.5	473	471

15:17	458.48	49.7	34.1	473	470
16:09	455.87	49.7	31.4	471	470
16:48	453.9	49.7	29.6	471	468
17:24	452.12	49.7	27.7	468	468
17:35	451.57	49.7	27.1	468	466
17:55	450.52	49.7	26.1	471	468
18:15	449.57	49.7	25.2	470	467
18:37	448.69	49.7	24.0	471	468
19:02	447.22	49.7	22.6	458	457
19:14	446.61	49.7	22.0	470	467
19:28	445.92	49.6	21.4	468	467
19:43	445.14	49.5	21.0	467	466
20:05	444.06	48.8	19.9	460	458
20:31	442.75	48.0	18.7	467	466
21:20	440.3	45.8	16.2	463	461
21:36	439.51	44.8	15.4	466	464
23:36	433.53	39.0	9.2	466	463
23:55	432.72	50.0	50.0	466	463
11:10	403.32	16.1	15.8	454	453

Table C.16 Experiment # 1, W-G-W-G, 7000 ppm TDS, gas injection

Exp #1: Gas Injection					
Time	Pump volume (cm ³)	Water level in burette (cm ³)	Oil level in burette (cm ³)	P _{in} (psi)	P _{out} (psi)
11:47	89.56	50.0	50.0	451	448
12:03	88.73	50.0	50.0	453	453
12:21	87.82	50.0	50.0	458	456
12:45	86.63	49.9	49.9	463	461
13:06	85.58	49.7	49.7	467	467
13:24	84.68	49.2	49.2	468	465
13:58	82.94	48.5	48.2	468	465
15:05	79.62	45.8	45.5	466	464
15:23	78.71	45.0	44.7	466	463
15:53	77.2	44.0	43.7	464	460
16:34	75.1	42.5	42.2	464	460
17:31	72.29	40.4	39.6	464	461
18:09	70.39	39.0	38.1	463	461
18:46	68.63	37.4	35.9	463	461
19:28	66.45	35.7	34.0	463	463

19:44	65.62	34.9	33.0	463	461
20:29	63.42	33.2	30.9	461	461
21:40	59.87	29.8	27.3	461	461
21:54	59.16	29.7	26.8	461	461
22:16	58.09	29.6	26.5	460	460
22:30	57.36	29.6	26.4	458	458
23:28	54.47	28.5	25.0	455	455

Table C.17 Experiment # 1, W-G-W-G, 7000 ppm TDS, water injection

Exp #1: Water injection					
Time	Pump volume (cm ³)	Water level in burette (cm ³)	Oil level in burette (cm ³)	P _{in} (psi)	P _{out} (psi)
11:02	0	50.0	50.0	457	457
11:12	0.47	50.0	50.0	457	450
11:45	2.14	50.0	50.0	464	454
11:56	2.7	50.0	50.0	466	458
12:34	4.57	50.0	50.0	464	459
12:48	5.26	50.0	50.0	466	463
13:14	6.59	49.9	49.8	466	462
13:25	7.14	49.4	49.3	466	459
13:47	8.22	48.6	48.5	466	462
14:28	10.27	46.5	46.3	466	465
14:46	11.19	45.6	45.4	466	461
15:39	13.8	43.0	42.8	464	464
16:11	15.43	41.3	41.1	463	462
17:11	17.91	39.0	38.8	463	463
17:27	19.22	37.8	37.5	463	463
17:49	20.33	36.7	36.4	461	459
18:25	22.15	35.9	35.6	461	460
18:52	23.5	33.5	33.2	461	459
19:24	25.09	32.0	31.7	463	463
20:24	28.08	29.1	28.8	463	463
21:12	30.47	26.5	26.2	463	463
21:27	31.24	25.8	25.5	463	463
23:17	35	20.1	19.8	461	461

Table C.18 Experiment # 1, W-G-W-G, 7000 ppm TDS, gas injection

Exp # 1: Gas Injection					
Time	Pump volume (cm ³)	Water level in burette (cm ³)	Oil level in burette (cm ³)	P _{in} (psi)	P _{out} (psi)
13:46	78.77	47.6	47.6	454	454
13:50	77.98	47.6	47.6	455	455
13:53	77.71	47.6	47.5	458	458
14:10	76.03	47.6	47.4	464	463
14:31	73.95	47.6	47.3	473	473
15:06	70.32	44.9	44.6	479	479
16:06	64.36	43.6	43.2	482	482
16:20	63.05	43.6	43.2	487	487
1:40	43.77	23.6	23.1	477	477

Table C.19 Experiment # 2, W-G-S-G, 7000 ppm TDS, Ivey-sol 108, 0.3 wt% + CMC, oil flooding

Exp # 2: Oil flooding						
Flow (cm ³ /min)	Time	P _{in} (psi)	Pump Volume (cm ³)	P _{out} (psi)	Water level in burette (cm ³)	Oil Level in burette (cm ³)
0.03	15:10	492	362.43	492	50.0	50.0
	15:11	483	362.37	483	49.5	49.5
	15:14	477	362.27	477	49.2	49.2
	15:24	473	361.99	473	49.0	49.0
	15:33	470	361.71	470	48.7	48.7
	15:45	468	361.34	467	48.2	48.2
	15:53	468	361.13	467	48.0	48.0
	16:07	466	360.7	466	47.5	47.5
	17:49	468	357.63	467	44.6	44.6
	20:28	466	352.87	466	40.2	40.2
	21:45	461	350.55	460	37.9	37.9
	21:56	460	350.2	458	49.7	49.7
	9:40	451	328.97	449	28.0	28.0
	10:13	448	328.1	445	27.0	27.0
	10:37	448	327.38	445	26.3	26.3
	11:08	448	326.47	445	25.6	25.6
	11:29	447	325.82	444	24.9	24.9

	11:55	447	325.04	444	24.2	24.2
	12:38	447	323.74	444	23.0	23.0
	12:44	447	323.59	445	22.9	22.9
	12:46	446	323.59	445	50.0	50.0
	13:09	446	322.82	445	49.4	49.4
	13:23	446	322.42	444	49.2	49.2
	13:58	446	321.37	444	48.2	48.2
	14:37	445	320.07	443	49.4	49.4
	15:05	444	319.31	442	46.1	46.1
	15:27	444	318.68	442	45.6	45.6
	15:45	444	318.14	442	44.8	44.8
	16:00	443	317.74	442	44.6	44.6
	16:29	442	316.82	441	43.7	43.7
	16:52	442	316.14	441	43.1	43.1
	17:36	442	314.83	441	41.7	41.7
	18:02	441	314.04	439	41.4	41.1
	18:30	438	313.21	435	41.4	40.3
0.08	10:44	524	312.95	522	50.0	47.4
	11:11	551	310.94	547	50.0	47.1
	11:40	558	308.6	553	49.9	45.3
	12:21	555	305.31	550	49.9	42.1
	12:46	557	303.25	551	49.9	40.0
	13:39	550	299.06	544	49.9	35.6
	14:55	592	292.99	586	49.6	30.4
	16:01	587	287.74	582	49.6	25.1
	17:12	583	282.05	577	49.4	19.2
	17:49	582	279.1	576	49.0	16.2
	20:03	571	268.33	566	48.5	4.7
	20:15	571	267.41	566	50.0	49.7
	21:17	567	262.4	561	50.0	45.3
0.5	21:25	567	261.8	560	49.8	44.6
	21:32	593	259.09	561	49.8	42.8
	22:32	587	228.87	555	48.8	11.5
	22:43	589	223.48	558	50.0	50.0
0.8	22:53	585	218.43	553	49.9	45.2
	22:59	603	214.1	558	49.8	41.0
	23:19	602	198.2	553	49.6	24.0
	23:23	602	195.27	553	49.5	19.7

Table C.20 Experiment # 2, W-G-S-G, 7000 ppm TDS, Ivey-sol 108, 0.3 wt% + CMC, secondary flooding

Exp # 2: Secondary waterflooding					
Time	Pump volume (cm ³)	Water level in burette (cm ³)	Oil Level in burette (cm ³)	P _{in} (psi)	P _{out} (psi)
11:02	174.96	49.5	49.5	508	500
11:21	174	49.5	49.3	516	513
11:34	173.36	49.5	48.4	516	513
11:45	172.79	49.5	50.0	518	513
12:03	171.91	49.5	49.4	516	513
12:32	170.49	49.5	48.0	513	511
12:53	169.4	49.5	47.0	513	511
13:40	166.97	49.5	44.4	511	506
14:07	165.69	49.5	43.1	509	506
14:28	164.68	49.5	42.1	509	506
14:58	163.17	49.5	40.6	508	505
15:55	160.34	49.5	37.8	506	502
16:02	159.98	49.5	37.3	506	502
16:37	158.2	49.5	35.4	503	500
17:24	155.87	49.5	33.0	500	497
18:03	153.94	49.5	31.1	497	495
19:11	150.52	49.5	26.8	493	490
19:26	149.77	49.5	24.5	495	490
19:48	148.68	48.5	23.8	489	487
19:56	148.26	48.5	22.5	489	486
20:05	147.83	48.2	49.7	489	486
22:43	132.93	41.3	41.3	484	482
9:28	107.67	9.4	8.2	461	458
10:03	105.94	7.7	6.5	460	457
10:12	105.47	7.4	6.1	458	455

Table C.21 Experiment # 2, W-G-S-G, 7000 ppm TDS, Ivey-sol 108, 0.3 wt% + CMC, gas injection

Exp # 2: Gas Injection					
Time	Pump volume (cm ³)	Water level in burette (cm ³)	Oil level in burette (cm ³)	P _{in} (psi)	P _{out} (psi)
10:35	68.35	49.6	49.0	451	450
10:53	67.51	49.6	49.0	455	455
11:12	66.5	49.6	49.1	463	463

11:20	66.15	49.6	49.0	464	464
11:32	65.54	49.6	49.0	468	467
11:40	65.12	49.6	48.8	470	470
11:55	64.4	49.6	49.6	474	474
12:27	62.78	49.6	49.6	484	484
13:09	60.71	49.5	48.8	495	494
13:28	59.75	49.7	47.9	495	492
14:07	57.76	47.4	46.5	495	490
14:23	56.98	46.5	45.7	492	485
15:00	54.83	44.9	44.0	490	487
15:18	54.22	44.4	43.5	489	488
15:53	52.36	42.7	41.6	487	485
16:14	51.43	42.0	40.9	486	485
16:36	50.37	41.1	40.0	486	484
17:11	48.58	39.8	38.7	484	481
17:37	47.31	38.8	37.7	483	480
18:17	45.26	37.0	35.9	483	481
18:53	43.47	35.2	33.5	480	479
19:07	42.75	35.0	33.4	480	479
19:15	42.37	34.9	32.6	480	479
19:27	41.78	33.5	30.9	480	479
19:46	40.82	33.2	30.5	479	477
20:03	39.99	32.3	29.2	479	478
20:17	39.29	31.7	29.0	474	474
20:28	38.75	31.6	28.5	470	470
20:47	37.79	31.4	28.4	470	469
21:37	35.31	31.1	28.0	471	470
22:00	34.12	31.1	28.0	471	471
22:09	33.71	31.1	28.0	471	471

Table C.22 Experiment # 2, W-G-S-G, 7000 ppm TDS, Ivey-sol 108, 0.3 wt% + CMC, surfactant injection

Exp # 2: Surfactant Injection					
Time	Pump volume (cm ³)	Water level in burette (cm ³)	Oil level in burette (cm ³)	P _{in} (psi)	P _{out} (psi)
11:10	0	50.0	50.0	460	460
11:11	0.04	50.0	50.0	473	473
11:13	0.17	50.0	50.0	474	474
11:22	0.6	50.0	50.0	480	480

11:42	1.58	50.0	50.0	497	494
11:58	2.39	50.0	50.0	513	508
12:07	2.87	50.0	50.0	519	514
12:23	3.66	50.0	50.0	525	512
12:53	5.13	50.0	50.0	524	512
13:08	5.89	50.0	50.0	522	510
13:26	6.78	50.0	50.0	522	514
13:46	7.81	49.9	49.8	522	517
13:58	8.39	49.4	49.1	521	517
14:23	9.63	48.4	48.1	519	514
15:08	11.91	46.3	46.0	518	516
15:34	13.2	44.9	44.6	516	512
15:57	14.36	43.6	43.3	516	515
16:29	16.01	42.4	42.0	515	514
17:17	18.37	40.2	39.6	512	511
19:07	23.83	34.8	34.1	509	509
19:27	24.88	33.9	33.1	509	509
19:47	25.86	32.9	32.1	509	509
20:15	27.23	31.4	30.6	508	508
21:03	28.83	28.6	27.8	508	505
21:36	30.5	27.9	26.7	507	504
23:40	36.53	23.7	22.0	504	501

Table C.23 Experiment # 2, W-G-S-G, 7000 ppm TDS, Ivey-sol 108, 0.3 wt% + CMC, gas injection

Exp # 2: Gas Injection					
Time	Pump volume (cm ³)	Water level in burette (cm ³)	Oil level in burette (cm ³)	P _{in} (psi)	P _{out} (psi)
10:48	68.14	50	50.0	479	476
10:50	68.14	50	50.0	479	476
10:52	68.02	50	50.0	479	475
10:59	67.67	49.2	48.9	477	474
11:09	67.19	49.2	48.9	477	472
11:17	66.78	48.5	48.2	474	470
11:28	66.25	48	47.7	474	469
11:45	65.39	46.3	45.9	474	471
11:55	64.9	45	44.6	471	466
12:14	63.95	44.4	44.0	471	469
12:40	62.65	43.8	43.3	467	465

13:00	61.63	43.5	43.0	461	461
13:13	61	43.5	43.0	460	459
13:19	60.66	43.5	43.0	461	460
22:30	33.35	43.5	43.0	460	460

Table C.24 Experiment # 3, W-S-G-S, 7000 ppm TDS, Ivey-sol 108, 0.3 wt% + CMC, oil flooding

Exp # 3: Oil flooding						
Flow (cm ³ /min)	Time	P _{in} (psi)	Pump Volume (cm ³)	P _{out} (psi)	Water level in burette (cm ³)	Oil level in burette (cm ³)
0.03	19:53	442	364.06	442	50.0	50.0
	20:01	463	362.92	463	50.0	50.0
	20:16	482	362.48	482	50.0	50.0
	20:36	499	361.85	499	49.6	49.6
	20:48	502	361.52	502	49.2	49.2
	20:53	503	361.35	503	49.1	49.1
	12:42	496	354.48	496	43.0	43.0
	1:48	496	352.51	493	39.9	39.9
	2:36	493	351.05	492	38.4	38.4
	9:39	473	338.38	471	25.0	25.0
	10:18	473	337.21	470	23.9	23.9
	11:29	470	335.08	468	21.5	21.5
	12:00	467	334.11	466	21.4	21.4
	12:30	467	333.29	466	20.4	20.4
	1:00	466	332.42	464	19.4	19.4
	1:30	464	331.48	463	18.4	18.4
	2:00	463	330.6	461	16.7	16.7
	2:30	460	329.7	458	15.8	15.8
	3:00	458	328.98	457	15.5	15.5
	3:30	454	327.93	453	14.0	14.0
	4:00	453	327.03	451	13.2	13.2
	4:28	451	326.1	450	12.4	12.4
	17:23	442	324.46	442	10.9	10.9
	18:17	445	322.85	444	9.3	9.3
	18:51	448	321.8	447	8.4	8.4
	19:00	438	321.54	438	7.7	7.7
	19:55	444	319.88	442	49.9	48.6
	21:13	438	317.56	435	49.9	46.6

	22:53	429	314.57	429	49.9	43.8
0.08	22:58	430	314.4	429	49.9	43.8
	23:28	431	312.05	431	49.9	41.8
	23:56	432	309.83	431	49.7	39.5
	12:30	420	307.11	416	49.3	37.1
	12:54	422	305.17	419	49.2	35.2
	1:56	429	300.21	426	49.2	30.3
	2:02	421	299.74	419	49.2	29.2
burette	2:10	429	299.11	426	50.0	49.9
	2:17	429	298.55	426	50.0	49.5
burette	9:56	408	261.88	405	48.1	6.5
0.5	10:10	413	256.61	405	50.0	49.2
	10:19	419	252.01	400	49.4	44.4
	10:39	413	242.06	402	49.2	34.5
	11:44	416	215.82	400	48.6	1.6
	11:44	416	209.52	400	50.0	49.8
0.8 ml/min	11:49	415	206.79	400	50.0	47.5
	11:56	425	201.93	400	50.0	42.2
	12:02	419	196.85	397	49.8	36.5
7.4 ml should add	14:10	419	179.17	392	49.4	18.7
1.25	14:18	410	173.07	389	49.4	6.0
	14:37	405	156.39	344	50.0	39.3
	14:56	421	134.77	374	49.7	17.4
	15:06	429	121.33	390	49.5	4.7
	15:08	425	119.38	379	49.5	2.6
	15:09	421	117.47	389	49.5	0.1
	15:22	420	95.77	415	50.0	15.0

Table C.25 Experiment # 3, W-S-G-S, 7000 ppm TDS, Ivey-sol 108, 0.3 wt% + CMC, secondary flooding

Exp # 3: Secondary waterflooding					
Time	Pump Volume (cm ³)	Water level in burette (cm ³)	Oil level in burette (cm ³)	P _{in} (psi)	P _{out} (psi)
9:07	463.39	50.0	50.0	450	450
9:13	462.46	50.0	50.0	492	492
9:07	462	50.0	48.5	499	499
9:13	461.68	50.0	48.5	508	508
9:57	459.48	50.0	47.1	509	506
10:50	456.8	50.0	44.5	505	503

11:15	455.36	50.0	43.0	502	500
11:50	453.87	50.0	41.4	500	499
12:20	452.38	50.0	39.8	497	496
12:50	450.8	50.0	38.1	490	487
1:20	449.28	50.0	36.6	493	492
1:50	447.69	50.0	35.1	492	490
2:20	446.31	50.0	33.6	489	487
2:50	444.91	50.0	32.1	487	486
3:20	443.58	50.0	30.9	486	483
3:50	441.9	50.0	29.1	484	482
16:15	440.55	50.0	27.6	482	480
16:57	438.44	50.0	25.6	479	476
17:46	436.03	50.0	23.2	474	473
18:01	435.26	50.0	22.0	458	453
18:22	434.21	49.7	21.1	450	450
19:31	430.76	46.1	17.3	421	421
19:54	429.62	45.6	16.8	463	461
20:39	427.35	43.8	15.0	460	457
22:05	423.06	38.9	9.9	450	448
12:02	417.22	33.0	3.8	447	445
12:17	416.45	33.0	3.6	447	445
12:19	416.35	32.2	2.7	447	444
12:34	415.61	31.6	1.9	445	444
1:30	412.8	28.6	28.4	445	444
2:30	409.83	25.4	25.2	447	446
3:30	406.25	22.1	21.9	445	444
6:30	397.41	13.0	12.8	443	443
7:30	394.38	10.1	9.9	442	441
8:30	391.42	7.7	7.5	440	440

Table C.26 Experiment # 3, W-S-G-S, 7000 ppm TDS, Ivey-sol 108, 0.3 wt% + CMC, surfactant injection

Exp # 3: Surfactant Injection					
Time	Pump volume (cm ³)	Water level in burette (cm ³)	Oil level in burette (cm ³)	P _{in} (psi)	P _{out} (psi)
10:40	367.19	50.0	50.0	503	503
10:47	366.86	50.0	50.0	513	513
10:56	366.42	50.0	50.0	529	529
11:25	364.87	49.4	49.3	550	549.4

12:01	363.17	48.5	48.3	571	569.5
12:20	362.25	47.8	47.6	571	568.8
12:43	361.05	46.8	46.5	569	565.8
13:11	359.6	45.6	45.1	567	562.6
13:29	358.77	44.8	44.3	560	554.8
14:26	355.92	42.1	41.6	557	549.1
15:07	353.86	40.8	40.3	553	543.8
16:53	348.56	35.1	34.6	547	532.1
18:28	343.8	30.5	30.0	537	517.5
18:47	342.86	29.5	29.0	532	511.5
19:30	338.61	25.1	24.6	535	510.1
20:15	334.1	20.4	19.9	534	504.4
20:29	332.74	19.1	18.6	531	500.1

Table C.27 Experiment # 3, W-S-G-S, 7000 ppm TDS, Ivey-sol 108, 0.3 wt% + CMC, gas injection

Exp # 3: Gas Injection					
Time	Pump volume (cm ³)	Water level in burette (cm ³)	Oil level in burette (cm ³)	P _{in} (psi)	P _{out} (psi)
21:15	70.35	50.0	50.0	533	526
21:38	69.21	48.3	48.2	528	524
21:58	68.21	47.4	47.3	526	522
23:16	64.3	42.6	42.5	515	512
23:58	62.22	40.6	40.5	511	505
12:39	60.63	38.9	38.8	509	504
1:40	57.1	35.1	35.0	503	501
3:34	51.42	30.2	30.0	506	505
4:16	49.3	28.7	27.0	500	500
5:28	45.68	27.8	25.4	493	493
6:55	41.36	27.8	23.4	487	487

Table C.28 Experiment # 3, W-S-G-S, 7000 ppm TDS, Ivey-sol 108, 0.3 wt% + CMC, surfactant injection

Exp # 3: Surfactant Injection					
Time	Pump volume (cm ³)	Water level in burette (cm ³)	Oil level in burette (cm ³)	P _{in} (psi)	P _{out} (psi)
10:35	474.93	50.0	50.0	467	466

10:47	474.29	50.0	50.0	466	465
11:20	472.68	50.0	50.0	466	465
11:42	471.57	50.0	50.0	468	467
12:38	468.75	50.0	50.0	487	480
13:19	466.73	48.4	48.4	489	480
14:06	464.39	46.2	46.2	486	477
16:44	456.47	38.3	38.3	479	474
17:22	454.58	36.3	36.3	477	474
18:08	452.29	34.1	34.1	474	471
18:29	451.22	33.0	33.0	474	473
19:40	447.68	29.4	29.4	470	468
20:23	445.51	27.2	27.2	470	469
20:33	436.34	22.1	22.1	502	500

Table C.29 Experiment #4, W-S-G-S, 21000 ppm TDS, TX-100, CMC, oil flooding

Exp # 4: Oil flooding						
Flow (cm ³ /min)	Time	P _{in} (psi)	Pump Volume (cm ³)	P _{out} (psi)	Water level in burette (cm ³)	Oil level in burette (cm ³)
0.03	10:51	460	361.88	458	49.0	49.0
	10:54	453	361.8	453	48.9	48.9
	11:07	461	361.4	461	48.8	48.8
	11:21	463	360.99	463	48.5	48.5
	11:42	464	360.36	464	47.7	47.7
	12:26	439	359.04	439	46.2	46.2
	14:08	453	355.96	453	43.2	43.2
	14:56	451	354.53	451	42.0	42.0
	17:36	447	349.74	445	36.8	36.8
	18:18	444	348.47	442	35.5	35.5
	18:35	444	347.96	442	35.0	35.0
burette	18:38	442	347.85	442	50.0	50.0
	20:57	441	343.7	439	45.7	45.7
	9:05	418	321.85	413	22.8	22.8
	9:29	416	321.17	413	22.0	22.0
	10:09	413	319.96	410	21.0	21.0
	10:55	412	318.56	409	19.4	19.4
	11:30	410	317.53	408	18.5	18.5
burette	12:04	416	316.49	412	17.1	17.1
	12:06	418	316.43	413	50.0	50.0

	12:22	416	315.97	413	49.8	49.7
	13:40	415	313.61	410	49.8	47.5
	14:40	412	311.74	409	49.8	45.6
	14:57	412	311.32	408	49.8	45.2
0.08	15:09	412	310.95	408	49.8	44.8
	16:30	412	304.53	405	48.7	38.6
	18:29	393	294.96	387	47.8	28.6
	19:26	399	290.4	392	47.8	24.2
	19:34	397	289.79	389	47.8	23.6
	10:04	393	282.84	393	50.0	50.0
	10:34	489	280.36	480	50.0	49.6
	12:00	484	273.51	476	49.8	43.0
	12:44	482	269.99	473	49.8	39.5
	14:13	480	262.84	473	49.7	32.1
	14:21	479	262.22	471	49.7	31.5
1.25	14:25	509	261.39	473	50.0	50.0
+7 ml	14:50	545	230.38	474	46.0	18.5
	14:57	545	222.46	473	50.0	50.0
	15:25	541	186.8	454	49.4	12.5
	15:30	545	180.62	473	49.1	6.5

Table C.30 Experiment #4, W-S-G-S, 21000 ppm TDS, TX-100, CMC, secondary flooding

Exp # 4: Secondary waterflooding					
Time	Pump volume (cm ³)	Water level in burette (cm ³)	Oil level in burette (cm ³)	P _{in} (psi)	P _{out} (psi)
16:35	169.14	50.0	50.0	471	468
17:24	166.62	50.0	48.2	470	466
18:54	162.13	50.0	43.4	463	458
19:25	160.56	50.0	41.8	463	458
20:09	158.39	50.0	37.9	461	457
20:13	158.2	50.0	49.5	460	457
10:01	116.78	23.1	7.0	437	432
10:03	116.71	50.0	34.6	437	431
10:44	114.63	47.9	32.1	435	431
12:34	109.12	42.5	26.6	431	426
13:35	106.07	39.4	23.4	429	425
14:37	102.99	36.3	20.2	429	421
14:48	102.43	35.8	19.7	426	421

15:30	100.35	33.7	17.6	425	419
-------	--------	------	------	-----	-----

Table C.31 Experiment #4, W-S-G-S, 21000 ppm TDS, TX-100, CMC, surfactant injection

Exp # 4: Surfactant Injection					
Time	Pump volume (cm ³)	Water level in burette (cm ³)	Oil level in burette (cm ³)	P _{in} (psi)	P _{out} (psi)
20:00	214.58	50.0	50.0	441	439
20:13	213.91	49.2	49.0	415	414
20:22	213.44	48.7	48.5	416	415
20:34	212.86	48.7	48.5	415	413
1:05	199.36	35.5	35.2	410	410
4:30	189.11	25.8	25.0	405	405
8:51	176.01	11.7	10.8	397	396

Table C.32 Experiment #4, W-S-G-S, 21000 ppm TDS, TX-100, CMC, gas injection

Exp # 4: Gas Injection						
Time	Pump volume (cm ³)	Water level in burette (cm ³)	Oil level in burette (cm ³)	Produced Gas * 10 (cm ³)	P _{in} (psi)	P _{out} (psi)
9:10	57.04	50.0	50.0	0	396	395
9:17	56.68	49.6	49.6	11	392	392
9:47	55.17	49.2	49.2	36	393	391
10:47	52.16	46.6	46.6	74	392	391
11:15	50.77	45.0	45.0	89	390	386
11:48	49.14	43.9	43.9	103	387	384
12:17	47.69	42.5	42.5	118	386	384
13:29	44.06	39.0	39.0	152	384	383
13:51	43	38.0	38.0	161	384	383
14:21	41.47	37.0	36.9	197	383	382
14:59	39.58	35.6	34.5	238	383	381
15:23	38.37	34.3	33.2	266	381	380
15:45	37.28	34.2	32.6	286	381	381
16:13	35.9	31.9	29.7	806	367	367
17:04	33.34	31.5	29.1	861	380	379
17:11	32.97	31.5	28.9	1017	377	376
18:10	30	31.0	28.2	1705	376	376
19:38	25.6	31.0	28.1	3170	365	365
20:22	23.42	30.5	27.6	3521	374	374

20:45	22.28	30.2	27.3	3678	374	374
-------	-------	------	------	------	-----	-----

Table C.33 Experiment #4, W-S-G-S, 21000 ppm TDS, TX-100, CMC, surfactant injection

Exp # 4: Surfactant Injection						
Time	Pump Volume (cm ³)	Water Level in burette (cm ³)	Oil level in burette (cm ³)	Produced Gas (*10 cm ³)	P _{in} (psi)	P _{out} (psi)
21:05	447.05	50.0	50.0	0	390	390
21:14	446.62	50.0	50.0	0	393	388
21:17	446.46	50.0	50.0	334	384	376
21:22	446.17	50.0	50.0	335	381	372
21:33	445.66	50.0	50.0	336	393	385
21:40	445.32	50.0	49.9	566	393	383
21:44	445.11	50.0	49.9	566	393	390
21:49	444.85	50.0	49.9	566	395	393
21:52	444.71	49.9	49.8	632	396	394
2:22	431.21	41.4	41.2	1175	410	410
8:25	413.04	25.6	25.2	2171	432	432
8:30	412.85	25.5	25.1	2175	432	432

Table C.34 Experiment # 5, W-S-G-S, 21000 ppm TDS, Ivey-sol 108, CMC, oil flooding

Exp # 5: Oil flooding						
Flow (cm ³ /min)	Time	P _{in} (psi)	Pump Volume (cm ³)	P _{out} (psi)	Water level in burette (cm ³)	Oil level in burette (cm ³)
0.03	18:50	511	468.17	511	50.0	50.0
	18:53	487	468.01	487	49.4	49.4
	19:02	470	467.77	470	49.3	49.3
	19:11	466	467.47	466	48.8	48.8
	20:03	461	465.88	460	47.3	47.3
	20:44	468	464.65	467	46.3	46.3
	9:10	448	442.3	447	23.0	23.0
	9:50	447	440.9	447	21.7	21.7
	10:23	447	440.07	447	21.0	21.0
	10:42	447	439.53	445	20.3	20.3
	11:19	438	438.41	437	19.3	19.3
	11:43	435	437.7	434	18.8	18.8
	12:18	431	436.64	431	17.8	17.8
	13:08	432	435.15	432	16.4	16.4

	13:34	434	434.38	434	15.7	15.7
	14:16	435	433.05	434	14.4	14.4
	14:54	344	431.98	341	13.7	13.7
	15:07	310	431.59	310	13.4	13.4
	15:15	294	431.34	294	13.3	13.3
	15:21	284	431.16	284	13.3	13.3
stop, filling oil acc.						12.8
	16:51	316	175.39	313	50.0	50.0
	16:52	323	175.34	323	50.0	50.0
	17:00	350	175.11	351	50.0	50.0
	17:49	444	173.65	442	49.7	49.7
	18:13	434	172.91	432	49.4	49.4
	19:05	424	171.37	421	48.2	48.2
	19:52	426	169.94	424	46.8	46.8
	20:10	429	169.43	425	46.5	46.5
	21:22	435	167.25	425	43.9	43.9
	21:49	438	166.43	425	43.3	43.3
	22:28	442	165.28	424	41.9	41.9
	22:53	444	164.52	422	41.2	41.2
	23:05	447	164.16	421	40.8	40.8
	23:34	450	163.3	421	39.9	39.9
	23:44	451	162.98	421	39.7	39.7
	12:01	453	162.48	421	39.2	39.2
	12:15	455	162.05	419	38.7	38.7
	8:38	511	146.96	425	34.4	23.1

Table C.35 Experiment # 5, W-S-G-S, 21000 ppm TDS, Ivey-sol 108, CMC, secondary flooding

Exp # 5: Secondary waterflooding						
Time	Pump Volume (cm ³)	Water level in burette (cm ³)	Oil level in burette (cm ³)	Produced Gas (10*cm ³)	P _{in} (psi)	P _{out} (psi)
9:05	132.28	50.0	50.0	0	467	464
9:20	131.57	50.0	49.6	0	516	512
9:29	131.11	50.0	49.3	0	529	524
9:40	130.59	50.0	48.8	0	509	504
9:50	130.07	50.0	48.0	0	487	483
10:02	129.45	50.0	47.2	0	487	484
10:42	127.45	50.0	45.0	0	487	482

11:09	126.12	50.0	43.7	0	486	480
11:41	124.53	50.0	42.1	0	486	482
11:57	123.8	50.0	41.4	0	485	480
12:26	122.3	50.0	40.0	0	485	481
13:34	118.82	50.0	36.5	0	483	475
14:03	117.41	50.0	35.1	0	483	478
14:27	116.21	50.0	34.1	0	480	474
15:05	114.31	50.0	32.3	0	479	474
15:31	112.99	50.0	31.0	0	477	471
15:57	111.68	50.0	29.8	0	477	473
16:18	110.12	50.0	28.3	0	475	470
17:27	107.21	48.0	25.2	0	475	471
18:18	104.66	45.7	22.9	0	475	467
18:36	103.77	44.5	21.9	0	472	467
21:11	96.03	36.8	14.0	0	472	466
22:02	83.91	50.0	50.0	0	472	466
22:17	83.16	49.3	49.0	0	473	467
22:50	81.48	47.9	47.6	0	473	467
9:13	50.33	16.6	12.1	0	453	447
9:44	48.81	15.1	10.6	0	453	447
10:11	47.49	13.9	9.4	0	453	447

Table C.36 Experiment # 5, W-S-G-S, 21000 ppm TDS, Ivey-sol 108, CMC, surfactant injection

Exp # 5: Surfactant Injection						
Time	Pump Volume (cm ³)	Water level in burette (cm ³)	Oil level in burette (cm ³)	Produced Gas (10*cm ³)	P _{in} (psi)	P _{out} (psi)
10:42	181.4	50.0	50.0	0	492	491
11:00	180.5	49.5	49.4	0	503	502
12:49	175.03	44.3	44.2	0	489	489
13:09	174.01	43.6	43.5	0	500	499
17:41	160.46	29.8	29.6	0	479	479
18:19	158.56	27.8	27.6	0	477	476
20:49	151.04	20.2	19.9	0	477	476
20:52	150.88	20.1	19.8	0	477	477
21:11	148.93	18.4	18.1	0	493	493
21:36	146.45	16.0	15.7	0	487	486
21:39	146.18	15.8	15.5	0	487	487

Table C.37 Experiment # 5, W-S-G-S, 21000 ppm TDS, Ivey-sol 108, CMC, gas injection

Exp # 5: Gas Injection						
Time	Pump Volume (cm ³)	Water level in burette (cm ³)	Oil level in burette (cm ³)	Produced Gas (10*cm ³)	P _{in} (psi)	P _{out} (psi)
10:02	35.09	50.0	50.0	0	322	322
10:04	35.08	50.0	50.0	3	328	327
10:55	32.54	50.0	50.0	24	355	353
13:37	24.4	50.0	50.0	70	457	454
13:46	23.97	50.0	50.0	72	460	457
14:16	22.47	48.8	48.7	87	466	464
14:53	20.61	47.9	47.7	106	484	483
15:44	18.07	45.0	44.8	142	454	451
16:14	16.56	43.5	43.3	160	447	444
16:44	15.07	42.2	42.0	174	442	440
17:21	13.28	40.7	40.5	191	441	439
18:35	9.52	37.6	37.4	229	448	448
18:42	9.17	37.5	37.3	229	453	453
19:52	5.66	35.7	34.7	274	458	455
20:29	(refill) 3.8	34.2	32.7	327	493	493
20:37	9.64	33.8	32.1	327	486	486
21:28	7.08	33.7	32.0	345	513	513
21:37	6.63	33.7	31.9	795	484	481
21:58	5.77	33.5	31.7	886	486	483
22:10	5.19	33.4	31.6	1071	484	481
22:16	4.85	33.4	31.6	1223	484	481

Table C.38 Experiment # 5, W-S-G-S, 21000 ppm TDS, Ivey-sol 108, CMC, surfactant injection

Exp # 5: Surfactant Injection						
Time	Pump Volume (cm ³)	Water level in burette (cm ³)	Oil level in burette (cm ³)	Produced Gas (10*cm ³)	P _{in} (psi)	P _{out} (psi)
10:40	469.68	50.0	50.0	1	486	478
10:59	468.49	50.0	50.0	234	506	504
11:03	468.21	50.0	50.0	283	516	513
11:17	467.53	50.0	50.0	514	515	511
11:29	466.96	50.0	50.0	572	512	512
12:29	463.89	47.6	47.6	590	506	506

9:44	436.2	23.6	23.3	1746	490	489
10:16	434.6	22.6	22.3	1781	483	482

Table C.39 Experiment # 6, W-S-G-S, 21000 ppm TDS, TX-100, 0.3 wt% + CMC, oil flooding

Exp # 6: Oil flooding						
Flow (cm ³ /min)	Time	P _{in} (psi)	Pump Volume (cm ³)	P _{out} (psi)	Water level in burette (cm ³)	Oil level in burette (cm ³)
0.03	15:32	522	339.86	522	50.0	50.0
	15:34	529	339.77	529	50.0	50.0
	16:01	542	338.97	542	49.0	48.5
	16:35	540	337.93	540	48.0	47.5
	16:57	540	337.29	540	47.7	47.2
	17:54	538	335.57	538	46.9	46.4
	18:11	537	335.06	537	45.5	45.0
	19:01	537	333.57	537	44.0	43.2
	8:24	500	309.48	499	19.0	18.5
	9:11	497	308.07	496	17.5	17.0
	9:57	496	306.67	493	16.0	15.5
	10:18	495	306.04	493	15.5	15.0
	11:04	492	304.68	489	14.2	13.7
	12:24	487	302.26	486	11.7	11.2
	12:41	486	301.76	484	11.0	10.5
	13:35	484	300.13	483	9.5	9.0
	15:04	482	297.46	479	7.0	6.5
	16:16	479	295.3	476	4.7	4.2
	16:24	477	295.08	476	4.6	4.1
	16:27	477	294.98	474	4.5	4.0
	16:28	477	294.94	474	50.0	49.5
	16:33	477	294.81	474	50.0	49.5
	16:44	477	294.46	474	49.8	49.3
	16:57	476	294.08	474	49.5	49.0
	17:05	476	293.84	474	49.3	48.8
	17:19	473	293.41	473	48.9	48.4
	17:34	476	292.98	473	48.5	48.0
	17:46	474	292.62	471	48.3	47.8
	17:50	474	292.49	471	48.2	47.7
	18:06	473	292.02	470	47.8	47.3
	18:14	473	291.75	470	47.5	47.0

	18:46	473	290.82	470	46.4	45.9
	19:15	471	289.94	470	45.5	45.0
	19:52	471	288.82	470	44.5	43.6
	20:07	471	288.33	470	44.5	43.5
	1:50	457	278.04	454	44.3	33.2
0.08	2:00	453	277.93	453	50.0	50.0
	2:06	460	277.5	455	50.0	49.8
	2:10	460	277.29	455	50.0	49.6
	2:19	460	276.49	455	50.0	49.0
	2:30	460	275.72	455	50.0	48.2
	2:48	457	274.2	453	50.0	46.7
	2:57	460	273.51	454	50.0	46.1

Table C.40 Experiment # 6, W-S-G-S, 21000 ppm TDS, TX-100, 0.3 wt% + CMC, secondary flooding

Exp # 6: Secondary waterflooding						
Time	Pump Volume (cm ³)	Water level in burette (cm ³)	Oil level in burette (cm ³)	Produced Gas (10*cm ³)	P _{in} (psi)	P _{out} (psi)
11:06	174.59	50	50.0	0	476	476
11:11	174.28	50	50.0	0	487	486
11:20	173.85	50	50.0	0	511	509
11:26	173.56	50	49.6	0	522	519
12:03	171.69	50	47.6	0	522	518
12:52	169.24	50	45.1	0	518	513
13:28	167.45	50	43.5	0	513	508
13:56	166.04	50	42.2	0	512	507
14:39	163.9	50	40.0	0	512	508
15:24	161.66	50	37.6	0	509	504
16:08	159.46	50	35.6	0	506	502
16:38	157.95	50	34.1	0	503	498
17:31	155.3	50	31.6	0	500	496
18:13	153.22	50	29.4	0	497	494
18:58	150.96	50	27.0	0	497	495
19:24	149.67	49.7	25.8	0	497	495
20:05	147.56	48.1	23.8	0	495	494
20:16	147.03	49.5	49.5	0	495	494
8:32	110.25	13.1	11.1	0	458	457
9:14	108.16	11.1	9.1	0	457	456
9:42	106.73	9.6	7.6	0	455	453

10:03	105.74	8.6	6.6	0	455	454
-------	--------	-----	-----	---	-----	-----

Table C.41 Experiment # 6, W-S-G-S, 21000 ppm TDS, TX-100, 0.3 wt% + CMC, surfactant injection

Exp # 6: Surfactant Injection						
Time	Pump Volume (cm ³)	Water level in burette (cm ³)	Oil level in burette (cm ³)	Produced Gas (10*cm ³)	P _{in} (psi)	P _{out} (psi)
10:23	96.51	50	0	0	474	473
10:24	96.5	50	0	0	474	474
10:26	96.31	50	0	0	484	483
10:38	95.78	49.3	0.1	0	487	487
11:19	93.72	47.6	0.3	0	486	485
11:48	92.28	46.5	0.5	0	482	482
12:39	89.75	43.9	0.5	0	479	478
14:14	84.96	39.4	0.5	0	474	473
14:57	82.81	37	0.6	0	473	472
15:47	80.33	34.4	0.5	0	471	471
17:38	74.78	29	0.8	0	467	465
18:14	72.98	26.9	0.8	0	464	464
19:17	69.83	23.6	0.9	0	461	460
19:37	68.82	22.5	1	0	461	460
19:45	68.44	22.2	1	0	461	461
20:21	64.89	18.8	1.1	0	461	461
20:33	63.69	17.5	1.1	0	461	460

Table C.42 Experiment # 6, W-S-G-S, 21000 ppm TDS, TX-100, 0.3 wt% + CMC, gas injection

Exp # 6: Gas Injection						
Time	Pump Volume (cm ³)	Water level in burette (cm ³)	Oil level in burette (cm ³)	Produced Gas (10*cm ³)	P _{in} (psi)	P _{out} (psi)
9:17	70.09	50	0.0	0	493	492
9:20	69.95	50	0.0	8	496	496
9:29	69.5	50	0.0	14	499	498
9:38	69.05	50	0.0	18	502	501
9:51	68.41	50	0.0	22	506	504
10:09	67.53	50	0.0	28	513	512
10:46	65.67	50	0.0	31	526	524
10:54	65.28	50	0.0	32	529	525
11:17	64.09	50	0.0	38	534	531

11:38	63.05	49.8	0.1	54	534	529
11:47	62.6	49.8	0.3	61	534	527
12:11	61.4	48.6	0.4	76	534	529
12:27	60.59	47.6	0.4	86	534	528
13:13	58.33	45.5	0.6	114	528	525
13:40	56.9	44.8	0.7	129	528	522
14:10	55.43	43.6	0.8	143	525	521
14:31	54.43	42.5	0.9	155	524	522
14:55	53.21	41.5	1.1	168	518	513
3:27	51.59	40.1	1.3	179	518	513
15:54	50.26	39	1.5	193	518	512
16:10	49.46	38.3	1.9	200	516	513
17:06	46.75	35.5	2	224	515	511
17:47	44.6	33.8	2.1	253	511	507
18:03	43.78	33.2	2.6	279	505	502
18:31	42.38	32	3.5	299	508	505
18:38	42.03	31.3	3.7	457	505	503
19:12	40.36	30.8	3.9	969	505	505
19:49	38.53	30.5	4.2	1502	506	505
20:11	37.43	30.5	4.4	1961	505	505
20:23	36.83	30.5	4.4	2258	502	502
20:45	35.73	30.5	4.4	2535	503	503

Table C.43 Experiment # 6, W-S-G-S, 21000 ppm TDS, TX-100, 0.3 wt% + CMC, surfactant injection

Exp # 6: Surfactant Injection						
Time	Pump Volume (cm ³)	Water level in burette (cm ³)	Oil level in burette (cm ³)	Produced Gas (10*cm ³)	P _{in} (psi)	P _{out} (psi)
21:02	322.04	30.5	30.5	0	506	506
21:04	321.95	30.5	30.5	112	502	502
21:08	321.76	30.5	30.5	202	502	495
21:14	321.45	30.5	30.3	365	499	491
21:20	321.13	30.5	30.3	439	500	492
21:24	320.93	30.5	30.3	482	503	496
21:35	320.41	30.5	30.3	663	505	497
21:50	319.67	30.5	30.3	850	509	498
21:53	319.56	30.5	30.3	852	511	506
22:25	317.92	30.1	29.9	1470	512	505
22:56	316.37	30.1	29.9	2107	511	501
23:14	315.45	30.1	29.9	2457	509	496

23:49	313.7	30.1	29.9	2706	509	507
0:06	312	29.9	29.4	2720	509	508
0:58	310.26	27.7	27.2	2763	506	506
2:01	306.8	23.1	22.3	2828	503	501
2:10	306.72	22.6	21.8	2876	503	501
2:35	305.41	22.1	21.2	2970	503	503
2:50	304.63	21.9	20.7	2984	500	499
3:03	304	21.2	20	3000	498	493
3:17	303.3	19.9	18.7	3021	497	495
3:32	302.55	19.4	18.2	3037	499	499
3:43	302	19.2	17.8	3048	499	498
8:45	286.88	5.3	3.4	3321	483	482

Table C.44 Experiment # 7, W-S-G-S, 21000 ppm TDS, Ivey-sol 108, 0.3 wt% + CMC, oil flooding

Exp # 7: Oil flooding						
Flow (cm ³ /min)	Time	P _{in} (psi)	Pump Volume (cm ³)	P _{out} (psi)	Water level in burette (cm ³)	Oil level in burette (cm ³)
0.03	16:58	522	373.56	522	50.0	50.0
	17:07	531	373.3	531	49.8	49.8
	17:28	531	372.67	531	49.5	49.5
	17:34	521	372.47	521	49.3	49.3
	18:04	511	371.59	511	48.3	48.3
	18:24	509	370.98	508	47.3	47.3
	18:52	509	370.11	508	46.8	46.8
	19:46	518	368.53	518	45.5	45.5
	20:04	522	367.98	521	45.3	45.3
	20:16	518	367.61	516	44.7	44.7
	20:34	512	367.09	511	44.3	44.3
	20:47	509	366.69	508	43.8	43.8
stop	21:17	513	365.79	512	43.5	43.5
run	21:24	499	345.15	499	43.3	43.3
	22:02	521	344.01	519	41.9	41.9
	22:17	519	343.58	518	41.6	41.6
	8:48	490	324.63	486	20.5	20.5
	9:05	487	324.13	483	20.0	20.0
	10:31	482	321.56	477	17.4	17.4

	11:06	479	320.49	476	16.2	16.2
	11:36	477	319.61	474	15.3	15.3
	12:08	474	318.64	470	14.3	14.3
	13:42	468	315.81	466	11.3	11.3
	14:08	467	315.05	464	10.7	10.7
burette	15:21	467	312.84	463	8.5	8.5
	15:23	467	312.78	463	50.0	50.0
	15:43	467	312.2	463	49.6	49.6
	16:25	466	310.94	463	48.3	48.3
	16:45	464	310.33	460	48.0	48.0
	17:07	460	309.66	455	47.5	47.5
	18:35	454	307.03	450	45.9	45.9
	19:28	458	305.43	457	43.4	43.4
	19:52	484	304.71	482	43.3	43.3
	20:02	492	304.43	487	43.2	43.2
	21:07	492	302.46	486	42.5	40.7
	22:48	486	299.43	480	42.4	37.9
0.08	22:55	486	299.22	482	50.0	50.0
	23:01	492	298.69	482	50.0	49.5
	23:07	489	298.27	479	50.0	49.1
	23:12	490	297.86	480	50.0	50.0
	8:45	467	251.2	455	47.5	46.8
0.5	9:35	460	248.89	454	50.0	49.9
	9:39	499	246.82	454	49.9	48.5
	9:42	499	245.54	454	49.7	48.3
	9:45	499	243.76	454	49.6	45.7
	10:02	497	235.31	450	49.0	36.9
	10:19	496	227.22	453	48.7	28.7
	10:27	497	223.17	451	48.6	24.3
	10:40	493	216.32	447	48.5	17.4
	10:49	493	212.17	447	48.5	13.2
0.8	10:54	467	211.56	442	50	14.4
	11:01	516	206.39	450	49.8	9.6
	11:10	515	199.42	448	49.6	2.4
	11:17	515	195.69	448	49.6	0.1
	11:25	513	188.15	448	50	43.2
	12:19	513	145.61	448	49.5	0.1

Table C.45 Experiment # 7, W-S-G-S, 21000 ppm TDS, Ivey-sol 108, 0.3 wt% + CMC, secondary flooding

Exp # 7: Secondary waterflooding						
Time	Pump Volume (cm ³)	Water level in burette (cm ³)	Oil level in burette (cm ³)	Produced Gas (10*cm ³)	P _{in} (psi)	P _{out} (psi)
13:13	104.45	50.0	50.0	0	450	450
13:15	104.42	50.0	49.9	0	451	451
13:20	104.07	50.0	49.8	0	444	441
13:32	103.52	50.0	49.7	0	441	438
13:48	102.77	50.0	48.6	0	441	438
14:12	101.54	50.0	47.1	0	441	437
14:33	100.53	50.0	46.3	0	437	432
14:59	99.22	50.0	44.7	0	438	432
15:14	98.44	50.0	44.1	0	438	432
15:38	97.27	50.0	42.6	0	437	431
16:11	95.64	50.0	40.9	0	432	426
16:37	94.31	50.0	39.6	0	431	426
17:14	92.49	50.0	37.8	0	429	424
18:01	90.09	50.0	35.9	0	427	422
19:43	85.02	50.0	30.3	0	425	419
20:37	82.33	50.0	27.5	0	422	420
20:55	81.42	50.0	26.5	0	421	420
21:05	80.91	50.0	26.0	0	421	420
21:54	78.44	50.0	23.4	0	422	421
22:18	77.25	49.6	22.0	0	424	424
22:27	76.8	50.0	50.0	0	421	420
22:37	76.34	49.5	49.3	0	422	421
9:23	44.01	17.1	16.7	0	397	396
10:39	40.23	13.4	12.8	0	393	392
11:10	38.68	11.7	11.1	0	392	392
11:17	38.31	11.4	10.8	0	392	391

Table C.46 Experiment # 7, W-S-G-S, 21000 ppm TDS, Ivey-sol 108, 0.3 wt% + CMC, surfactant injection

Exp # 7: Surfactant Injection						
Time	Pump Volume (cm ³)	Water level in burette (cm ³)	Oil level in burette (cm ³)	Produced Gas (10*cm ³)	P _{in} (psi)	P _{out} (psi)
12:07	251.21	50.0	50.0	0	444	443
12:37	249.52	49.5	49.5	0	516	516

13:12	247.81	48.0	47.6	0	512	511
14:27	244.02	44.6	44.1	0	506	506
15:22	241.32	42.1	41.6	0	506	506
16:05	239.15	40.0	39.5	0	506	505
17:55	233.67	34.6	34.1	0	497	497
19:21	229.37	30.2	29.7	0	495	494
20:01	227.22	28.0	27.4	0	493	492
20:05	227.12	27.9	27.3	0	495	495
20:18	225.89	26.8	26.2	0	495	489
20:48	222.81	23.7	23.1	0	499	496
21:26	219.04	19.7	19.1	0	497	496
21:41	217.45	18.6	18.0	0	497	496
21:55	216.6	17.7	17.1	0	497	496

Table C.47 Experiment # 7, W-S-G-S, 21000 ppm TDS, Ivey-sol 108, 0.3 wt% + CMC, gas injection

Exp # 7: Gas Injection						
Time	Pump Volume (cm ³)	Water level in burette (cm ³)	Oil level in burette (cm ³)	Produced Gas (10*cm ³)	P _{in} (psi)	P _{out} (psi)
10:34	74.32	50.0	50.0	0	541	539
10:38	74.11	50.0	50.0	0	541	540
12:31	68.46	44.8	44.8	98	535	534
12:57	67.14	43.2	43.2	113	529	528
14:10	63.53	40.2	40.2	145	529	529
14:18	63.15	40.2	40.2	145	532	531
14:46	61.72	40.1	40.1	145	541	538
15:21	59.96	40.1	40.1	145	553	552
15:49	58.58	40.1	40.1	145	561	560
15:53	58.36	50.0	50.0	145	564	562
16:15	57.27	50.0	50.0	145	571	571
16:19	57.09	49.9	49.9	145	571	569
16:26	56.75	49.8	49.8	148	574	572
16:31	56.48	49.5	49.5	149	574	573
16:46	55.72	48.6	48.5	160	574	572
17:34	53.32	47.5	46.6	199	574	574
17:41	52.97	47.2	46.0	217	571	571
17:53	52.37	47.0	45.3	228	570	562
18:03	51.9	46.7	44.5	297	573	566
18:18	51.15	46.4	43.9	523	571	570

18:20	51.05	46.3	43.8	10	571	571
18:26	50.72	46.3	43.8	568	564	564
18:28	50.46	46.3	43.8	568	560	560
12:28	32.62	44.5	41.6	7830	545	545

Table C.48 Experiment # 7, W-S-G-S, 21000 ppm TDS, Ivey-sol 108, 0.3 wt% + CMC, surfactant injection

Exp # 7: Surfactant Injection						
Time	Pump Volume (cm ³)	Water level in burette (cm ³)	Oil level in burette (cm ³)	Produced Gas (10*cm ³)	P _{in} (psi)	P _{out} (psi)
12:58	394.37	50.0	50.0	0	545	545
1:04	394.13	50.0	50.0	103	542	542
1:17	393.44	50.0	50.0	429	542	541
1:23	393.19	50.0	49.5	498	548	541
1:26	393.07	50.0	49.5	500	551	544
10:11	366.76	31.0	30.4	3156	524	523
10:38	365.39	29.7	29.1	3179	522	522
12:09	360.84	25.3	24.7	3250	516	516
12:55	358.54	22.8	22.2	3289	513	513

Table C.49 Experiment # 8, SLS-S-G-S, 21000 ppm TDS, Ivey-sol 108, 0.3 wt% + CMC, oil flooding

Exp # 8: Oil flooding						
Flow (cm ³ /min)	Time	P _{in} (psi)	Pump Volume (cm ³)	P _{out} (psi)	Water level in burette (cm ³)	Oil level in burette (cm ³)
0.03	22:08	339	339.38	339	49.6	49.6
	22:18	342	339.08	342	49.1	49.1
	23:03	328	337.73	328	48.0	48.0
	9:11	315	319.49	315	32.3	32.3
	9:53	309	318.21	309	31.4	31.4
	10:27	305	317.21	305	30.5	30.5
	11:10	305	315.87	305	29.6	29.6
	11:50	306	314.7	305	28.5	28.5
	12:55	306	312.76	306	27.1	27.1

	14:15	316	310.35	315	25.1	25.1
	14:35	319	309.78	318	24.8	24.8
	15:09	318	308.74	316	23.7	23.7
	15:40	315	307.81	313	23.0	23.0
	16:10	313	306.92	312	22.0	22.0
	16:40	312	306.06	312	21.4	21.4
	19:09	312	301.54	312	17.4	17.4
	20:19	310	299.44	310	15.5	15.5
	20:22	310	299.37	310	49.9	49.9
	20:44	310	298.71	309	49.5	49.5
	9:44	326	275.31	326	35.1	28.0
	10:25	326	274.07	325	35.1	27.0
0.08	10:50	323	273.32	321	34.8	26.1
	10:54	323	273.13	321	50.0	41.5
	11:15	334	271.41	332	49.5	40.1
	12:00	329	267.84	326	49.5	36.1
	12:45	329	264.1	326	49.2	33.4
	14:17	325	256.91	322	48.7	26.5
	14:55	323	253.81	321	48.7	23.6
	15:30	323	251.05	321	48.7	21.0
1.25	16:08	328	248.01	326	48.2	18.3
	16:17	389	238.7	360	47.5	9.5
	16:20	390	234.33	361	47.1	5.5

Table C.50 Experiment # 8, SLS-S-G-S, 21000 ppm TDS, Ivey-sol 108, 0.3 wt% + CMC, secondary flooding

Exp # 8: Secondary water flooding (SLS)						
Time	Pump Volume (cm ³)	Water level in burette (cm ³)	Oil level in burette (cm ³)	Produced Gas (10*cm ³)	P _{in} (psi)	P _{out} (psi)
17:35	372.62	50.0	50.0	0	403	400
18:32	369.75	50.0	48.5	0	455	453
19:26	367.04	50.0	46.1	0	455	453
19:52	365.75	50.0	45.0	0	454	452
20:23	364.2	50.0	43.5	0	453	448
20:26	364.05	50.0	50.0	0	454	450
10:18	322.48	27.5	8.9	0	424	420
10:48	320.96	26.3	7.3	0	422	421
10:51	320.83	50.0	31.7	0	421	420
11:09	319.92	49.1	30.7	0	421	420

12:02	317.25	47.0	28.2	0	418	417
14:05	311.1	41.7	22.3	0	415	414
16:02	305.25	36.4	16.6	0	408	408
16:24	304.17	35.4	15.6	0	408	406
16:26	304.06	50.0	31.5	0	408	406
17:53	299.71	46.1	27.2	0	409	408
18:22	298.26	44.7	25.7	0	405	404
18:25	297.81	50.0	31.2	0	410	410
18:30	292.4	45.0	25.5	0	416	416
18:34	290.82	43.8	24.1	0	418	417
18:38	289.2	42.6	22.5	0	419	419

Table C.51 Experiment # 8, SLS-S-G-S, 21000 ppm TDS, Ivey-sol 108, 0.3 wt% + CMC, surfactant injection

Exp # 8: Surfactant Injection						
Time	Pump Volume (cm ³)	Water level in burette (cm ³)	Oil level in burette (cm ³)	Produced Gas (10*cm ³)	P _{in} (psi)	P _{out} (psi)
9:39	356.5	49.3	49.3	0	458	457
9:49	355.99	49.3	49.3	0	473	471
9:55	355.72	49.3	49.3	0	483	483
10:21	354.41	49.0	49.0	0	482	480
10:46	353.16	48.8	47.7	0	477	475
11:21	351.38	48.7	46.7	0	500	498
13:33	344.81	42.4	40.4	0	496	495
15:08	340.04	38.0	35.9	0	492	492
15:31	338.9	37.2	35.1	0	492	490
15:34	338.74	49.5	47.4	0	492	492
19:12	327.85	38.8	36.7	0	489	489
19:43	326.3	37.4	35.3	0	487	487
20:16	324.67	35.8	33.3	0	487	486
20:27	324.09	50.0	47.5	0	489	488
21:08	322.08	48.9	46.4	0	487	487
21:13	321.82	48.7	46.2	0	487	487

Table C.52 Experiment # 8, SLS-S-G-S, 21000 ppm TDS, Ivey-sol 108, 0.3 wt% + CMC, gas injection

Exp # 8: Gas Injection						
Time	Pump Volume (cm ³)	Water level in burette (cm ³)	Oil level in burette (cm ³)	Produced Gas (10*cm ³)	P _{in} (psi)	P _{out} (psi)
9:39	65.62	50.0	50.0	0	495	495
10:01	60.88	47.5	47.5	70	468	465
10:11	59.94	45.5	45.5	109	453	451
11:15	56.74	37.9	37.9	186	424	422
12:19	53.55	36.6	36.6	205	431	431
13:40	49.52	35.6	35.6	216	448	446
13:50	48.99	35.5	35.5	216	453	451
14:08	48.13	35.5	35.5	219	455	453
14:20	47.53	35.2	35.2	219	460	458
14:33	46.87	35.0	35.0	221	461	460
14:36	46.71	35.0	35.0	224	463	461
14:38	46.59	34.9	34.9	224	463	463
14:44	46.29	34.8	34.8	224	464	464
14:48	46.12	34.7	34.7	224	466	466
14:54	45.79	34.7	34.7	224	468	466
15:04	45.3	34.7	34.7	224	470	468
15:49	43.05	33.7	32.7	264	474	474
16:13	41.03	32.5	31.4	305	473	472
16:51	39.95	31.2	29.2	355	474	473
16:57	39.64	31.0	28.9	621	468	467
17:34	37.81	30.4	27.5	1123	468	467
17:56	36.7	30.0	27.2	1391	468	468
18:43	34.35	29.8	26.8	2308	464	464
20:00	30.5	29.4	26.4	3680	460	460
20:06	30.21	29.4	50.0	3682	463	463

Table C.53 Experiment # 8, SLS-S-G-S, 21000 ppm TDS, Ivey-sol 108, 0.3 wt% + CMC, surfactant injection

Exp 8: Surfactant Injection						
Time	Pump Volume (cm ³)	Water level in burette (cm ³)	Oil level in burette (cm ³)	Produced Gas (10*cm ³)	P _{in} (psi)	P _{out} (psi)
20:25	473.32	50.0	50.0	0	463	462
20:28	473.18	50.0	50.0	209	461	457
21:09	471.13	50.0	50.0	824	467	460

21:20	470.6	49.9	49.9	971	470	469
21:43	469.43	49.9	49.9	1391	471	469
8:07	438.23	23.2	22.9	1715	457	457
8:27	437.25	22.2	21.9	1725	454	453

Table C.54 Experiment # 9, SLS-G-S-G, 7000 ppm TDS, TX-100, 0.3 wt% + CMC, oil flooding

Exp #9: Oil flooding						
Flow (cm ³ /min)	Time	P _{in} (psi)	Pump Volume (cm ³)	P _{out} (psi)	Water level in burette (cm ³)	Oil level in burette (cm ³)
0.03	18:13	345	299.24	350	50.0	50.0
	18:19	368	299.05	370	50.0	50.0
	18:42	408	298.39	408	49.8	49.8
	19:01	422	297.8	424	49.5	49.5
	19:30	376	296.9	376	47.8	47.8
	20:00	357	295.99	357	46.3	46.3
	20:30	355	295.08	355	45.5	45.5
	21:00	360	294.2	358	44.7	44.7
	21:30	363	293.31	363	44.0	44.0
	22:00	365	292.32	367	42.9	42.9
	22:30	365	291.51	365	42.5	42.5
	23:00	363	290.61	363	41.2	41.2
	23:30	361	289.71	361	40.6	40.6
	0:00	361	288.81	361	39.7	39.7
	0:30	360	287.86	360	38.9	38.9
	1:00	358	287	358	38.0	38.0
	1:30	358	286.14	358	37.0	37.0
	2:00	357	285.21	357	36.5	36.5
	2:30	355	284.3	355	35.5	35.5
	3:00	355	283.4	355	34.5	34.5
	3:30	358	282.51	358	33.8	33.8
	4:00	363	281.61	361	32.8	32.8
	4:30	364	280.63	364	32.0	32.0
	5:00	360	279.76	360	31.0	31.0
burette	10:05	345	270.68	342	21.5	21.5
	10:07	345	270.62	342	50.0	50.0
	10:16	344	270.35	342	49.8	49.8
	10:30	342	269.95	341	49.2	49.2

	12:05	335	267.07	332	46.7	46.7
	12:30	331	266.24	329	45.6	45.6
	13:00	328	265.42	326	44.7	44.7
	13:30	326	264.55	325	43.8	43.8
	14:00	326	263.6	325	43.1	43.1
	14:30	326	262.74	325	42.2	42.2
	15:00	328	261.71	326	41.1	41.1
	15:35	329	260.79	326	40.4	40.4
	16:02	329	259.99	328	39.6	39.6
	16:40	329	258.85	328	38.3	38.3
	17:10	336	257.93	332	37.7	37.7
	17:34	332	257.2	332	36.6	36.6
	17:39	334	257.08	332	36.5	36.5
	17:40	334	257.03	331	36.4	36.4
	17:43	332	256.96	331	36.3	36.3
	17:54	330	256.62	328	36.0	36.0
	18:06	329	256.25	326	35.6	35.6
	18:15	328	256	326	34.5	34.5
burette	9:35	408	249.97	403	50.0	50.0
	10:04	383	249.1	383	49.8	49.8
	10:33	381	248.23	381	49.0	49.0
	11:08	393	247.19	393	48.1	48.1
	11:33	400	246.43	400	47.3	47.3
	12:02	399	245.56	399	47.3	46.4
	12:32	397	244.66	397	47.3	45.6
	13:03	396	243.72	395	47.0	44.7
	13:32	395	242.85	395	47.0	44.0
	14:02	395	241.96	393	47.0	43.1
	14:30	393	241.08	393	47.0	42.4
	15:05	393	240.06	392	47.0	41.3
	16:09	390	238.16	389	47.0	39.5
	16:37	389	237.31	387	47.0	38.8
	17:12	387	236.24	387	47.0	37.6
	17:29	389	235.76	387	47.0	37.1
0.08	17:35	390	235.52	387	47.0	37.1
	17:53	393	234.04	389	47.0	35.6
	18:28	393	231.3	390	47.0	32.6
	18:57	393	228.94	390	47.0	30.3
	19:58	392	224.02	387	46.9	25.7
	20:05	392	223.53	387	46.9	25.1
	20:10	390	223.13	387	46.9	24.9

Table C.55 Experiment # 9, SLS-G-S-G, 7000 ppm TDS, TX-100, 0.3 wt% + CMC, secondary flooding

Exp # 9: Secondary waterflooding (SLS)						
Time	Pump Volume (cm ³)	Water level in burette (cm ³)	Oil level in burette (cm ³)	Produced Gas (10*cm ³)	P _{in} (psi)	P _{out} (psi)
21:37	456.14	50.0	50.0	0	512	510
21:45	455.1	50.0	48.9	0	479	477
22:28	453.1	50.0	47.0	0	481	480
23:01	451.1	49.9	45.3	0	480	477
23:32	449.3	49.9	43.5	0	480	476
0:05	447.8	49.9	41.9	0	477	474
0:31	446.9	49.8	40.9	0	477	473
1:00	446.02	49.8	39.8	0	476	471
1:30	444.45	49.8	37.6	0	475	471
2:03	442.87	49.8	36.0	0	471	466
3:09	439.55	49.7	32.7	0	473	468
4:15	436.25	49.7	29.5	0	473	470
4:40	434.98	49.7	28.1	0	467	464
5:08	430.1	49.7	23.1	0	454	453
5:11	430.02	50.0	50.0	0	452	450
5:36	427.2	49.0	48.5	0	454	453
11:08	415.6	36.0	34.6	0	442	440
11:15	415.28	36.0	34.2	0	441	440
11:17	415.17	50.0	49.1	0	441	440
12:19	412.06	49.8	47.5	0	441	441
12:42	410.9	49.1	48.0	0	439	439
13:14	409.3	47.1	45.8	0	439	439
13:49	407.56	45.2	43.9	0	439	438
14:30	405.49	43.2	42.0	0	436	436
15:00	403.99	41.6	40.4	0	436	436
15:34	402.3	40.0	38.6	0	435	435
16:01	400.95	38.5	37.2	0	434	433
16:58	398.11	35.6	34.2	0	434	434
17:33	396.37	33.8	32.4	0	432	432
18:02	394.89	32.6	31.1	0	432	432
19:02	391.9	29.6	28.1	0	431	430
19:34	390.29	28.0	26.3	0	434	433
20:06	388.72	26.5	24.8	0	432	430
20:29	387.56	25.5	23.8	0	429	428
20:58	386.12	24.5	22.8	0	428	427

Table C.56 Experiment # 9, SLS-G-S-G, 7000 ppm TDS, TX-100, 0.3 wt% + CMC, gas injection

Exp # 9: Gas Injection						
Time	Pump Volume (cm ³)	Water level in burette (cm ³)	Oil level in burette (cm ³)	Produced Gas (10*cm ³)	P _{in} (psi)	P _{out} (psi)
21:33	51.61	50.0	50.0	0	421	420
21:42	51.17	50.0	50.0	8	419	418
22:11	49.7	50.0	50.0	24	425	423
22:51	47.69	49.2	49.2	47	429	427
23:39	45.29	47.2	47.2	77	429	426
0:11	43.73	45.5	45.5	91	425	421
1:15	40.46	42.6	42.6	125	418	412
1:32	39.67	42.5	42.5	130	418	409
1:47	38.88	42.3	42.3	131	422	416
2:14	37.56	40.7	39.7	137	425	420
2:50	25.63	39.5	38.5	160	429	427
3:34	33.56	39.0	36.7	217	429	426
4:00	32.29	37.9	35.1	259	428	426
4:06	31.98	37.3	33.4	571	419	416
4:26	30.96	36.7	32.8	1216	405	402
4:52	29.65	36.3	32.3	1409	405	404
5:15	28.54	36.1	32.1	1502	407	406
8:59	17.3	35.0	30.3	4567	384	382
9:21	16.22	35.0	30.3	4664	389	389

Table C.57 Experiment # 9, SLS-G-S-G, 7000 ppm TDS, TX-100, 0.3 wt% + CMC, surfactant injection

Exp # 9: Surfactant Injection						
Time	Pump Volume (cm ³)	Water level in burette (cm ³)	Oil level in burette (cm ³)	Produced Gas (10*cm ³)	P _{in} (psi)	P _{out} (psi)
10:47	449.09	50.0	50.0	2	512	512
10:48	448.98	50.0	49.8	410	505	505
10:54	448.7	50.0	49.8	860	457	455
11:10	447.88	49.9	49.7	957	460	458
11:26	447.09	49.9	49.7	960	480	478
11:30	446.89	49.9	49.7	962	481	470
12:20	444.38	48.7	48.5	1001	477	466
12:46	443.08	47.7	47.5	1020	471	459
13:55	439.65	44.0	43.5	1069	471	466

14:26	438.08	42.6	42.1	1085	476	473
14:52	436.8	41.3	40.2	1112	474	469
15:08	435.98	40.7	39.5	1128	475	468
15:42	434.31	40.0	38.8	1144	474	473
16:15	432.6	37.4	36.2	1168	473	473
17:01	430.4	35.3	33.9	1198	473	470
17:32	428.82	33.7	32.3	1222	471	468
18:03	427.22	32.3	30.7	1242	471	469
18:52	424.8	29.9	28.3	1276	471	470
19:53	421.71	27.9	26.3	1322	470	469
20:28	419.99	25.0	23.7	1344	470	469
21:04	418.18	23.3	21.8	1368	468	468
21:34	416.71	22.0	20.5	1388	467	466
22:03	415.26	20.5	18.9	1407	467	466
22:25	413.89	19.5	17.9	1424	465	464

Table C.58 Experiment # 9, SLS-G-S-G, 7000 ppm TDS, TX-100, 0.3 wt% + CMC, gas injection

Exp # 9: Gas Injection						
Time	Pump Volume (cm ³)	Water level in burette (cm ³)	Oil level in burette (cm ³)	Produced Gas (10*cm ³)	P _{in} (psi)	P _{out} (psi)
10:46	60.76	50.0	50.0	0	463	457
10:49	60.54	50.0	50.0	7	461	457
11:38	58.12	47.8	47.8	35	463	457
12:08	56.6	46.7	46.7	58	463	458
12:58	54.1	44.0	44.0	94	461	458
2:01	50.08	41.5	41.5	152	464	463
2:31	49.43	40.6	40.0	218	467	464
2:42	48.87	39.9	39.3	705	457	450
3:00	47.97	39.2	38.4	1225	448	448
3:31	46.32	38.7	37.8	1626	447	444
4:04	44.8	38.5	37.4	2027	444	444
4:29	45.55	38.5	37.4	2378	442	442
5:00	42.06	38.2	36.5	2978	436	435
10:19	26.04	37.6	34.2	6685	442	441
10:31	25.48	37.6	34.2	6687	445	445

APPENDIX D: Sample Calculation

D-1: Dead Volume Calculation (volume of outlet section):

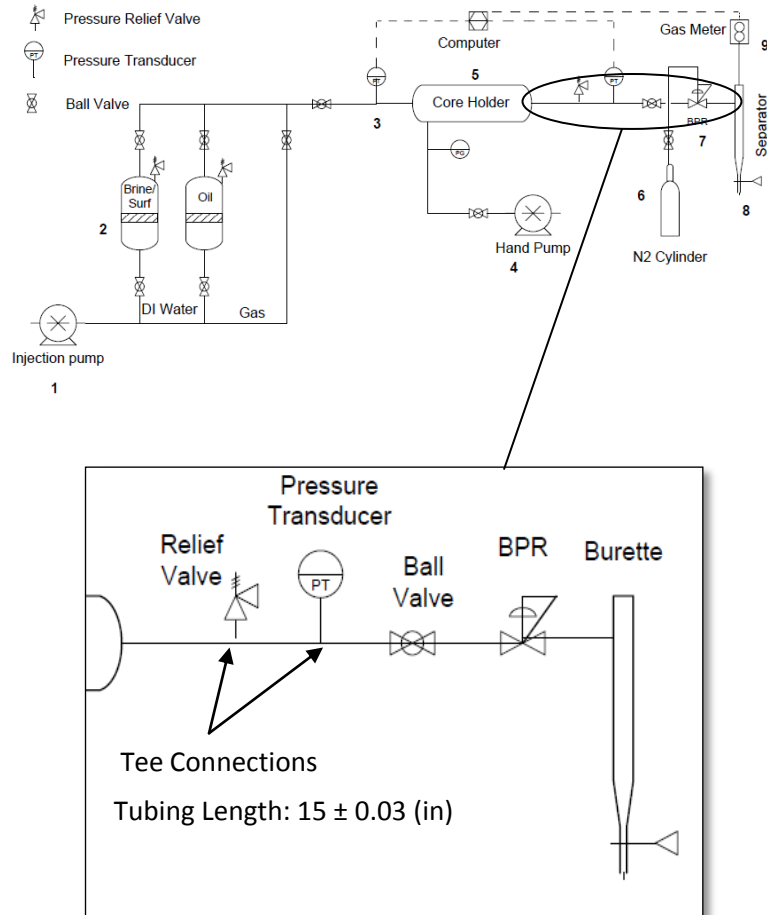


Figure D.1 Coreflooding apparatus outlet section

$$\text{Outlet Dead Volume} = 2 \times (\text{volume of Tee connection}) + (\text{volume of ball valve}) + (\text{volume of BPR}) + (\text{volume of 15'' length tubing})$$

1) Tee Connections (Swagelok SS-200-3-4TTM)

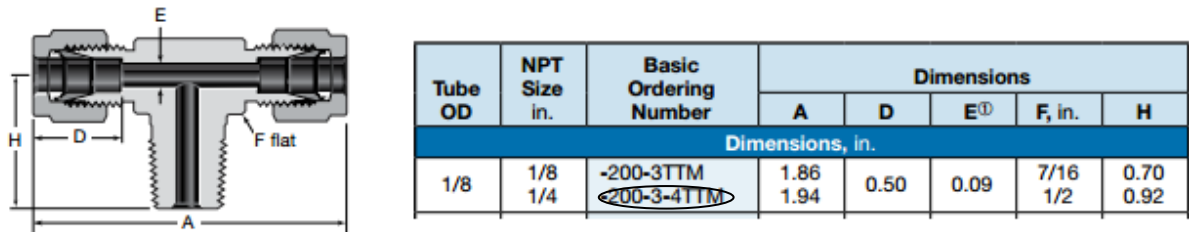


Figure D.2 Tee connection dimensions (Swagelok Web Catalog, 2014)

2 Tee Connections volume:

$$2 \times \left[\frac{(E)^2}{4} \times 3.14 \times (A + H) \right] =$$

$$2 \times \left[\frac{(0.09 \text{ (in)})^2}{4} \times 3.14 \times (2.86 \text{ (in)}) \right] = 0.036 \text{ (in}^3\text{)} = 0.59 \text{ (cm}^3\text{)}$$

2) Ball Valve (Swagelok SS-41GS2-1466)

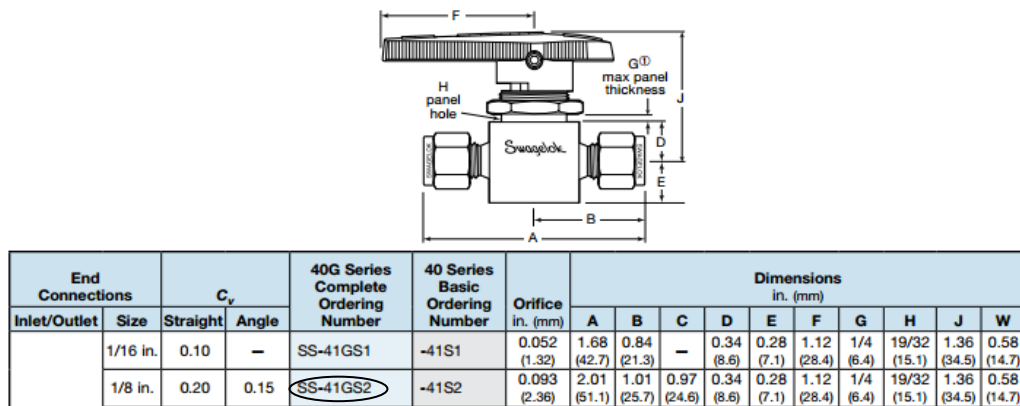


Figure D.3 Ball valve dimensions (Swagelok Web Catalog, 2014)

The ball valve volume assumed to be equal to A” length of 1/8” tubing with 0.028” wall thickness:

$$\text{Ball valve volume} = \frac{(1/8 - (2 \times 0.028))^2}{4} \times 3.14 \times 2.01 = 0.0075 \text{ (in}^3\text{)} = 0.12 \text{ (cm}^3\text{)}$$

3) BPR (Equilibar (EB1LF1) with 1/8” NPT tube fitting)

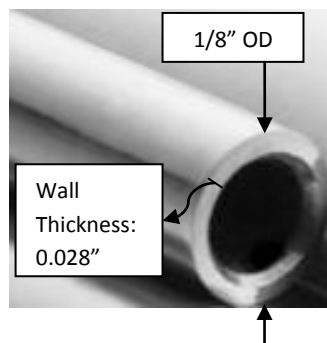
According to the reference below:

<http://www.equiblar.com/back-pressure-regulators/severe-services/low-dead-volume/>

BPR volume = 3 (cm³)

4) Tubing (Swagelok SS-T2-S-028-20)

Volume of 15” length 1/8” OD Swagelok **tubing** with 0.028 wall thickness



Tube OD in.	Tube Wall in.	Ordering Number	Weight lb/ft	Working Pressure psig
1/8	0.028	SS-T2-S-028-20	0.029	8 500

Figure D.4 1/8” tubing dimensions (Swagelok Web Catalog, 2014)

Volume of tubing =

$$\frac{[1/8 - (2 \times 0.028)]^2}{4} \times 3.14 \times (15 \pm 0.03 \text{ (in)}) = 0.056 \pm 0.001 \text{ (in}^3) = 0.92 \pm 0.01 \text{ (cm}^3)$$

Outlet Dead Volume = 2 × (volume of **Tee connection**) + (volume of **ball valve**) + (volume of **BPR**) + (volume of 15" length **tubing**)

$$\text{Outlet Dead Volume} = 0.59 \text{ (cm}^3) + 3 \text{ (cm}^3) + 0.12 \text{ (cm}^3) + (0.92 \pm 0.01) = 4.63 \pm 0.01 \text{ (cm}^3)$$

D-2: Coreflooding Material Balance Calculation

From Appendix B-1, Actual Pore Volume = $65.4 \pm 0.1 \text{ (cm}^3)$

From Appendix D-1, Outlet Dead Volume = $4.63 \pm 0.01 \text{ (cm}^3)$

In order to minimize errors in calculations:

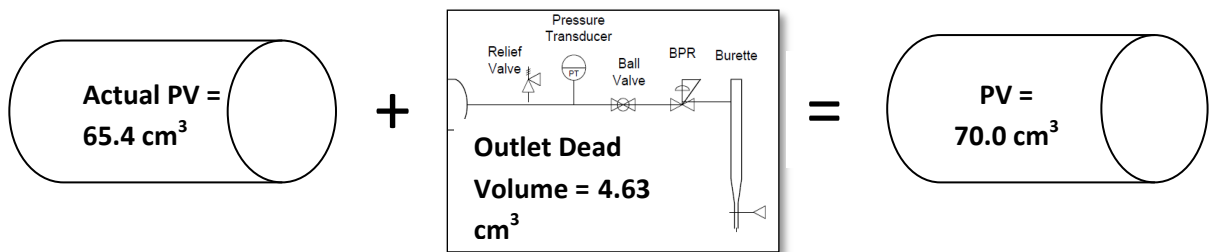


Figure D.5 Pore volume in coreflooding experiments

$$\text{PV} = \text{Actual PV} + \text{Outlet Dead Volume} = (65.4 \pm 0.1) + (4.63 \pm 0.01) = 70.0 \pm 0.1 \text{ (cm}^3)$$

This new value for PV was used during coreflooding and material balance calculation.

Coreflooding:

Experiment # 1: WAG experiment with brine salinity 7000 ppm TDS

Experiment # 1 has the following steps:

1. Primary Waterflooding
2. Oil flooding
3. Secondary Waterflooding (1 PV)
4. Tertiary Injection (0.5 PV Gas - 0.5 PV Water - 0.5 PV Gas)

Step 1) Primary Waterflooding (100% water saturated core)

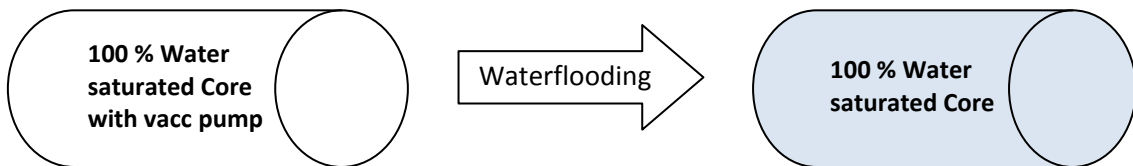


Figure D.6 Primary waterflooding

Total volume of water inside the core = PV = 70.0 ± 0.1 (cm³)

Step 2) Oil flooding until no more water production

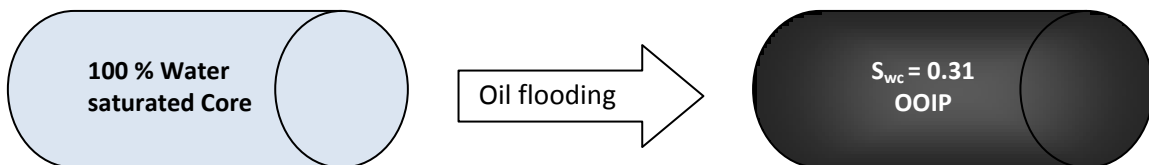


Figure D.7 Oil flooding

According to Appendix C-3, Table C.14 (oil flooding raw data for experiment #1), there were seven times burette draining during oil flooding in experiment # 1:

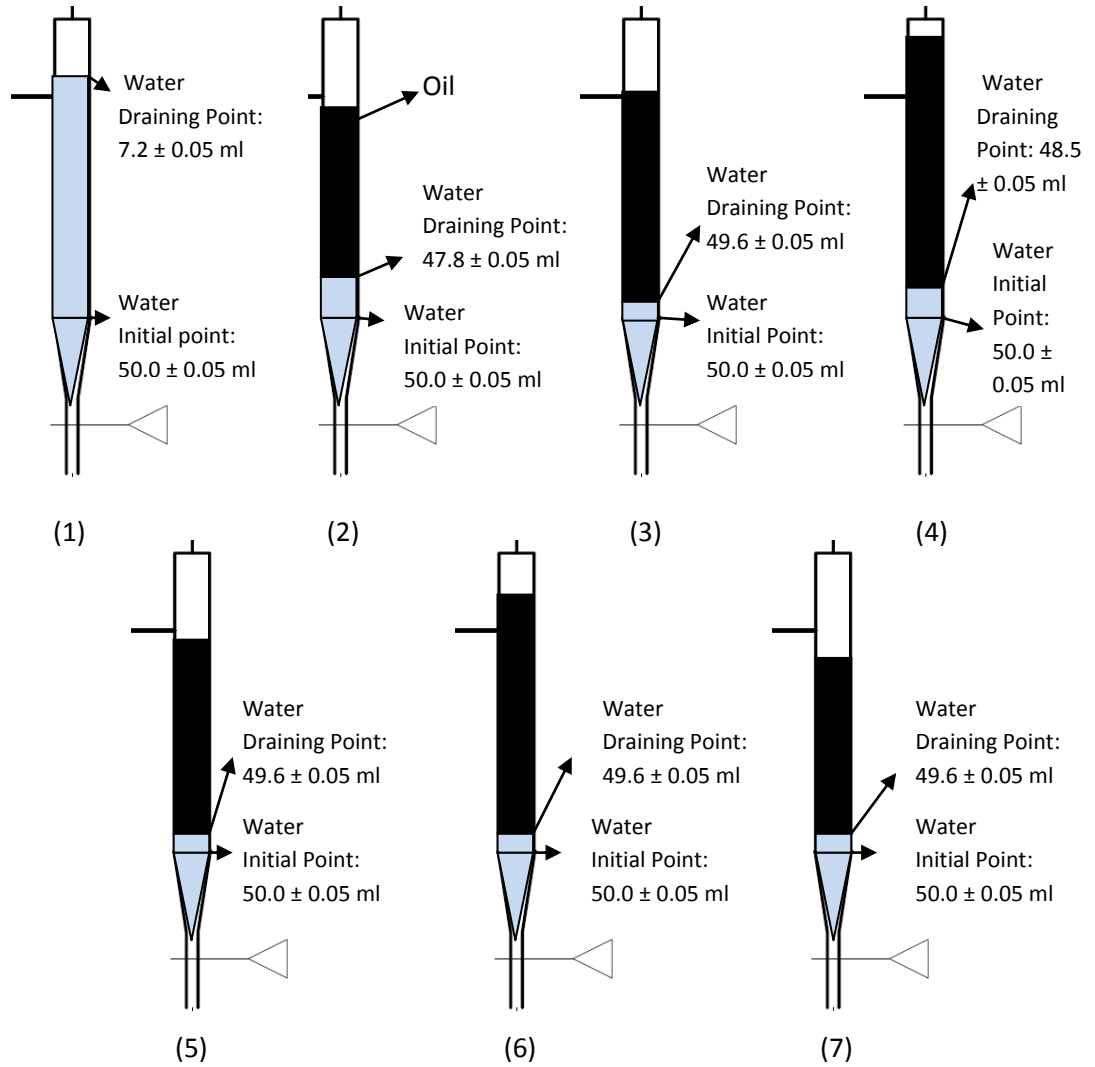


Figure D.8 Burette reading during oil flooding in experiment # 1

Table D.1 Burette reading during oil flooding in experiment # 1

Oil flooding		
Burette Draining #	Water Level Initial Point (cm ³)	Water Level Draining Point (cm ³)
1	50.0 ± 0.05	7.2 ± 0.05
2	50.0 ± 0.05	47.8 ± 0.05
3	50.0 ± 0.05	49.6 ± 0.05
4	50.0 ± 0.05	48.5 ± 0.05
5	50.0 ± 0.05	49.6 ± 0.05
6	50.0 ± 0.05	49.6 ± 0.05
7	50.0 ± 0.05	49.6 ± 0.05

Step 2-1)

$$\begin{aligned} \text{Produced water during oil flooding} &= \sum (\text{Water Level at Initial Point} - \\ &\text{Water Level at Draining Point}) = [(50.0 \pm 0.05) - (7.2 \pm 0.05)] + [(50.0 \pm \\ &0.05) - (47.8 \pm 0.05)] + [(50.0 \pm 0.05) - (49.6 \pm 0.05)] + [(50.0 \pm 0.05) - \\ &(48.5 \pm 0.05)] + [(50.0 \pm 0.05) - (49.6 \pm 0.05)] + [(50.0 \pm 0.05) - (49.6 \pm \\ &0.05)] + [(50.0 \pm 0.05) - (49.6 \pm 0.05)] = 48.1 \pm 0.2 \end{aligned}$$

Step 2-2)

$$\text{Original oil in place, OOIP} = \text{produced water during this step} = 48.1 \pm 0.2 \text{ (cm}^3\text{)}$$

$$\text{Connate water saturation, } S_{wc} =$$

$$\frac{\text{PV}(\text{cm}^3) - \text{OOIP}(\text{cm}^3)}{\text{PV}(\text{cm}^3)} = \frac{(70.0 \pm 0.1) - (48.1 \pm 0.2)}{(70.0 \pm 0.1)} = 0.31 \pm 0.003$$

Step 3) Secondary Waterflooding (1 PV injection)

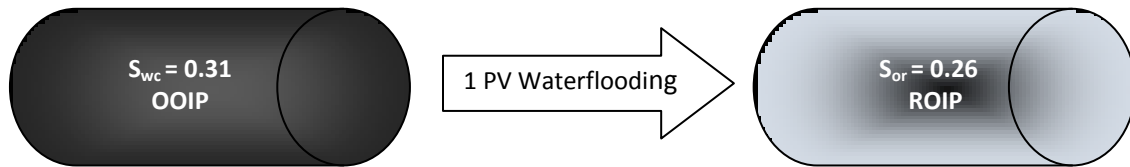


Figure D.9 Secondary waterflooding

According to Appendix C-3, Table C.15 (secondary waterflooding raw data for experiment #1), there were two times burette draining during secondary waterflooding in experiment # 1:

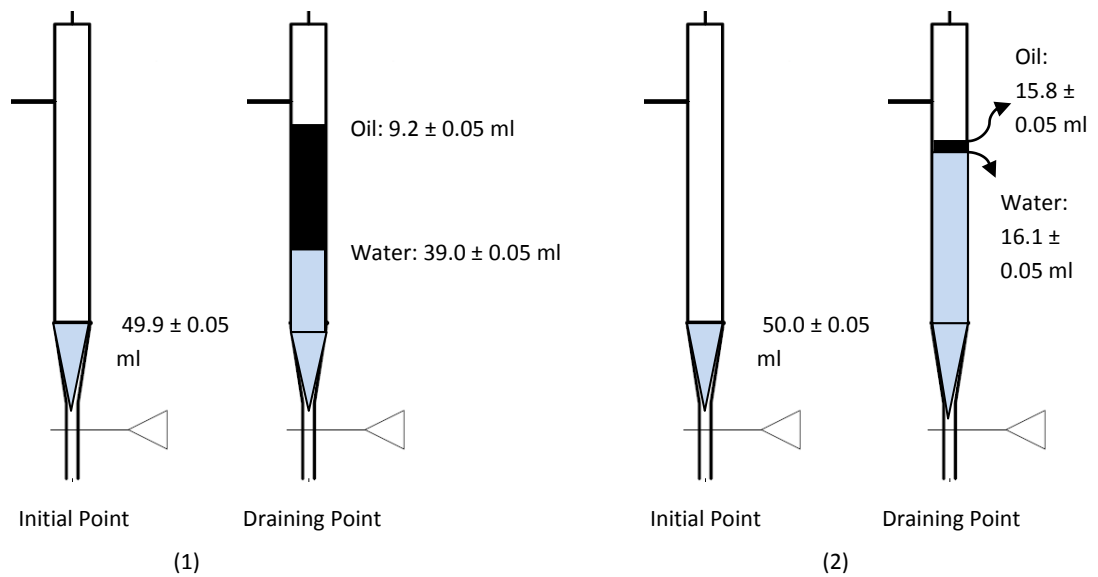


Figure D.10 Burette reading during secondary waterflooding in experiment # 1

Table D.2 Burette reading during secondary waterflooding in experiment # 1

Secondary Waterflooding				
Burette Draining #	Water Level (cm ³) Initial point	Oil Level (cm ³) Initial Point	Water Level (cm ³) Draining Point	Oil Level (cm ³) Draining Point
1	49.9 ± 0.05	49.9 ± 0.05	39.0 ± 0.05	9.2 ± 0.05
2	50.0 ± 0.05	50.0 ± 0.05	16.1 ± 0.05	15.8 ± 0.05

Step 3-1)

Produced oil during secondary waterflooding, $O_1 = \sum (\text{Water Level at Draining Point} - \text{Oil Level at Draining Point}) = [(39.0 \pm 0.05) - (9.2 \pm 0.05)] + [(16.1 \pm 0.05) - (15.8 \pm 0.05)] = 30.1 \pm 0.09 \text{ (cm}^3\text{)}$

Step 3-2)

Residual oil in place, $ROIP = (48.1 \pm 0.2) - (30.1 \pm 0.09) = 18.0 \pm 0.2 \text{ (cm}^3\text{)}$

Step 3-3)

Residual oil saturation, $S_{or} =$

$$\frac{OOIP \text{ (cm}^3\text{)} - O_1 \text{ (cm}^3\text{)}}{PV \text{ (cm}^3\text{)}} = \frac{(48.1 \pm 0.2) - (30.1 \pm 0.09)}{70.0 \pm 0.1} = 0.26 \pm 0.003$$

Step 3-4)

Waterflood recovery =

$$\frac{O_1 \text{ (cm}^3\text{)}}{OOIP \text{ (cm}^3\text{)}} \times 100 = \frac{30.1 \pm 0.09 \text{ (cm}^3\text{)}}{48.1 \pm 0.2 \text{ (cm}^3\text{)}} \times 100 = 62.6 \pm 0.3 \text{ (\% OOIP)}$$

Step 4) Tertiary Injection (0.5 PV Gas - 0.5 PV Water - 0.5 PV Gas)

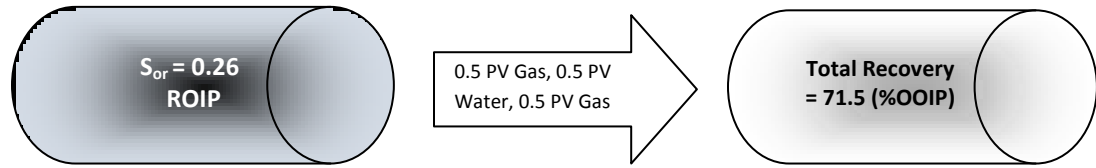
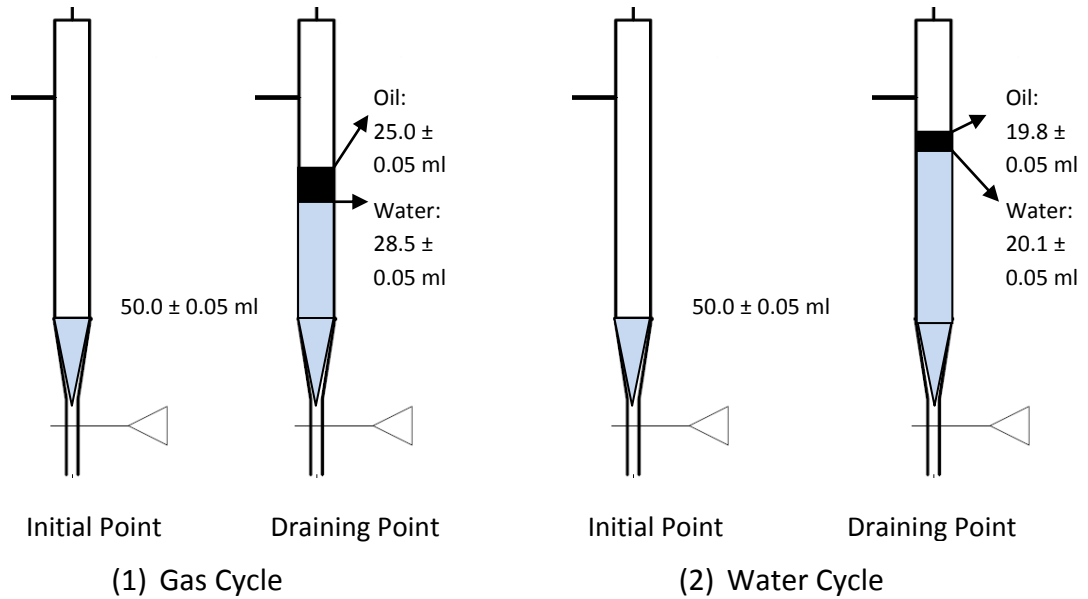
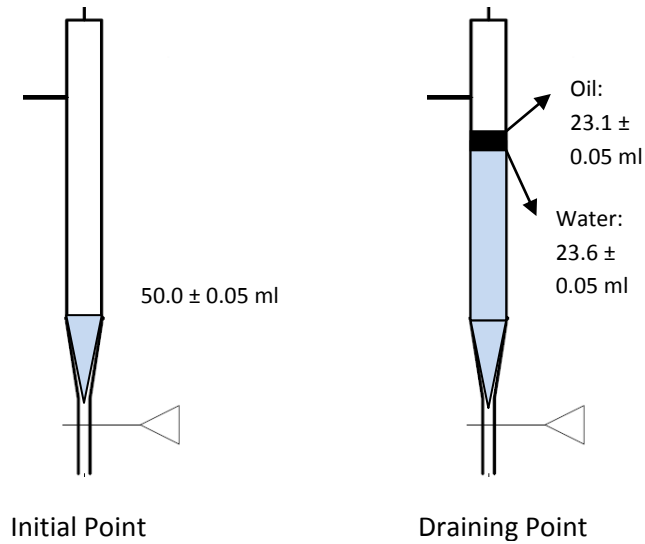


Figure D.11 Tertiary injection

According to Appendix C-3, Table C.16 to Table C.18 (Gas, Water, Gas injections raw data for experiment #1) there was one time burette draining in each water or gas cycle:





(3) Gas Cycle

Figure D.12 Burette reading during tertiary injection in experiment # 1

Table D.3 Burette reading during tertiary injection in experiment # 1

Tertiary Injections					
Burette Draining #	Cycle	Water Level (cm ³) Initial Point	Oil Level (cm ³) Initial Point	Water Level (cm ³) Draining Point	Oil Level (cm ³) Draining Point
1	Gas	50.0 ± 0.05	50.0 ± 0.05	28.5 ± 0.05	25.0 ± 0.05
2	Water	50.0 ± 0.05	50.0 ± 0.05	20.1 ± 0.05	19.8 ± 0.05
3	Gas	50.0 ± 0.05	50.0 ± 0.05	23.6 ± 0.05	23.1 ± 0.05

Step 4-1)

Total produced oil during tertiary recovery (0.5 PV Gas - 0.5 PV Water - 0.5 PV Gas), $O_2 = \sum (\text{Water Level at Draining Point} - \text{Water Level at$

$$\text{Initial Point} = [(28.5 \pm 0.05) - (25.0 \pm 0.05)] + [(20.1 \pm 0.05) - (19.8 \pm 0.05)] + [(23.6 \pm 0.05) - (23.1 \pm 0.05)] = 4.3 \pm 0.1 (\text{cm}^3)$$

Step 4-2)

$$\begin{aligned} \text{Total produced oil, O3} &= \text{Produced oil during secondary flooding} + \\ &\text{Produced oil during tertiary recovery} = (30.1 \pm 0.09) + (4.3 \pm 0.1) = 34.4 \\ &\pm 0.1 (\text{cm}^3) \end{aligned}$$

Step 4-3)

Total oil recovery =

$$\frac{\text{O3} (\text{cm}^3)}{\text{OOIP} (\text{cm}^3)} \times 100 = \frac{34.4 \pm 0.1 (\text{cm}^3)}{48.1 \pm 0.2 (\text{cm}^3)} \times 100 = 71.5 \pm 0.4 (\% \text{ OOIP})$$

Step 4-4)

$$\begin{aligned} \text{Incremental oil recovery} &= \text{total oil recovery} - \text{waterflood recovery (step} \\ &3-4) = (71.5 \pm 0.4 \text{ cm}^3) - (62.6 \pm 0.3 \text{ cm}^3) = 8.9 \pm 0.5 (\% \text{ OOIP}) \end{aligned}$$

Step 4-5)

Residual oil recovery =

$$\frac{\text{O2} (\text{cm}^3)}{\text{ROIP} (\text{cm}^3)} \times 100 = \frac{4.3 \pm 0.1 (\text{cm}^3)}{18.0 \pm 0.2 (\text{cm}^3)} \times 100 = 23.9 \pm 0.6 (\% \text{ ROIP})$$

D-3: IFT and Contact Angle Sample Calculation

According to the raw data in Table C.12 for TX-100 at 0.3 wt% above CMC in 7000 ppm TDS brine, the best estimate of a quantity x measured n times (interfacial tension or contact angle in our case), is assumed to be the average or mean value of x (Taylor, 1982).

$$\text{IFT} = \bar{x} = \frac{1}{n} \sum_1^n x_i = \frac{1}{5} (0.41 + 0.43 + 0.43 + 0.43 + 0.43) = 0.43$$

The standard deviation of x (IFT) is given by

$$\sigma = \sqrt{\frac{\sum_1^n (x_i - \bar{x})^2}{n-1}} = \sqrt{\frac{(0.41-0.43)^2 + (0.43-0.43)^2 + (0.43-0.43)^2 + (0.43-0.43)^2 + (0.43-0.43)^2}{5-1}} = 0.01$$

For contact angle the average between the measured left and right angles is calculated:

Contact angle =

$$\frac{1}{13} (72.6 + 70.7 + 71.6 + 71.3 + 70.3 + 70.7 + 70.6 + 70.6 + 69.4 + 70.9 + 69.4 + 62.9 + 63.2) + \frac{1}{13} (75.5 + 76.2 + 72.4 + 75.8 + 72.4 + 72.6 + 72.5 + 76 + 76.9 + 76.4 + 72.4 + 70.5 + 69.5) = 71.2$$

The standard deviation of contact angle is given by

$$\sigma = \sqrt{\frac{\sum_{i=1}^n (x_i - \bar{x})^2}{n-1}} =$$

$$\sqrt{\frac{(72.6 - 71.2)^2 + (70.7 - 71.2)^2 + (71.6 - 71.2)^2 + (71.3 - 71.2)^2 + (70.3 - 71.2)^2 + (70.7 - 71.2)^2}{26-1}} +$$

$$\sqrt{\frac{(70.6 - 71.2)^2 + (70.6 - 71.2)^2 + (69.4 - 71.2)^2 + (70.9 - 71.2)^2 + (69.4 - 71.2)^2 + (62.9 - 71.2)^2}{26-1}} +$$

$$\sqrt{\frac{(63.2 - 71.2)^2 + (75.5 - 71.2)^2 + (76.2 - 71.2)^2 + (72.4 - 71.2)^2 + (75.8 - 71.2)^2 + (72.4 - 71.2)^2}{26-1}} +$$

$$\sqrt{\frac{(72.6 - 71.2)^2 + (72.5 - 71.2)^2 + (76 - 71.2)^2 + (76.9 - 71.2)^2 + (76.4 - 71.2)^2 + (72.4 - 71.2)^2}{26-1}} +$$

$$\sqrt{\frac{(69.5 - 71.2)^2 + (70.5 - 71.2)^2}{26-1}} = 3.5$$

APPENDIX E: Economic Analysis

Table E.1 NPV calculation for experiment 9 (Optimized SAG Scenario, TX-100 at 0.3 wt% + CMC in 7000 ppm TDS)

year (i)	cumulative inj fluid (m ³)	inj fluid (m ³)	Cumulative produced oil (m ³)	Produced oil in each year(m ³)	Produced oil in each year(bbl)	Gross Revenue in each year[price(\$ USD/bbl)*produced oil (bbl)]	inj chemical in each year (kg)	cost of chemical in each year (\$ USD)	c _i (Net Revenue in period i after production starts \$ USD)	c _i [*] (Capex in period -i before production \$ USD)	NPV revenue (\$ USD)	NPV Capex (\$ USD)	NPV (\$ USD)
0	0.0000E+00	0.0000E+00	0.0000E+00	0.0000E+00	0.0000E+00	0.0000E+00	0.0000E+00	0.0000E+00	0.0000E+00	8.8500E+06	0.0000E+00	9.3810E+06	-9.3810E+06
1	1.7962E+07	1.7962E+07	1.6713E+07	1.6713E+07	1.0512E+08	7.8843E+09	8.9811E+04	2.6943E+04	7.8843E+09	0.0000E+00	7.4380E+09	9.3810E+06	7.4286E+09
2	3.9207E+07	2.1245E+07	3.6038E+07	1.9325E+07	1.2155E+08	9.1162E+09	1.0622E+05	3.1867E+04	9.1162E+09	0.0000E+00	1.5551E+10	9.3810E+06	1.5542E+10
3	5.5567E+07	1.6360E+07	5.6408E+07	2.0369E+07	1.2812E+08	9.6090E+09	8.1801E+04	2.4540E+04	9.6090E+09	0.0000E+00	2.3619E+10	9.3810E+06	2.3610E+10
4	7.2295E+07	1.6728E+07	7.0118E+07	1.3710E+07	8.6235E+07	6.4676E+09	8.3640E+04	2.5092E+04	6.4676E+09	0.0000E+00	2.8742E+10	9.3810E+06	2.8733E+10
5	9.1229E+07	1.8934E+07	7.1946E+07	1.8280E+06	1.1498E+07	8.6235E+08	9.4669E+04	2.8401E+04	8.6232E+08	0.0000E+00	2.9387E+10	9.3810E+06	2.9377E+10
6	1.1305E+08	2.1822E+07	7.5602E+07	3.6561E+06	2.2996E+07	1.7247E+09	1.0911E+05	3.2734E+04	1.7247E+09	0.0000E+00	3.0602E+10	9.3810E+06	3.0593E+10
7	1.2757E+08	1.4522E+07	7.7430E+07	1.8280E+06	1.1498E+07	8.6235E+08	7.2610E+04	2.1783E+04	8.6232E+08	0.0000E+00	3.1176E+10	9.3810E+06	3.1166E+10
8	1.4866E+08	2.1087E+07	7.7691E+07	2.6115E+05	1.6426E+06	1.2319E+08	1.0544E+05	3.1631E+04	1.2316E+08	0.0000E+00	3.1253E+10	9.3810E+06	3.1244E+10
9	1.6477E+08	1.6111E+07	7.8083E+07	3.9172E+05	2.4638E+06	1.8479E+08	8.0554E+04	2.4166E+04	1.8476E+08	0.0000E+00	3.1362E+10	9.3810E+06	3.1353E+10
10	1.8382E+08	1.9052E+07	7.8605E+07	5.2229E+05	3.2851E+06	2.4638E+08	9.5260E+04	2.8578E+04	2.4636E+08	0.0000E+00	3.1500E+10	9.3810E+06	3.1491E+10
11	2.0247E+08	1.8645E+07	7.8605E+07	0.0000E+00	0.0000E+00	0.0000E+00	0.0000E+00	0.0000E+00	0.0000E+00	0.0000E+00	3.1500E+10	9.3810E+06	3.1491E+10
12	2.2072E+08	1.8251E+07	8.1217E+07	2.6115E+06	1.6426E+07	1.2319E+09	0.0000E+00	0.0000E+00	1.2319E+09	0.0000E+00	3.2112E+10	9.3810E+06	3.2103E+10
13	2.3805E+08	1.7332E+07	8.8920E+07	7.7038E+06	4.8456E+07	3.6342E+09	0.0000E+00	0.0000E+00	3.6342E+09	0.0000E+00	3.3816E+10	9.3810E+06	3.3807E+10
14	2.5916E+08	2.1113E+07	8.9965E+07	1.0446E+06	6.5702E+06	4.9277E+08	0.0000E+00	0.0000E+00	4.9277E+08	0.0000E+00	3.4034E+10	9.3810E+06	3.4025E+10
15	2.7534E+08	1.6176E+07	9.0879E+07	9.1401E+05	5.7490E+06	4.3117E+08	0.0000E+00	0.0000E+00	4.3117E+08	0.0000E+00	3.4214E+10	9.3810E+06	3.4205E+10
16	2.9705E+08	2.1710E+07	9.1793E+07	9.1401E+05	5.7490E+06	4.3117E+08	6.8602E+04	5.0766E+06	4.2610E+08	0.0000E+00	3.4382E+10	9.3810E+06	3.4372E+10
17	3.1119E+08	1.4141E+07	9.4013E+07	2.2197E+06	1.3962E+07	1.0471E+09	4.4686E+04	3.3068E+06	1.0438E+09	0.0000E+00	3.4769E+10	9.3810E+06	3.4760E+10
18	3.2999E+08	1.8803E+07	9.4796E+07	7.8344E+05	4.9277E+06	3.6958E+08	5.9416E+04	4.3968E+06	3.6518E+08	0.0000E+00	3.4897E+10	9.3810E+06	3.4888E+10
19	3.4867E+08	1.8671E+07	9.5057E+07	2.6115E+05	1.6426E+06	1.2319E+08	5.9001E+04	4.3661E+06	1.1883E+08	0.0000E+00	3.4937E+10	9.3810E+06	3.4927E+10
20	3.6740E+08	1.8737E+07	9.5057E+07	2.9802E-08	1.8745E-07	1.4059E-05	5.9209E+04	4.3814E+06	-4.3814E+06	0.0000E+00	3.4935E+10	9.3810E+06	3.4926E+10
21	3.8514E+08	1.7734E+07	9.5057E+07	0.0000E+00	0.0000E+00	0.0000E+00	0.0000E+00	0.0000E+00	0.0000E+00	0.0000E+00	3.4935E+10	9.3810E+06	3.4926E+10
22	4.0340E+08	1.8264E+07	9.7277E+07	2.2197E+06	1.3962E+07	1.0471E+09	0.0000E+00	0.0000E+00	1.0471E+09	0.0000E+00	3.5226E+10	9.3810E+06	3.5216E+10
23	4.3779E+08	3.4388E+07	1.0172E+08	4.4395E+06	2.7924E+07	2.0943E+09	0.0000E+00	0.0000E+00	2.0943E+09	0.0000E+00	3.5774E+10	9.3810E+06	3.5765E+10
24	4.4831E+08	1.0517E+07	1.0283E+08	1.1099E+06	6.9809E+06	5.2357E+08	0.0000E+00	0.0000E+00	5.2357E+08	0.0000E+00	3.5903E+10	9.3810E+06	3.5894E+10
25	4.5882E+08	1.0517E+07	1.0394E+08	1.1099E+06	6.9809E+06	5.2357E+08	0.0000E+00	0.0000E+00	5.2357E+08	0.0000E+00	3.6025E+10	9.3810E+06	3.6016E+10

NPV_{SAG} = \$ 3.6016E+10 USD

Table E.2 NPV calculation for experiment 1 (WAG, 7000 ppm TDS)

year (i)	cumulative inj fluid (m ³)	inj fluid (m ³)	Cumulative produced oil (m ³)	Produced oil in each year(m ³)	produced oil in each year(bbl)	Gross Revenue in each year[price(\$ USD/bbl)*produced oil (bbl)]	inj chemical in each year (kg)	cost of chemical in each year (\$ USD)	ci(Net Revenue in period i after production starts \$ USD)	ci* (Capex in period -i before production \$ USD)	NPV revenue (\$ USD)	NPV capex (\$ USD)	NPV (\$ USD)
0	0.0000E+00	0.0000E+00	0.0000E+00	0.0000E+00	0.0000E+00	0.0000E+00	0.0000E+00	0.0000E+00	0.0000E+00	0.0000E+00	0.0000E+00	0.0000E+00	0.0000E+00
1	2.0063E+07	2.0063E+07	1.8028E+07	1.8028E+07	1.1339E+08	8.5045E+09	0.0000E+00	0.0000E+00	8.5045E+09	0.0000E+00	8.0231E+09	0.0000E+00	8.0231E+09
2	3.6738E+07	1.6675E+07	3.3755E+07	1.5727E+07	9.8917E+07	7.4188E+09	0.0000E+00	0.0000E+00	7.4188E+09	0.0000E+00	1.4626E+10	0.0000E+00	1.4626E+10
3	5.6408E+07	1.9669E+07	5.3828E+07	2.0074E+07	1.2626E+08	9.4695E+09	0.0000E+00	0.0000E+00	9.4695E+09	0.0000E+00	2.2577E+10	0.0000E+00	2.2577E+10
4	7.4737E+07	1.8330E+07	7.2879E+07	1.9051E+07	1.1983E+08	8.9870E+09	0.0000E+00	0.0000E+00	8.9870E+09	0.0000E+00	2.9695E+10	0.0000E+00	2.9695E+10
5	9.7374E+07	2.2637E+07	7.5692E+07	2.8129E+06	1.7693E+07	1.3269E+09	0.0000E+00	0.0000E+00	1.3269E+09	0.0000E+00	3.0687E+10	0.0000E+00	3.0687E+10
6	1.0735E+08	9.9790E+06	7.6204E+07	5.1143E+05	3.2168E+06	2.4126E+08	0.0000E+00	0.0000E+00	2.4126E+08	0.0000E+00	3.0857E+10	0.0000E+00	3.0857E+10
7	1.2647E+08	1.9118E+07	7.6396E+07	1.9179E+05	1.2063E+06	9.0473E+07	0.0000E+00	0.0000E+00	9.0473E+07	0.0000E+00	3.0917E+10	0.0000E+00	3.0917E+10
8	1.4559E+08	1.9118E+07	7.6587E+07	1.9179E+05	1.2063E+06	9.0473E+07	0.0000E+00	0.0000E+00	9.0473E+07	0.0000E+00	3.0974E+10	0.0000E+00	3.0974E+10
9	1.6471E+08	1.9118E+07	7.6779E+07	1.9179E+05	1.2063E+06	9.0473E+07	0.0000E+00	0.0000E+00	9.0473E+07	0.0000E+00	3.1027E+10	0.0000E+00	3.1027E+10
10	1.8382E+08	1.9118E+07	7.6971E+07	1.9179E+05	1.2063E+06	9.0473E+07	0.0000E+00	0.0000E+00	9.0473E+07	0.0000E+00	3.1078E+10	0.0000E+00	3.1078E+10
11	2.0557E+08	2.1744E+07	7.7738E+07	7.6715E+05	4.8252E+06	3.6189E+08	0.0000E+00	0.0000E+00	3.6189E+08	0.0000E+00	3.1268E+10	0.0000E+00	3.1268E+10
12	2.2180E+08	1.6229E+07	7.7738E+07	0.0000E+00	0.0000E+00	0.0000E+00	0.0000E+00	0.0000E+00	0.0000E+00	0.0000E+00	3.1268E+10	0.0000E+00	3.1268E+10
13	2.3879E+08	1.6991E+07	8.0807E+07	3.0686E+06	1.9301E+07	1.4476E+09	0.0000E+00	0.0000E+00	1.4476E+09	0.0000E+00	3.1947E+10	0.0000E+00	3.1947E+10
14	2.5713E+08	1.8343E+07	8.3364E+07	2.5572E+06	1.6084E+07	1.2063E+09	0.0000E+00	0.0000E+00	1.2063E+09	0.0000E+00	3.2481E+10	0.0000E+00	3.2481E+10
15	2.7597E+08	1.8842E+07	8.5921E+07	2.5572E+06	1.6084E+07	1.2063E+09	0.0000E+00	0.0000E+00	1.2063E+09	0.0000E+00	3.2984E+10	0.0000E+00	3.2984E+10
16	2.9472E+08	1.8751E+07	8.6177E+07	2.5572E+05	1.6084E+06	1.2063E+08	0.0000E+00	0.0000E+00	1.2063E+08	0.0000E+00	3.3032E+10	0.0000E+00	3.3032E+10
17	3.1221E+08	1.7489E+07	8.6432E+07	2.5572E+05	1.6084E+06	1.2063E+08	0.0000E+00	0.0000E+00	1.2063E+08	0.0000E+00	3.3076E+10	0.0000E+00	3.3076E+10
18	3.3175E+08	1.9538E+07	8.6688E+07	2.5572E+05	1.6084E+06	1.2063E+08	0.0000E+00	0.0000E+00	1.2063E+08	0.0000E+00	3.3119E+10	0.0000E+00	3.3119E+10
19	3.4971E+08	1.7962E+07	8.6688E+07	0.0000E+00	0.0000E+00	0.0000E+00	0.0000E+00	0.0000E+00	0.0000E+00	0.0000E+00	3.3119E+10	0.0000E+00	3.3119E+10
20	3.6788E+08	1.8172E+07	8.6688E+07	0.0000E+00	0.0000E+00	0.0000E+00	0.0000E+00	0.0000E+00	0.0000E+00	0.0000E+00	3.3119E+10	0.0000E+00	3.3119E+10
21	3.8531E+08	1.7424E+07	8.7455E+07	7.6715E+05	4.8252E+06	3.6189E+08	0.0000E+00	0.0000E+00	3.6189E+08	0.0000E+00	3.3225E+10	0.0000E+00	3.3225E+10
22	4.0573E+08	2.0418E+07	8.7711E+07	2.5572E+05	1.6084E+06	1.2063E+08	0.0000E+00	0.0000E+00	1.2063E+08	0.0000E+00	3.3259E+10	0.0000E+00	3.3259E+10
23	4.2303E+08	1.7306E+07	8.7711E+07	0.0000E+00	0.0000E+00	0.0000E+00	0.0000E+00	0.0000E+00	0.0000E+00	0.0000E+00	3.3259E+10	0.0000E+00	3.3259E+10
24	4.4667E+08	2.3634E+07	8.7967E+07	2.5572E+05	1.6084E+06	1.2063E+08	0.0000E+00	0.0000E+00	1.2063E+08	0.0000E+00	3.3288E+10	0.0000E+00	3.3288E+10
25	4.5956E+08	1.2893E+07	8.7967E+07	0.0000E+00	0.0000E+00	0.0000E+00	0.0000E+00	0.0000E+00	0.0000E+00	0.0000E+00	3.3288E+10	0.0000E+00	3.3288E+10

$NPV_{WAG} = \$ 3.3288E+10 \text{ USD}$

APPENDIX F: Paper

Moayedi, M., James, L. A., Mahmoodi, M. (2014). An Experimental Study on Optimization of SAG Process Utilizing Nonionic Surfactants and Sodium Lignosulfonate. *The Society of Core Analysts*, SCA2014-087.

http://www.scaweb.org/assets/papers/2014_papers/SCA2014-087.pdf